

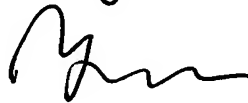
VERIFICATION OF TRANSLATION

I, Yoshito FUKUSHIMA of 3F ESAKA MITAKA BLDG. 4-1,  
HIROSHIBA-CHO, SUITA-SHI, OSAKA 564-0052, JAPAN,  
hereby verify that the attached translation is a  
true and accurate translation of a certified copy  
of Japanese Patent Application NO.2003-089077.

Date

July 10, 2008

Signature



Yoshito FUKUSHIMA

日 本 国 特 許 庁  
JAPAN PATENT OFFICE

別紙添付の書類に記載されている事項は下記の出願書類に記載されて  
る事項と同一であることを証明する。

This is to certify that the annexed is a true copy of the following application as filed  
with this Office.

出 願 年 月 日                      2 0 0 3 年    3 月 2 7 日  
Date of Application:

願 番 号                      特 願 2 0 0 3 - 0 8 9 0 7 7  
Application Number:

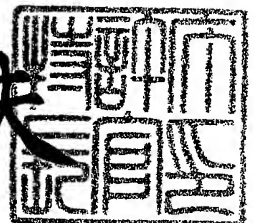
[T. 10/C]:                      [ J P 2 0 0 3 - 0 8 9 0 7 7 ]

願                      人                      三 洋 電 機 株 式 会 社  
Applicant(s):

2 0 0 4 年    2 月    3 日

特許庁長官  
Commissioner,  
Japan Patent Office

今 井 康 夫



出証番号    出証特 2 0 0 4 - 3 0 0 5 8 2 6

【Document Name】	Petition for Patent
【Docket No.】	NPX1030009
【Filing Date】	March 27, 2003
【Address】	Commissioner, Patent Office
【International Patent Classification】	H01M 4/02 H01M 4/04
【Inventor】	
【Address】	c/o SANYO ELECTRIC CO., LTD. 2-5-5, Keihanhondori, Moriguchi-shi, Osaka 570-8677, JAPAN
【Name】	Masaharu ITAYA
【Inventor】	
【Address】	c/o SANYO ELECTRIC CO., LTD. 2-5-5, Keihanhondori, Moriguchi-shi, Osaka 570-8677, JAPAN
【Name】	Masahide MIYAKE
【Inventor】	
【Address】	c/o SANYO ELECTRIC CO., LTD. 2-5-5, Keihanhondori, Moriguchi-shi, Osaka 570-8677, JAPAN
【Name】	Masahisa FUJIMOTO
【Applicant】	
【Identification No.】	000001889
【Name】	SANYO ELECTRIC CO., LTD.
【Attorney】	
【Identification No.】	100098305
【Patent Attorney】	
【Name】	Yoshito FUKUSHIMA
【Telephone No.】	06-6330-5625
【Payment of Fees】	
【Prepayment Book No.】	032920
【Amount to be paid】	¥21,000
【Attached Documents】	

【Item】	Specification	1
【Item】	Drawings	1
【Item】	Abstract	1
【Identification No. of General Power】	0006012	
【Requirement of Proof】	Yes	.



[Document Name] Specification

[Title of the Invention] Non-aqueous electrolyte secondary battery

[Scope of Claim for Patent]

5           [Claim 1] A non-aqueous electrolyte secondary battery characterized by comprising a positive electrode, a negative electrode, and a non-aqueous electrolyte, wherein

          said positive electrode includes elemental sulfur, and said negative electrode includes silicon that stores lithium.

10          [Claim 2] The non-aqueous electrolyte secondary battery as recited in Claim 1, characterized in that

          said non-aqueous electrolyte includes a room temperature molten salt having a melting point of not higher than 60°C.

15          [Claim 3] The non-aqueous electrolyte secondary battery as recited in Claim 1 or 2, characterized in that

          said non-aqueous electrolyte includes a quaternary ammonium salt.

20          [Claim 4] The non-aqueous electrolyte secondary battery as recited in Claim 2 or 3, characterized in that

          said non-aqueous electrolyte further includes at least one type of solvent selected from the group consisting of cyclic ether, chain ether, and fluorinated carbonate.

          [Claim 5] A non-aqueous electrolyte secondary battery

characterized by comprising a positive electrode, a negative electrode, and a non-aqueous electrolyte, wherein

said negative electrode includes silicon that stores lithium, and

5       said non-aqueous electrolyte includes a room temperature molten salt having a melting point of not higher than 60°C and a reduction product of elemental sulfur.

[Claim 6] The non-aqueous electrolyte secondary battery as recited in Claim 5, characterized in that

10       said positive electrode includes elemental sulfur.

[Claim 7] The non-aqueous electrolyte secondary battery as recited in Claim 5 or 6, characterized in that

15       said reduction product of elemental sulfur is obtained by reducing elemental sulfur in a room temperature molten salt having a melting point of not higher than 60°C and an organic electrolyte.

[Claim 8] The non-aqueous electrolyte secondary battery as recited in any of Claims 1 to 7, characterized in that

20       said silicon is an amorphous silicon thin film or a microcrystalline silicon thin film.

[Claim 9] The non-aqueous electrolyte secondary battery as recited in Claim 2 or any of Claims 5 to 7, characterized in that

said room temperature molten salt includes at least one type selected from the group consisting of

trimethylpropylammonium

bis(trifluoromethylsulfonyl)imide, trimethyloctylammonium

5 bis(trifluoromethylsulfonyl)imide, trimethylallylammonium

bis(trifluoromethylsulfonyl)imide, trimethylhexylammonium

bis(trifluoromethylsulfonyl)imide, trimethylethylammonium

2,2,2-trifluoro-N-(trifluoromethylsulfonyl)acetamide,

trimethylallylammonium

10 2,2,2-trifluoro-N-(trifluoromethylsulfonyl)acetamide,

trimethylpropylammonium

2,2,2-trifluoro-N-(trifluoromethylsulfonyl)acetamide,

tetraethylammonium

2,2,2-trifluoro-N-(trifluoromethylsulfonyl)acetamide,

15 triethylmethylammonium

2,2,2-trifluoro-N-(trifluoromethylsulfonyl)acetamide,

1-ethyl-3-methylimidazolium

bis(pentafluoroethylsulfonyl)imide,

1-ethyl-3-methylimidazolium

20 bis(trifluoromethylsulfonyl)imide,

1-ethyl-3-methylimidazolium tetrafluoroborate, and

1-ethyl-3-methylimidazolium pentafluoroborate.

[Claim 10] The non-aqueous electrolyte secondary battery as recited in Claim 3, characterized in that

said quaternary ammonium salt includes at least one type selected from the group consisting of

trimethylpropylammonium

bis(trifluoromethylsulfonyl)imide, trimethyloctylammonium

5 bis(trifluoromethylsulfonyl)imide, trimethylallylammonium

bis(trifluoromethylsulfonyl)imide, trimethylhexylammonium

bis(trifluoromethylsulfonyl)imide, trimethylethylammonium

2,2,2-trifluoro-N-(trifluoromethylsulfonyl)acetamide,

trimethylallylammonium

10 2,2,2-trifluoro-N-(trifluoromethylsulfonyl)acetamide,

trimethylpropylammonium

2,2,2-trifluoro-N-(trifluoromethylsulfonyl)acetamide,

tetraethylammonium

2,2,2-trifluoro-N-(trifluoromethylsulfonyl)acetamide,

15 triethylmethylammonium

2,2,2-trifluoro-N-(trifluoromethylsulfonyl)acetamide,

tetramethylammonium tetrafluoroborate, tetramethylammonium

hexafluorophosphate, tetraethylammonium tetrafluoroborate,

and tetraethylammonium hexafluorophosphate.

20 [Claim 11] The non-aqueous electrolyte secondary battery as recited in Claim 4, characterized in that

said cyclic ether include at least one type selected from the group consisting of 1,3-dioxolane,

4-methyl-1,3-dioxolane, tetrahydrofuran, 2-methyl

25 tetrahydrofuran, propylene oxide, 1,2-butylene oxide,

1,4-dioxiane, 1,3,5-trioxane, furan, 2-methy furan,  
1,8-cineole, and crown ether; said chain ether includes at  
lest one type selected from the group consisting of  
1,2-dimethoxyethane, diethyl ether, dipropyl ether,  
5 diisopropyl ether, dibutyl ether, dihexyl ether, ethyl vinyl  
ether, butyl vinyl ether, methyl phenyl ether, ethyl phenyl  
ether, butyl phenyl ether, pentyl phenyl ether,  
methoxytoluene, benzyl ethyl ether, diphenyl ether, dibenzyl  
ether, o-dimethoxybenzene, 1,2-diethoxyethane,  
10 1,2-dibutoxyethane, diethylene glycol dimethyl ether,  
diethylene glycol diethyl ether, diethylene glycol dibutyl  
ether, 1,1-dimethoxymethane, 1,1-diethoxyethane,  
triethylene glycol dimethyl ether, and tetraethylene glycol  
dimethyl ether; and said fluorinated carbonate includes at  
15 least one type selected from the group consisting of  
trifluoropropylene carbonate and fluoroethyl carbonate.

[Claim 12] The non-aqueous electrolyte secondary  
battery as recited in any of Claims 1 to 11, characterized  
in that

20 a conductive agent is added to said positive electrode.

[Claim 13] The non-aqueous electrolyte secondary  
battery as recited in any of Claims 1 to 12, characterized  
in that

said non-aqueous electrolyte includes  $\gamma$ -butyrolactone.

25 [Detailed Description of the Invention]

[0001]

[Technical Field to which the Invention Belongs]

The present invention relates to a non-aqueous electrolyte secondary battery composed of a positive  
5 electrode, a negative electrode and non-aqueous electrolyte.

[0002]

[Conventional Art]

In recent years, as one of the secondary batteries having high power and high energy density, non-aqueous  
10 electrolyte secondary batteries with high electromotive forces have been made available in which the oxidation and reduction of lithium using non-aqueous electrolytes is utilized.

[0003]

15 The currently practical lithium secondary batteries have lithium cobaltate ( $\text{LiCoO}_2$ ) or lithium manganate ( $\text{LiMn}_2\text{O}_4$ ) as positive electrode materials, and carbon materials as negative electrode materials. In addition, these batteries have non-aqueous electrolytes including  
20 electrolyte salts of lithium salts, such as  $\text{LiBF}_4$  and  $\text{LiPF}_6$ , dissolved in organic solvents of ethylene carbonate, diethyl carbonate, or the like.

[0004]

However, portable equipment requires secondary  
25 batteries having longer duration, and hence further increased

capacity and energy density of lithium secondary batteries are required.

[0005]

As a negative electrode material capable of storage and  
5 release of lithium while exhibiting high capacity, the use  
of a silicon thin film formed by being deposited on a negative  
electrode current collector has been proposed (refer to  
Patent Documents 1 and 2.) This negative electrode material  
allows a negative electrode capacity of at least 3000 to 4000  
10 mAh/g.

[0006]

[Patent Document 1]

JP-2001-266851-A

[Patent Document 2]

15 JP-2002-83594-A

[Patent Document 3]

JP-4-267073-A

[Patent Document 4]

JP-8-115724-A

20 [0007]

[Problems to be Solved by the Invention]

However, for the preparation of a lithium secondary  
battery having the silicon material as a negative electrode  
and lithium cobaltate as a positive electrode, it is required  
25 to considerably increase the thickness of the positive

electrode active material layer in order to balance the positive and negative electrode capacities. This may make it difficult for the electrolyte to penetrate into the positive electrode active material layer during a manufacturing process, and may further cause a shortage of the electrolyte in the positive electrode active material layer during charge-discharge cycles, resulting in deterioration of the charge-discharge cycle characteristics. For this reason, there exists a need for the development of positive electrode materials having a high electrode capacity balanced with the high negative electrode capacity.

[0008]

In recent years, the use of an organic disulfide compound, such as DMcT (2,5-dimercapto-1,3,4-thiadiazole), as a positive electrode material for achieving high capacity and high energy density has been proposed. However, the organic disulfide compound used as a positive electrode material react reversibly with lithium only at elevated temperatures of 60°C or higher. Therefore, the use of organic disulfide compound in general non-aqueous electrolyte secondary batteries has been difficult.

[0009]

Moreover, in recent years, a secondary battery has been proposed capable of the charge-discharge reaction at room temperature using a positive electrode material obtained from



the above-mentioned organic disulfide compound, such as DMcT, mixed with a conductive polymer, such as polyaniline (refer to Patent Documents 3 and 4.)

[0010]

5           In the case of the above-mentioned positive electrode active material using the organic disulfide compound, however, the disulfide bonds are involved with the charge-discharge reaction, and other parts including carbon atoms and hydrogen atoms do not contribute to the reaction.  
10 Therefore, it has been difficult to further increase a capacity per weight.

[0011]

          An object of the present invention is to provide a non-aqueous electrolyte secondary battery having increased  
15 capacity and energy density.

[0012]

[Means for Solving the Problems and Effects of the Invention]

          A non-aqueous electrolyte secondary battery according to a first invention comprises a positive electrode, a  
20 negative electrode, and a non-aqueous electrolyte, the positive electrode including elemental sulfur, the negative electrode including silicon that stores lithium.

[0013]

          In the non-aqueous electrolyte secondary battery  
25 according to the present invention, the combination of the

positive electrode including elemental sulfur and the negative electrode including silicon that stores lithium enables the elemental sulfur in the positive electrode and the silicon in the negative electrode to react reversibly with lithium at relatively low temperatures. In this case, the use of silicon that stores lithium can result in increased negative electrode capacity. Moreover, the use of elemental sulfur in the positive electrode enables increased capacity per unit weight, compared with that obtained using an organic disulfide compound. Accordingly, the negative electrode capacity and positive electrode capacity can be easily balanced, so that increased capacity and energy density can be realized.

[0014]

The non-aqueous electrolyte may include a room temperature molten salt having a melting point of not higher than 60°C. In this case, the reversible reaction of the silicon in the negative electrode and the elemental sulfur in the positive electrode with lithium can be easily carried out also at room temperature, so as to facilitate the charging/discharging reaction at room temperature. Room temperature molten salts having melting points of not higher than 60°C are liquids containing only ions, having fire-resistance and no vapor pressure, and therefore, they are not decomposed or burned even at the time of abnormal

operations, such as overcharging, and can be safely used without the provision of a protection circuit or the like.

[0015]

The non-aqueous electrolyte may include a quaternary ammonium salt. In this case, the reversible reaction of the silicon in the negative electrode and the elemental sulfur in the positive electrode with lithium can be easily carried out also at room temperature, so as to facilitate the charging/discharging reaction at room temperature.

10 [0016]

The non-aqueous electrolyte may further include at least one type of solvent selected from the group consisting of cyclic ether, chain ether, and fluorinated carbonate. In this case, the reversible reaction of the silicon in the negative electrode and the elemental sulfur in the positive electrode with lithium can be more easily carried out also at room temperature, so as to further facilitate the charging/discharging reaction at room temperature.

[0017]

20 A non-aqueous electrolyte secondary battery according to a second invention comprises a positive electrode, a negative electrode, and a non-aqueous electrolyte, the negative electrode including silicon that stores lithium, the non-aqueous electrolyte including a room temperature molten

salt having a melting point of not higher than 60°C and a reduction product of elemental sulfur.

[0018]

In the non-aqueous electrolyte secondary battery  
5 according to the present invention, the inclusion of the room temperature molten salt having a melting point of not higher than 60°C and the reduction product of elemental sulfur in the non-aqueous electrolyte enables the silicon in the negative electrode to easily react with lithium also at room  
10 temperature, so as to facilitate the charging/discharging at room temperature. Accordingly, increased capacity and energy density can be realized.

[0019]

The positive electrode may include elemental sulfur. In  
15 this case, the combination of the positive electrode including elemental sulfur and the negative electrode including silicon that stores lithium enables the elemental sulfur in the positive electrode and the silicon in the negative electrode to reversibly react with lithium. In this  
20 case, the use of silicon that stores lithium for the negative electrode can increase the negative electrode capacity, and the use of elemental sulfur for the positive electrode can increase the positive electrode capacity. Accordingly, the negative electrode capacity and the positive electrode

capacity can be easily balanced, so that further increased capacity and energy density can be realized.

[0020]

The reduction product of elemental sulfur may be  
5 obtained by reducing elemental sulfur in a room temperature molten salt having a melting point of not higher than 60°C and an organic electrolyte. In this case, the reversible reaction of the silicon in the negative electrode and the elemental sulfur in the positive electrode with lithium can  
10 be more easily carried out also at room temperature, so as to further facilitate the charging/discharging reaction at room temperature.

[0021]

The silicon may be an amorphous silicon thin film or a  
15 microcrystalline silicon thin film. In this case, further increased negative electrode capacity can be achieved.

[0022]

The room temperature molten salt may include at least one type selected from the group consisting of  
20 trimethylpropylammonium bis(trifluoromethylsulfonyl)imide  
 $((\text{CH}_3)_3\text{N}^+(\text{C}_3\text{H}_7)\text{N}^-(\text{SO}_2\text{CF}_3)_2)$ , trimethyloctylammonium  
bis(trifluoromethylsulfonyl)imide  
 $((\text{CH}_3)_3\text{N}^+(\text{C}_8\text{H}_{17})\text{N}^-(\text{SO}_2\text{CF}_3)_2)$ , trimethylallylammonium  
bis(trifluoromethylsulfonyl)imide  
25  $((\text{CH}_3)_3\text{N}^+(\text{Allyl})\text{N}^-(\text{SO}_2\text{CF}_3)_2)$ , trimethylhexylammonium

bis(trifluoromethylsulfonyl)imide  
 ((CH<sub>3</sub>)<sub>3</sub>N<sup>+</sup>(C<sub>6</sub>H<sub>13</sub>)N<sup>-</sup>(SO<sub>2</sub>CF<sub>3</sub>)<sub>2</sub>), trimethylethylammonium  
 2,2,2-trifluoro-N-(trifluoromethylsulfonyl)acetamide  
 ((CH<sub>3</sub>)<sub>3</sub>N<sup>+</sup>(C<sub>2</sub>H<sub>5</sub>)(CF<sub>3</sub>CO)N<sup>-</sup>(SO<sub>2</sub>CF<sub>3</sub>)), trimethylallylammonium  
 5 2,2,2-trifluoro-N-(trifluoromethylsulfonyl)acetamide  
 ((CH<sub>3</sub>)<sub>3</sub>N<sup>+</sup>(Allyl)(CF<sub>3</sub>CO)N<sup>-</sup>(SO<sub>2</sub>CF<sub>3</sub>)), trimethylpropylammonium  
 2,2,2-trifluoro-N-(trifluoromethylsulfonyl)acetamide  
 ((CH<sub>3</sub>)<sub>3</sub>N<sup>+</sup>(C<sub>3</sub>H<sub>7</sub>)(CF<sub>3</sub>CO)N<sup>-</sup>(SO<sub>2</sub>CF<sub>3</sub>)), tetraethylammonium  
 2,2,2-trifluoro-N-(trifluoromethylsulfonyl)acetamide  
 10 ((C<sub>2</sub>H<sub>5</sub>)<sub>4</sub>N<sup>+</sup>(CF<sub>3</sub>CO)N<sup>-</sup>(SO<sub>2</sub>CF<sub>3</sub>)), triethylmethylanmonium  
 2,2,2-trifluoro-N-(trifluoromethylsulfonyl)acetamide  
 ((C<sub>2</sub>H<sub>5</sub>)<sub>3</sub>N<sup>+</sup>(CH<sub>3</sub>)(CF<sub>3</sub>CO)N<sup>-</sup>(SO<sub>2</sub>CF<sub>3</sub>)),  
 1-ethyl-3-methylimidazolium  
 bis(pentafluoroethylsulfonyl)imide  
 15 ((C<sub>2</sub>H<sub>5</sub>)(C<sub>3</sub>H<sub>3</sub>N<sub>2</sub>)<sup>+</sup>(CH<sub>3</sub>)N<sup>-</sup>(SO<sub>2</sub>C<sub>2</sub>F<sub>5</sub>)<sub>2</sub>),  
 1-ethyl-3-methylimidazolium  
 bis(trifluoromethylsulfonyl)imide  
 ((C<sub>2</sub>H<sub>5</sub>)(C<sub>3</sub>H<sub>3</sub>N<sub>2</sub>)<sup>+</sup>(CH<sub>3</sub>)N<sup>-</sup>(SO<sub>2</sub>CF<sub>3</sub>)<sub>2</sub>),  
 1-ethyl-3-methylimidazolium tetrafluoroborate  
 20 ((C<sub>2</sub>H<sub>5</sub>)(C<sub>3</sub>H<sub>3</sub>N<sub>2</sub>)<sup>+</sup>(CH<sub>3</sub>)BF<sub>4</sub><sup>-</sup>), and 1-ethyl-3-methylimidazolium  
 pentafluoroborate ((C<sub>2</sub>H<sub>5</sub>)(C<sub>3</sub>H<sub>3</sub>N<sub>2</sub>)<sup>+</sup>(CH<sub>3</sub>)PF<sub>6</sub><sup>-</sup>).  
 [0023]

The quaternary ammonium salt may include at least one  
 type selected from the group consisting of

25 trimethylpropylammonium

bis(trifluoromethylsulfonyl)imide, trimethyloctylammonium  
 bis(trifluoromethylsulfonyl)imide, trimethylallylammonium  
 bis(trifluoromethylsulfonyl)imide, trimethylhexylammonium  
 bis(trifluoromethylsulfonyl)imide, trimethylethylammonium  
 5 2,2,2-trifluoro-N-(trifluoromethylsulfonyl)acetamide,  
 trimethylallylammonium  
 2,2,2-trifluoro-N-(trifluoromethylsulfonyl)acetamide,  
 trimethylpropylammonium  
 2,2,2-trifluoro-N-(trifluoromethylsulfonyl)acetamide,  
 10 tetraethylammonium  
 2,2,2-trifluoro-N-(trifluoromethylsulfonyl)acetamide,  
 triethylmethylammonium  
 2,2,2-trifluoro-N-(trifluoromethylsulfonyl)acetamide,  
 tetramethylammonium tetrafluoroborate, tetramethylammonium  
 15 hexafluorophosphate, tetraethylammonium tetrafluoroborate,  
 and tetraethylammonium hexafluorophosphate.  
 [0024]

The cyclic ether may include at least one type selected  
 from the group consisting of 1,3-dioxolane,  
 20 4-methyl-1,3-dioxolane, tetrahydrofuran, 2-methyl  
 tetrahydrofuran, propylene oxide, 1,2-butylene oxide,  
 1,4-dioxane, 1,3,5-trioxane, furan, 2-methyl furan,  
 1,8-cineole, and crown ether; the chain ether may include at  
 least one type selected from the group consisting of  
 25 1,2-dimethoxyethane, diethyl ether, dipropyl ether,

diisopropyl ether, dibutyl ether, dihexyl ether, ethyl vinyl ether, butyl vinyl ether, methyl phenyl ether, ethyl phenyl ether, butyl phenyl ether, pentyl phenyl ether, methoxytoluene, benzyl ethyl ether, diphenyl ether, dibenzyl ether, o-dimethoxybenzene, 1,2-diethoxyethane, 1,2-dibutoxyethane, diethylene glycol dimethyl ether, diethylene glycol diethyl ether, diethylene glycol dibutyl ether, 1,1-dimethoxymethane, 1,1-diethoxyethane, triethylene glycol dimethyl ether, and tetraethylene glycol dimethyl ether; and the fluorinated carbonate may include at least one type selected from the group consisting of trifluoropropylene carbonate and fluoroethyl carbonate.

[0025]

A conductive agent may be added to the positive electrode. This enhances the conductivity of the positive electrode. As a result, the charge-discharge characteristics can be enhanced.

[0026]

Further, the non-aqueous electrode may include  $\gamma$ -butyrolactone. In this case also, the reversible reaction of the silicon in the negative electrode and the elemental sulfur in the positive electrode with lithium can be easily carried out at room temperature, so as to facilitate the charging/discharging reaction at room temperature.

[0027]



[Embodiments of the Invention]

Description will, hereinafter, be made of a non-aqueous electrolyte secondary battery according to one embodiment of the present invention.

5 [0028]

The non-aqueous electrolyte secondary battery according to the present embodiment comprises a negative electrode, a positive electrode, and a non-aqueous electrolyte.

10 [0029]

The positive electrode has a positive electrode active material made of a mixture of elemental sulfur, a conductive agent, and a binder. As the conductive agent, a conductive carbon material, for example, may be used. It is noted that  
15 addition of too small an amount of conductive carbon material cannot sufficiently enhance the conductivity in the positive electrode, whereas addition of an excessive amount of the material decreases the ratio of elemental sulfur in the positive electrode, and fails to achieve high capacity.  
20 Accordingly, the amount of carbon material may be set in the range of 5 to 84% by weight of the whole positive electrode active material, preferably, in the range of 5 to 54% by weight, more preferably, in the range of 5 to 20% by weight.  
[0030]

As the negative electrode, silicon that stores lithium is used. For example, an amorphous silicon thin film or a microcrystalline silicon film is formed on a current collector made of a copper foil having an electrolytically treated surface. A thin film made of a mixture of amorphous silicon and microcrystalline silicon may also be used. As a film formation method, sputtering, plasma CVD (chemical vapor deposition), or the like may be used. In particular, it is preferable to use silicon with large capacity, as proposed in JP-2001-266851-A and JP-2002-83594-A. This enables a non-aqueous electrolyte secondary battery having increased energy density. In place of the silicon thin film, silicon powder formed using a binder may also be used.

[0031]

As the non-aqueous electrolyte, a non-aqueous electrolyte including a room temperature molten salt having a melting point of not higher than 60°C and a lithium salt may be used. Room temperature molten salts are liquids containing only ions, having fire-resistance and no vapor pressure. Hence, they are not decomposed or burned even at the time of abnormal operations, such as overcharging, and can be safely used without the provision of a protection circuit or the like.

[0032]

It is necessary for the room temperature molten salt to remain liquid in a broad room temperature range, in general, in the range of -20°C to 60°C. It is desired that the room temperature molten salt have a conductivity of not less than  
5  $10^{-4}$ S/cm.

[0033]

By the addition of a lithium salt, a room temperature molten salt will probably have a lower melting point than the melting point of each of the two types of salts alone, and  
10 these are maintained in a liquid state.

[0034]

As the non-aqueous electrolyte salt, a non-aqueous electrolyte salt including a quaternary ammonium salt and a lithium salt may also be used.

15 [0035]

Further, as the non-aqueous electrolyte salt, a non-aqueous electrolyte salt including a room temperature molten salt having a melting point of not higher than 60°C and a reduction product of elemental sulfur may be used. The  
20 reduction product of elemental sulfur may be obtained by reducing elemental sulfur in a room temperature molten salt having a melting point of not higher than 60°C and an organic electrolyte.

[0036]

As the non-aqueous electrolyte,  $\gamma$ -butyrolactone may also be used.

As the room temperature molten salt, a quaternary ammonium salt or an imidazolium salt may be used, for example.

- 5 Specifically, as the room temperature molten salt, at least one type selected from trimethylpropylammonium bis(trifluoromethylsulfonyl)imide  
 $((\text{CH}_3)_3\text{N}^+(\text{C}_3\text{H}_7)\text{N}^-(\text{SO}_2\text{CF}_3)_2)$ , trimethyloctylammonium bis(trifluoromethylsulfonyl)imide  
10  $((\text{CH}_3)_3\text{N}^+(\text{C}_8\text{H}_{17})\text{N}^-(\text{SO}_2\text{CF}_3)_2)$ , trimethylallylammonium bis(trifluoromethylsulfonyl)imide  
 $((\text{CH}_3)_3\text{N}^+(\text{Allyl})\text{N}^-(\text{SO}_2\text{CF}_3)_2)$ , trimethylhexylammonium bis(trifluoromethylsulfonyl)imide  
 $((\text{CH}_3)_3\text{N}^+(\text{C}_6\text{H}_{13})\text{N}^-(\text{SO}_2\text{CF}_3)_2)$ , trimethylethylammonium  
15 2,2,2-trifluoro-N-(trifluoromethylsulfonyl)acetamide  
 $((\text{CH}_3)_3\text{N}^+(\text{C}_2\text{H}_5)(\text{CF}_3\text{CO})\text{N}^-(\text{SO}_2\text{CF}_3))$ , trimethylallylammonium 2,2,2-trifluoro-N-(trifluoromethylsulfonyl)acetamide  
 $((\text{CH}_3)_3\text{N}^+(\text{Allyl})(\text{CF}_3\text{CO})\text{N}^-(\text{SO}_2\text{CF}_3))$ , trimethylpropylammonium 2,2,2-trifluoro-N-(trifluoromethylsulfonyl)acetamide  
20  $((\text{CH}_3)_3\text{N}^+(\text{C}_3\text{H}_7)(\text{CF}_3\text{CO})\text{N}^-(\text{SO}_2\text{CF}_3))$ , tetraethylammonium 2,2,2-trifluoro-N-(trifluoromethylsulfonyl)acetamide  
 $((\text{C}_2\text{H}_5)_4\text{N}^+(\text{CF}_3\text{CO})\text{N}^-(\text{SO}_2\text{CF}_3))$ , triethylmethylammonium 2,2,2-trifluoro-N-(trifluoromethylsulfonyl)acetamide  
 $((\text{C}_2\text{H}_5)_3\text{N}^+(\text{CH}_3)(\text{CF}_3\text{CO})\text{N}^-(\text{SO}_2\text{CF}_3))$ ,  
25 1-ethyl-3-methylimidazolium

bis(pentafluoroethylsulfonyl)imide

$((C_2H_5)(C_3H_3N_2)^+(CH_3)N^-(SO_2C_2F_5)_2)$ ,

1-ethyl-3-methylimidazolium

bis(trifluoromethylsulfonyl)imide

5  $((C_2H_5)(C_3H_3N_2)^+(CH_3)N^-(SO_2CF_3)_2)$ ,

1-ethyl-3-methylimidazolium tetrafluoroborate

$((C_2H_5)(C_3H_3N_2)^+(CH_3)BF_4^-)$ , 1-ethyl-3-methylimidazolium

pentafluoroborate  $((C_2H_5)(C_3H_3N_2)^+(CH_3)PF_6^-)$ , and the like.

[0037]

10 As the quaternary ammonium salt, instead of the  
above-mentioned quaternary ammonium salt for use as a room  
temperature molten salt, at least one type selected from  
tetramethylammonium tetrafluoroborate  $((CH_3)_4N^+BF_4^-)$ ,  
tetramethylammonium hexafluorophosphate  $((CH_3)_4N^+PF_6^-)$ ,  
15 tetraethylammonium tetrafluoroborate  $((C_2H_5)_4N^+BF_4^-)$ ,  
tetraethylammonium hexafluorophosphate  $((C_2H_5)_4N^+PF_6^-)$ , and  
the like may be use.

[0038]

It is noted that the above-mentioned non-aqueous  
20 electrolyte may include an organic solvent, such as ethylene  
carbonate, diethyl carbonate, dimethyl carbonate, propylene  
carbonate, cyclic ether, chain ether, fluorinated carbonate,  
in addition to the room temperature molten salt or quaternary  
ammonium salt.

25 [0039]

As the cyclic ether, at least one type selected from 1,3-dioxolane, 4-methyl-1,3-dioxolane, tetrahydrofuran, 2-methyl tetrahydrofuran, propylene oxide, 1,2-butylene oxide, 1,4-dioxane, 1,3,5-trioxane, furan, 2-methyl furan, 5 1,8-cineole, crown ether, and the like may be used.

[0040]

As the chain ether, at least one type selected from 1,2-dimethoxyethane, diethyl ether, dipropyl ether, diisopropyl ether, dibutyl ether, dihexyl ether, ethyl vinyl 10 ether, butyl vinyl ether, methyl phenyl ether, ethyl phenyl ether, butyl phenyl ether, pentyl phenyl ether, methoxytoluene, benzyl ethyl ether, diphenyl ether, dibenzyl ether, o-dimethoxybenzene, 1,2-diethoxyethane, 1,2-dibutoxyethane, diethylene glycol dimethyl ether, 15 diethylene glycol diethyl ether, diethylene glycol dibutyl ether, 1,1-dimethoxymethane, 1,1-diethoxyethane, triethylene glycol dimethyl ether, tetraethylene glycol dimethyl ether, and the like may be used. As the fluorinated carbonate, at least one type selected from trifluoropropylene 20 carbonate, fluoroethyl carbonate, and the like may be used.

[0041]

As the lithium salt to be added to the non-aqueous electrolyte, a lithium salt used as an electrolyte in general non-aqueous electrolyte secondary battery may be used. For 25 example, at least one type selected from  $\text{LiBF}_4$ ,  $\text{LiPF}_6$ ,  $\text{LiCF}_3$

$\text{SO}_3$ ,  $\text{LiC}_4\text{F}_9\text{SO}_3$ ,  $\text{LiN}(\text{CF}_3\text{SO}_2)_2$ ,  $\text{LiN}(\text{C}_2\text{F}_5\text{SO}_2)_2$ ,  $\text{LiN}(\text{CF}_3\text{SO}_2)(\text{COCF}_3)$ , and  $\text{LiAsF}_6$  may be used.

[0042]

Another possibility is the gelation of the non-aqueous electrolyte using polyethylene oxide (PEO), for example, for preventing the elution of elemental sulfur to allow the reversible reaction of the elemental sulfur. As the non-aqueous electrolyte, a gelled polymer electrolyte in which a polymer electrolyte such as polyethylene oxide, polyacrylonitrile, or the like is impregnated with an electrolyte salt, or an inorganic solid electrolyte such as  $\text{LiI}$  or  $\text{Li}_3\text{N}$  may also be used.

[0043]

In the non-aqueous electrolyte secondary battery according to the present embodiment, the combination of the positive electrode including elemental sulfur and the negative electrode including silicon that stores lithium allows the elemental sulfur in the positive electrode and the silicon in the negative electrode to react reversibly with the lithium at relatively low temperatures. In this case, high negative electrode capacity can be obtained using silicon that stores lithium. Moreover, the use of elemental sulfur in the positive electrode allows increased capacity per unit weight compared with that obtained using an organic disulfide compound. Consequently, the negative and positive

electrode capacities can be easily balanced, and increased capacity and energy density can be realized.

[0044]

In the case of the non-aqueous electrolyte including a room temperature molten salt having a melting point of not higher than 60°C, a quaternary ammonium salt, a reduction product of elemental sulfur, or  $\gamma$ -butyrolactone, the silicon in the negative electrode and elemental sulfur in the positive electrode easily react reversibly with lithium also at room temperature, and hence the charge-discharge reaction at room temperature can be facilitated.

[0045]

(Examples)

It will now be apparent from the citation of Examples that the non-aqueous electrolyte secondary battery according to the present invention in which elemental sulfur is used for the positive electrode and a silicon material is used for the negative electrode can be appropriately charged/discharged at room temperature, and has much increased energy density. It will be recognized that the following examples merely illustrate the practice of the non-aqueous electrolyte secondary battery in the present invention but are not intended to be limiting thereof. Suitable changes and modifications can be effected without departing the scope of the present invention.



[0046]

In Inventive Examples 1 to 20 and Comparative Examples 1 to 5 described below, the test cell shown in Fig. 1 was prepared to evaluate a positive electrode including sulfur and a negative electrode including a silicon material.

[0047]

As shown in Fig. 1, a non-aqueous electrolyte 14 was poured into a test cell vessel 10, and a working electrode 11 and a reference electrode 13 were immersed in the non-aqueous electrolyte 14.

[0048]

In Inventive Examples 1, 3, 5, 7, 9, 11, 13, 15, 17, 19, and Inventive Examples 1 to 5, positive electrodes including elemental sulfur as active materials were evaluated, whereas in Inventive Examples 2, 4, 6, 8, 10, 12, 14, 16, 18, and 20, negative electrodes made of silicon materials were evaluated.

[0049]

Tables 1 and 2 summarize the compositions of test cells in Inventive Examples 1 to 20 and Comparative Examples 1 to 5.

[0050]

(Table 1)

	working electrode	counter electrode	solute	non-aqueous electrolyte
Inventive example 1	sulfur	Li metal	$\text{LiN}(\text{CF}_3\text{SO}_2)_2$	room temperature molten salt 1(quaternary ammonium salt)
Comparative example 1	sulfur	Li metal	$\text{LiPF}_6$	EC/DEC
Inventive example 2	amorphous silicon thin film	Li metal	$\text{LiN}(\text{CF}_3\text{SO}_2)_2$	room temperature molten salt 1(quaternary ammonium salt)
Inventive example 3	sulfur	Li metal	$\text{LiPF}_6$	fluorinated carbonate 1 : room temperature molten salt 1(quaternary ammonium salt)
Comparative example 2	sulfur	Li metal	$\text{LiPF}_6$	fluorinated carbonate 1
Inventive example 4	amorphous silicon thin film	Li metal	$\text{LiPF}_6$	fluorinated carbonate 1 : room temperature molten salt 1(quaternary ammonium salt)
Inventive example 5	sulfur	Li metal	$\text{LiN}(\text{CF}_3\text{SO}_2)_2$	room temperature molten salt 2(quaternary ammonium salt)
Inventive example 6	amorphous silicon thin film	Li metal	$\text{LiN}(\text{CF}_3\text{SO}_2)_2$	room temperature molten salt 2(quaternary ammonium salt)
Inventive example 7	sulfur	Li metal	$\text{LiN}(\text{CF}_3\text{SO}_2)_2$	room temperature molten salt 3(quaternary ammonium salt)
Inventive example 8	amorphous silicon thin film	Li metal	$\text{LiN}(\text{CF}_3\text{SO}_2)_2$	room temperature molten salt 3(quaternary ammonium salt)
Inventive example 9	sulfur	Li metal	$\text{LiN}(\text{CF}_3\text{SO}_2)_2$	cyclic ether 1 : room temperature molten salt 1(quaternary ammonium salt)=50 : 50
Inventive example 10	amorphous silicon thin film	Li metal	$\text{LiN}(\text{CF}_3\text{SO}_2)_2$	cyclic ether 1 : room temperature molten salt 1(quaternary ammonium salt)=50 : 50

[0051]

(Table 2)

	working electrode	counter electrode	solute	non-aqueous electrolyte
Inventive example 11	sulfur	Li metal	$\text{LiN}(\text{CF}_3\text{SO}_2)_2$	cyclic ether 1 : room temperature molten salt 1(quaternary ammonium salt)=25 : 75
Inventive example 12	amorphous silicon thin film	Li metal	$\text{LiN}(\text{CF}_3\text{SO}_2)_2$	cyclic ether 1 : room temperature molten salt 1(quaternary ammonium salt)=25 : 75
Comparative example 3	sulfur	Li metal	$\text{LiN}(\text{CF}_3\text{SO}_2)_2$	cyclic ether 1
Inventive example 13	sulfur	Li metal	$\text{LiN}(\text{CF}_3\text{SO}_2)_2$	cyclic ether 2 : room temperature molten salt 1(quaternary ammonium salt)=50 : 50
Inventive example 14	amorphous silicon thin film	Li metal	$\text{LiN}(\text{CF}_3\text{SO}_2)_2$	cyclic ether 2 : room temperature molten salt 1(quaternary ammonium salt)=50 : 50
Inventive example 15	sulfur	Li metal	$\text{LiN}(\text{CF}_3\text{SO}_2)_2$	cyclic ether 2 : room temperature molten salt 1(quaternary ammonium salt)=25 : 75
Inventive example 16	amorphous silicon thin film	Li metal	$\text{LiN}(\text{CF}_3\text{SO}_2)_2$	cyclic ether 2 : room temperature molten salt 1(quaternary ammonium salt)=25 : 75
Comparative example 4	sulfur	Li metal	$\text{LiN}(\text{CF}_3\text{SO}_2)_2$	cyclic ether 2
Inventive example 17	sulfur	Li metal	$\text{LiN}(\text{CF}_3\text{SO}_2)_2$	chain ether 1 : room temperature molten salt 1(quaternary ammonium salt)=50 : 50
Inventive example 18	amorphous silicon thin film	Li metal	$\text{LiN}(\text{CF}_3\text{SO}_2)_2$	chain ether 1 : room temperature molten salt 1(quaternary ammonium salt)=50 : 50
Inventive example 19	sulfur	Li metal	$\text{LiN}(\text{CF}_3\text{SO}_2)_2$	chain ether 1 : room temperature molten salt 1(quaternary ammonium salt)=25 : 75
Inventive example 20	amorphous silicon thin film	Li metal	$\text{LiN}(\text{CF}_3\text{SO}_2)_2$	chain ether 1 : room temperature molten salt 1(quaternary ammonium salt)=25 : 75
Comparative example 5	sulfur	Li metal	$\text{LiN}(\text{CF}_3\text{SO}_2)_2$	chain ether 1

[0052]

(Inventive Example 1)

In Inventive Example 1, a non-aqueous electrolyte including a lithium salt,  $\text{LiN}(\text{CF}_3\text{SO}_2)_2$ , dissolved at a concentration of 0.3 mol/l in a room temperature molten salt, trimethylpropylammonium bis(trifluoromethylsulfonyl)imide ( $(\text{CH}_3)_3\text{N}^+(\text{C}_3\text{H}_7)\text{N}^-(\text{SO}_2\text{CF}_3)_2$ ) was used.

[0053]

For a positive electrode, 20% by weight of elemental sulfur, 70% by weight of acetylene black as conductive agent, and 10% by weight of polytetrafluoroethylene as binder were mixed, and the resultant mixture was ground in a mortar for 30 minutes, then pressed in a mold for five seconds under a pressure of  $150 \text{ kg/cm}^2$  to give a disk-shaped material having a diameter of 10.3 mm. This material was wrapped in a net made of aluminum to be used as a positive electrode.

[0054]

As shown in Fig. 1, the above-mentioned non-aqueous electrolyte 14 was poured into the test cell vessel 10, while the above-mentioned positive electrode was used for a working electrode 11, and lithium metal was used for each of a negative electrode as a counter electrode 12 and a reference electrode 13, to prepare a test cell of Inventive Example 1.

[0055]

25 (Comparative Example 1)

In Comparative Example 1, a non-aqueous electrolyte including a lithium salt,  $\text{LiPF}_6$  dissolved at a concentration of 1 mol/l in a mixed solvent of ethylene carbonate (EC) and diethyl carbonate (DEC) at a volume ratio of 1:1 was used. Otherwise, the test cell of Comparative Example 1 was prepared as in the case of the above-mentioned Inventive Example 1. [0056]

(Evaluation 1)

Using the test cell of Inventive Example 1 prepared as shown above, the potential of the active electrode 11 (positive electrode) relative to the reference electrode 13 was scanned starting at an initial potential of 2.9 V (vs.  $\text{Li/Li}^+$ ) in a reduction direction, and then in an oxidation direction for two cycles, at a scan rate of 0.5 mV/s in a scan range of 1.0 to 5.0 V (vs.  $\text{Li/Li}^+$ ), to measure the cyclic voltammetry in each cycle. The results are given in Fig. 2. [0057]

Using the test cell of Comparative Example 1 prepared as shown above, the potential of the active electrode 11 (positive electrode) relative to the reference electrode 13 was scanned starting at an initial potential of 3.0 V (vs.  $\text{Li/Li}^+$ ) in a reduction direction, and then in an oxidation direction for two cycles, at a scan rate of 0.5 mV/s in a scan range of 1.0 to 4.2 V (vs.  $\text{Li/Li}^+$ ), to measure the cyclic voltammetry in each cycle. The results are given in Fig. 3.

[0058]

As a result, in the case of the test cell of Inventive Example 1, an abrupt reduction current began to flow at around 2.3 V or lower (vs.  $\text{Li/Li}^+$ ) during scanning in the reduction direction, and so it is presumed that the elemental sulfur was reduced. In addition, there were oxidation peaks between around 2.6 and 3.9 V (vs.  $\text{Li/Li}^+$ ) during scanning in the oxidation direction, and so it is presumed that the above-mentioned reduced elemental sulfur was oxidized in this potential range. The same result was obtained also in the second cycle. It is therefore presumed that the reversible reaction of elemental sulfur was carried out.

[0059]

In the case of the test cell of Comparative Example 1, a reduction current began to flow at around 2.4 V or lower (vs.  $\text{Li/Li}^+$ ) during scanning in the reduction direction, and so it is presumed that the elemental sulfur was reduced. However, there were no oxidation peaks during scanning in the oxidation direction, and so it is presumed that the above-mentioned reduced elemental sulfur was not oxidized. In addition, a small amount of reduction current flowed at around 2.4 V or lower (vs.  $\text{Li/Li}^+$ ) during scanning in the oxidation direction. This is probably due to the reduction of the residual elemental sulfur that was not reduced in the earlier reaction.

[0060]

The test cell of Inventive Example 1 was discharged to a discharge cutoff potential of 1.0 V (vs. Li/Li<sup>+</sup>) at a discharge current of 0.13 mA/cm<sup>2</sup>, and then charged to a charge cutoff potential of 2.7 V (vs. Li/Li<sup>+</sup>) at a charge current of 0.13 mA/cm<sup>2</sup>, to examine the initial charge-discharge characteristics. The results are given in Fig. 4. Note that the solid line represents a discharge curve showing the relationship between the potential and the capacity per 1g of elemental sulfur during discharging, and the broken line represents a charge curve showing the relationship between the potential and the capacity per 1 g of elemental sulfur during charging.

[0061]

As a result, in the test cell of Inventive Example 1, the initial specific discharge capacity was approximately 654 mAh/g per 1 g of elemental sulfur, which was lower than the theoretical capacity of 1675 mAh/g, but the specific discharge capacity was markedly increased, compared with that of LiCoO<sub>2</sub> used as a general positive electrode. Moreover, the initial specific discharge capacity per 1 g of elemental sulfur exhibited a value as large as approximately 623 mAh/g, and the reversible reaction of elemental sulfur was also proved.

[0062]

Further, with this test cell of Inventive Example 1, the operation of discharging the cell to a discharge cutoff potential of 1.0 V (vs. Li/Li<sup>+</sup>) at a discharge current of 0.13 mA/cm<sup>2</sup>, and then charging the cell to a charge cutoff potential of 2.7 V (vs. Li/Li<sup>+</sup>) at a charge current of 0.13 mA/cm<sup>2</sup> was repeated, to measure the charge capacity Q<sub>a</sub> (mAh/g) and discharge capacity Q<sub>b</sub> (mAh/g) in each cycle, and also find out the charge-discharge efficiency (%) in each cycle in accordance with the following equation. In Fig. 5, the white circle and solid line represent the discharge capacity (mAh/g) in each cycle, and the triangle and broken line represent the charge-discharge efficiency (%) in each cycle. [0063]

$$\text{Charge-discharge efficiency} = (Q_b/Q_a) \times 100$$

As a result, in this test cell of Inventive Example 1, the specific discharge capacities in the third cycle and thereafter were kept constant at approximately 490 mAh/g, and the charge-discharge efficiencies were also kept constant at approximately 100%.

[0064]

It is noted that in the test cell of Inventive Example 1, the average discharge voltage was approximately 2 V and the energy density per 1 g of elemental sulfur was approximately 980 mWh/g. The energy density was markedly increased, compared with the energy density per 1g of LiCoO<sub>2</sub>



(approximately 540 mWh/g) used as a general positive electrode.

[0065]

(Inventive Example 2)

5 In Inventive Example 2, the same non-aqueous electrolyte as that in the above-mentioned Inventive Example 1 was used. As a working electrode 11, an amorphous silicon thin film formed by sputtering on a copper foil having an electrolytically treated surface and formed into a 2 cm x 2  
10 cm size was used.

[0066]

A DC pulse sputtering apparatus was used. An argon (Ar) gas was used for atmospheric gas, and a 99.999% single silicon crystal for a target. The flow rate of the argon gas was set  
15 to 60 sccm, and the pressure of the sputtering atmosphere was set to  $2 \times 10^{-1}$  Pa. The electric power of sputtering was set to 2000 W ( $6.7 \text{ W/cm}^2$ .)

[0067]

The initial substrate temperature was set to 25°C. The  
20 maximum temperature was approximately 100°C.

[0068]

As shown in Fig. 1, the above-mentioned non-aqueous electrolyte 14 was poured into the test cell vessel 10, while the above-mentioned working electrode 11 was used, and  
25 lithium metal was used for each of a counter electrode 12 and

a reference electrode 13, to prepare a test cell of Inventive Example 2.

[0069]

(Evaluation 1)

5       The test cell of Inventive Example 2 was discharged to a discharge cutoff potential of 0.0 V (vs.  $\text{Li/Li}^+$ ) at a discharge current of  $0.05 \text{ mA/cm}^2$ , and then charged to a charge cutoff potential of 2.0 V (vs.  $\text{Li/Li}^+$ ) at a charge current of  $0.05 \text{ mA/cm}^2$ , to examine the initial charge-discharge  
10 characteristics. The results are given in Fig. 6. Note that the solid line represents a charge curve showing the relationship between the potential and the active material per 1g of elemental sulfur during charging, and the broken line represents a discharge curve showing the relationship  
15 between the potential and the active material per 1 g of elemental sulfur during discharging.

[0070]

As a result, in the test cell of Inventive Example 2, the initial specific charge and discharge capacities per 1  
20 g of the active material were approximately 3417 mAh/g and 2989 mAh/g, respectively. The specific charge/discharge capacity was markedly increased, compared with that of a carbon material used as a general negative electrode. Moreover, the reversible reaction of elemental sulfur was  
25 also proved.

[0071]

Further, with this test cell of Inventive Example 2, the operation of charging the cell to a charge cutoff potential of 0.0 V (vs. Li/Li<sup>+</sup>) at a charge current of 0.05 mA/cm<sup>2</sup>, and  
5 then discharging the cell to a discharge cutoff potential of 2.0 V (vs. Li/Li<sup>+</sup>) at a discharge current of 0.05 mA/cm<sup>2</sup> was repeated, to measure the charge capacity Q<sub>a</sub> (mAh/g) and discharge capacity Q<sub>b</sub> (mAh/g) in each cycle, and also find out the charge-discharge efficiency (%) in each cycle in  
10 accordance with the above-mentioned equation. In Fig. 7, the white circle and solid line represent the discharge capacity (mAh/g) in each cycle, and the triangle and broken line represent the charge-discharge efficiency (%) in each cycle.  
[0072]

15 As a result, in this test cell of Inventive Example 2, the discharge capacities in the third cycle and thereafter were kept constant at approximately 3243 mAh/g, and the charge-discharge efficiencies were also kept constant at approximately 94%.

20 [0073]

(Inventive Example 3)

In Inventive Example 3, a non-aqueous electrolyte including a lithium salt, LiPF<sub>6</sub> dissolved at a concentration of 1 mol/l in a mixed solvent of tetrafluoropropylene

carbonate and a quaternary ammonium salt,  
trimethylpropylammonium bis(trifluoromethylsulfonyl)imide  
( $(\text{CH}_3)_3\text{N}^+(\text{C}_3\text{H}_7)\text{N}^-(\text{SO}_2\text{CF}_3)_2$ ) at a volume ratio of 1:1 was used.  
Otherwise, test cell of Inventive Example 3 was prepared as  
5 in the case of the above-mentioned Inventive Example 1.

[0074]

(Comparative Example 2)

In Comparative Example 2, a non-aqueous electrolyte  
including a lithium salt,  $\text{LiPF}_6$  dissolved at a concentration  
10 of 1 mol/l in tetrafluoropropylene carbonate was used.  
Otherwise, the test cell of Comparative Example 2 was prepared  
as in the case of the above-mentioned Inventive Example 1.

[0075]

(Evaluation 3)

15 Using each of the test cells of Inventive Example 3 and  
Comparative Example 2 thus prepared, the electrode 11  
relative to the reference electrode 13 was scanned starting  
at an initial potential of 3.34 V (vs.  $\text{Li}/\text{Li}^+$ ) in a reduction  
direction, and then in an oxidation direction, at a scan rate  
20 of 1.0 mV/s in a scan range of 1.0 to 4.7 V (vs.  $\text{Li}/\text{Li}^+$ ), to  
measure the cyclic voltammetry in each cycle. The scanning  
operations were performed for four cycles in the test cell  
of Inventive Example 3, and for three cycles in the test cell  
of Comparative Example 2. The results of the test cell of

Inventive Example 3 are given in Fig. 8, and the results of the test cell of Comparative Example 2 are given in Fig. 9.  
[0076]

As a result, in the case of the test cell of Inventive  
5 Example 3, a reduction current began to flow at around 2.3 V or lower (vs.  $\text{Li/Li}^+$ ) during scanning in the reduction direction, and so it is presumed that elemental sulfur was reduced. In addition, there were oxidation peaks between 2.0 and 3.0 V (vs.  $\text{Li/Li}^+$ ) during scanning in the oxidation  
10 direction, and so it is presumed that the above-mentioned reduced elemental sulfur was oxidized in this potential range. The same result was obtained also in the second cycle. It is therefore presumed that the reversible reaction of elemental sulfur was carried out.

15 [0077]

In the case of the test cell of Comparative Example 2, a reduction current began to flow at around 2.2 V or lower (vs.  $\text{Li/Li}^+$ ) during scanning in the reduction direction, and so it is presumed that the elemental sulfur was reduced.  
20 However, there was an oxidation peak around 4.0 V (vs.  $\text{Li/Li}^+$ ) during scanning in the oxidation direction, and the energy efficiency was very poor. In the second cycle and thereafter, the oxidation peaks and the reduction currents abruptly decreased in size, and the resultant reversibility was poor.

25 [0078]

The discharge potential of elemental sulfur given by the results of the above-mentioned test cell of Inventive Example 3 was approximately 2.0 V (vs. Li/Li<sup>+</sup>), and the energy density of elemental sulfur converted from the theoretical specific capacity of 1675 mAh/g was 3350 Wh/g. The energy density was  
5 markedly increased, compared with that of LiCoO<sub>2</sub> (approximately 540 mWh/g) used in a general positive electrode.

[0079]

10 (Inventive Example 4)

In Inventive Example 4, the same non-aqueous electrolyte as that in the above-mentioned Inventive Example 3 was used. Otherwise, the test cell of Example 3 was prepared as in the case of the above-mentioned Inventive Example 2.

15 [0080]

(Evaluation 4)

The test cell of Inventive Example 4 was charged to a charge cutoff potential of 0.0 V (vs. Li/Li<sup>+</sup>) at a charge current of 0.05 mA/cm<sup>2</sup>, and then discharged to a discharge  
20 cutoff potential of 2.0 V (vs. Li/Li<sup>+</sup>) at a discharge current of 0.05 mA/cm<sup>2</sup>, to examine the initial charge-discharge characteristics. The results are given in Fig.10. Note that the solid line represents a discharge curve showing the relationship between the potential and the capacity per 1 g  
25 of active material during charging, and the broken line

represents a charge curve showing the relationship between the potential and capacity per 1 g of active material during discharging.

[0081]

5       As a result, in the test cell of Inventive Example 4, the initial specific charge and discharge capacities per 1 g of the active material were approximately 3417 mAh/g and 2989 mAh/g, respectively. The specific charge/discharge capacity was markedly increased, compared with that of a  
10 carbon material used in a general negative electrode. Moreover, the reversible reaction of the silicon thin film was also proved.

[0082]

15       Further, with this test cell of Inventive Example 4, the operation of charging the cell to a charge cutoff potential of 0.0 V (vs. Li/Li<sup>+</sup>) at a charge current of 0.05 mA/cm<sup>2</sup>, and then discharging the cell to a discharge cutoff potential of 2.0 V (vs. Li/Li<sup>+</sup>) at a discharge current of 0.05 mA/cm<sup>2</sup> was repeated, to measure the charge capacity  $Q_a$  (mAh/g) and  
20 discharge capacity  $Q_b$  (mAh/g) in each cycle, and also find out the charge-discharge efficiency (%) in each cycle in accordance with the above-mentioned equation. In Fig. 11, the white circle and solid line represent the specific discharge capacity (mAh/g) in each cycle, and the triangle

and broken line represent the charge-discharge efficiency (%) in each cycle.

[0083]

As a result, in the test cell of Inventive Example 4,  
5 the specific discharge capacities in the third cycle and thereafter were kept constant at approximately 3243 mAh/g, and the charge-discharge efficiencies were also kept constant at approximately 94%.

[0084]

10 (Inventive Example 5)

In Inventive Example 5, a non-aqueous electrolyte including a lithium salt,  $\text{LiN}(\text{CF}_3\text{SO}_2)_2$  dissolved at a concentration of 0.5 mol/l in a room temperature molten salt, triethylmethylammonium

15 2,2,2-trifluoro-N-(trifluoromethylsulfonyl)acetamide

( $(\text{C}_2\text{H}_5)_3\text{N}^+(\text{CH}_3)(\text{CF}_3\text{CO})\text{N}^-(\text{SO}_2\text{CF}_3)$ ) was used. Otherwise, the test cell of Example 5 was prepared as in the case of the above-mentioned Inventive Example 1.

[0085]

20 (Evaluation 5)

Using the test cell of Inventive Example 5 thus prepared, the potential of the active electrode 11 relative to the reference electrode 13 was scanned starting at an initial potential of 3.0 V (vs.  $\text{Li}/\text{Li}^+$ ) in a reduction  
25 direction, and then in an oxidation direction for three



cycles, at a scan rate of 1.0 mV/s in a scan range of 1.0 to 4.7 V (vs. Li/Li<sup>+</sup>), to measure the cyclic voltammetry in each cycle. The results are given in Fig. 12.

[0086]

5        As a result, in the case of the test cell of Inventive Example 5, a reduction current began to flow at around 2.3 V or lower (vs. Li/Li<sup>+</sup>) during scanning in the reduction direction, and so it is presumed that elemental sulfur was reduced. In addition, there was an oxidation peak around 3.8  
10 V (vs. Li/Li<sup>+</sup>) during scanning in the oxidation direction, and so it is presumed that the above-mentioned reduced elemental sulfur was oxidized at around this potential. The same results were obtained also in the second cycle and thereafter. It is therefore presumed that the reversible  
15 reaction of elemental sulfur was carried out.

[0087]

      The test cell of Inventive Example 5 was discharged to a discharge cutoff potential of 1.0 V (vs. Li/Li<sup>+</sup>) at a discharge current of 0.13 mA/cm<sup>2</sup>, and then charged to a charge  
20 cutoff potential of 3.5 V (vs. Li/Li<sup>+</sup>) at a charge current of 0.13 mA/cm<sup>2</sup>, to examine the initial charge-discharge characteristics. The results are given in Fig. 13. Note that the solid line represents a discharge curve showing the relationship between the potential and the capacity per 1g  
25 of elemental sulfur during discharging, and the broken line

represents a charge curve showing the relationship between the potential and the capacity per 1 g of elemental sulfur during charging.

[0088]

5       As a result, in the test cell of Inventive Example 5, the initial specific discharge capacity per 1 g of elemental sulfur was approximately 1138 mAh/g. The specific discharge capacity was markedly increased, compared with that of  $\text{LiCoO}_2$  used in a general positive electrode.

10   [0089]

(Inventive Example 6)

In Inventive Example 6, the same non-aqueous electrolyte as that in the above-mentioned Inventive Example 5 was used. Otherwise, the test cell of Example 6 was prepared  
15 as in the case of the above-mentioned Inventive Example 2.

[0090]

(Evaluation 6)

Using the test cell of Inventive Example 6 thus prepared, the potential of the active electrode 11 relative  
20 to the reference electrode 13 was scanned starting at an initial potential of 2.6 V (vs.  $\text{Li/Li}^+$ ) in a reduction direction, and then in an oxidation direction for three cycles, at a scan rate of 1.0 mV/s in a scan range of 0.0 to 2.75 V (vs.  $\text{Li/Li}^+$ ), to measure the cyclic voltammetry in each  
25 cycle. The results are given in Fig. 14.

[0091]

As a result, in the case of the test cell of Example 6, there was a reduction peak around 0.03 V (vs. Li/Li<sup>+</sup>) during scanning in the reduction direction, and there was an  
5 oxidation peak around 0.7 V (vs. Li/Li<sup>+</sup>) during scanning in the oxidation direction. It is presumed that insertion/release of lithium into/from silicon occurred at around this potential. The same results were obtained in the second cycle and thereafter, and so it is presumed that the  
10 reversible reaction of silicon with lithium was carried out.

[0092]

(Inventive Example 7)

In Inventive Example 7, a non-aqueous electrolyte including a lithium salt, LiN(CF<sub>3</sub>SO<sub>2</sub>)<sub>2</sub> dissolved at a  
15 concentration of 0.5 mol/l in a room temperature molten salt, trimethylhexylammonium bis(trifluoromethylsulfonyl)imide ((CH<sub>3</sub>)<sub>3</sub>N<sup>+</sup>(C<sub>6</sub>H<sub>13</sub>)N<sup>-</sup>(SO<sub>2</sub>CF<sub>3</sub>)<sub>2</sub>) was used. Otherwise, the test cell of Inventive Example 7 was prepared as in the case of the above-mentioned test cell of Inventive Example 1.

20 [0093]

(Evaluation 7)

Using the test cell of Inventive Example 7 thus prepared, the potential of the active electrode 11 relative to the reference electrode 13 was scanned starting at an  
25 initial potential of 2.8 V (vs. Li/Li<sup>+</sup>) in a reduction

direction, and then in an oxidation direction for three cycles, at a scan rate of 1.0 mV/s in a scan range of 1.0 to 4.7 V (vs. Li/Li<sup>+</sup>), to measure the cyclic voltammetry in each cycle. The results are given in Fig. 15.

5 [0094]

As a result, in the case of the test cell of Inventive Example 7, a reduction current began to flow at around 2.3 V or lower (vs. Li/Li<sup>+</sup>) during scanning in the reduction direction, and so it is presumed that the elemental sulfur  
10 was reduced. In addition, there was an oxidation peak around 2.6 V (vs. Li/Li<sup>+</sup>) during scanning in the oxidation direction, and so it is presumed that the above-mentioned reduced elemental sulfur was oxidized at around this potential. The same results were obtained also in the second cycle and  
15 thereafter. It is therefore presumed that the reversible reaction of elemental sulfur was carried out.

[0095]

Further, the test cell of Inventive Example 7 was discharged to a discharge cutoff potential of 1.0 V (vs. Li/Li<sup>+</sup>) at a discharge current of 0.13 mA/cm<sup>2</sup>, and then charged  
20 to a charge cutoff potential of 3.5 V (vs. Li/Li<sup>+</sup>) at a charge current of 0.13 mA/cm<sup>2</sup>, to examine the initial charge-discharge characteristics. The results are given in Fig. 16. Note that the solid line represents a discharge curve  
25 showing the relationship between the potential and the

capacity per 1g of elemental sulfur during discharging, and the broken line represents a charge curve showing the relationship between the potential and the capacity per 1 g of elemental sulfur during charging.

5 [0096]

As a result, in the test cell of Example 7, the initial specific discharge capacity per 1 g of elemental sulfur was 588 mAh/g, and the specific discharge capacity was markedly increased, compared with that of  $\text{LiCoO}_2$  used in a general positive electrode.

[0097]

(Inventive Example 8)

In Inventive Example 8, the same non-aqueous electrolyte as that in the above-mentioned Inventive Example 7 was used. Otherwise, the test cell of Example 8 was prepared as in the case of the above-mentioned Inventive Example 2.

[0098]

(Evaluation 8)

The test cell of Inventive Example 8 was charged to a charge cutoff potential of 0.0 V (vs.  $\text{Li/Li}^+$ ) at a charge current of  $0.05 \text{ mA/cm}^2$ , and then discharged to a discharge cutoff potential of 2.0 V (vs.  $\text{Li/Li}^+$ ) at a discharge current of  $0.05 \text{ mA/cm}^2$ , to examine the initial charge-discharge characteristics. The results are given in Fig.17. Note that the solid line represents a discharge curve showing the

relationship between the potential and the capacity per 1 g of active material during charging, and the broken line represents a charge curve showing the relationship between the potential and capacity per 1 g of active material during  
5 discharging.

[0099]

As a result, in the test cell of Example 8, the initial specific charge and discharge capacities per 1 g of active material were 3417 mAh/g and 2989 mAh/g, respectively. The  
10 specific charge/discharge capacity was markedly increased, compared with that of a carbon material used in a general positive electrode. Moreover, the reversible reaction of the silicon thin film was also proved.

[0100]

15 Further, with the test cell of Inventive Example 8, the operation of charging the cell to a charge cutoff potential of 0.0 V (vs. Li/Li<sup>+</sup>) at a charge current of 0.05 mA/cm<sup>2</sup>, and then discharging the cell to a discharge cutoff potential of 2.0 V (vs. Li/Li<sup>+</sup>) at a discharge current of 0.05 mA/cm<sup>2</sup> was  
20 repeated, to measure the charge capacity  $Q_a$  (mAh/g) and discharge capacity  $Q_b$  (mAh/g) in each cycle, and also find out the charge-discharge efficiency (%) in each cycle in accordance with the above-mentioned equation. In Fig. 18, the white circle and solid line represent the discharge  
25 capacity (mAh/g) in each cycle, and the triangle and broken

line represent the charge-discharge efficiency (%) in each cycle.

[0101]

As a result, in the test cell of Inventive Example 8,  
5 the specific discharge capacities in the third cycle and thereafter were kept constant at approximately 3243 mAh/g, and the charge-discharge efficiencies were also kept constant at approximately 94%.

[0102]

10 (Inventive Example 9)

In Inventive Example 9, a non-aqueous electrolyte including a lithium salt, or  $\text{LiN}(\text{CF}_3\text{SO}_2)_2$  dissolved at a concentration of 0.5 mol/l in a mixture of 50% by volume of 1,3-dioxolane and 50% by volume of trimethylpropylammonium  
15 bis (trifluoromethylsulfonyl)imide  
 $((\text{CH}_3)_3\text{N}^+(\text{C}_3\text{H}_7)\text{N}^-(\text{SO}_2\text{CF}_3)_2)$  was used. Otherwise, the test cell of Inventive Example 9 was prepared as in the case of the above-mentioned Inventive Example 1.

[0103]

20 (Evaluation 9)

Using the test cell of Inventive Example 9 thus prepared, the potential of the active electrode 11 relative to the reference electrode 13 was scanned starting at an initial potential of 2.4 V (vs.  $\text{Li}/\text{Li}^+$ ) in a reduction  
25 direction, and then in an oxidation direction for three

cycles, at a scan rate of 1.0 mV/s in a scan range of 1.0 to 3.0 V (vs. Li/Li<sup>+</sup>), to measure the cyclic voltammetry in each cycle. The results are given in Fig. 19.

[0104]

5        As a result, in the case of the test cell of Inventive Example 9, a reduction current began to flow at around 2.3 V or lower (vs. Li/Li<sup>+</sup>) during scanning in the reduction direction, and so it is presumed that elemental sulfur was reduced. In addition, there was an oxidation peak around 2.6  
10 V (vs. Li/Li<sup>+</sup>) during scanning in the oxidation direction, and so it is presumed that the above-mentioned reduced elemental sulfur was oxidized at around this potential. The same results were obtained also in the second cycle and thereafter. It is therefore presumed that the reversible  
15 reaction of elemental sulfur was carried out.

[0105]

      The test cell of Inventive Example 9 was discharged to a discharge cutoff potential of 1.0 V (vs. Li/Li<sup>+</sup>) at a discharge current of 0.13 mA/cm<sup>2</sup>, and then charged to a charge  
20 cutoff potential of 3.0 V (vs. Li/Li<sup>+</sup>) at a charge current of 0.13 mA/cm<sup>2</sup>, to examine the initial charge-discharge characteristics. The results are given in Fig. 20. Note that the solid line represents a discharge curve showing the relationship between the potential and the capacity per 1 g  
25 of elemental sulfur during discharging, and the broken line



represents a charge curve showing the relationship between the potential and capacity per 1 g of elemental sulfur during charging.

[0106]

5           As a result, in the test cell of Inventive Example 9, the initial specific discharge capacity per 1 g of elemental sulfur was 2230 mAh/g. The specific discharge capacity was markedly increased, compared with that of  $\text{LiCoO}_2$  used in a general positive electrode. Further, the mixture of

10 1,3-dioxolane and trimethylpropylammonium bis (trifluoromethylsulfonyl)imide  $((\text{CH}_3)_3\text{N}^+(\text{C}_3\text{H}_7)\text{N}^-(\text{SO}_2\text{CF}_3)_2)$  increases the specific capacities at around 2.0 V or higher during discharging, compared with that obtained using 1,3-dioxolane alone, and the specific discharge capacity was  
15 also greater than that obtained using trimethylpropylammonium bis (trifluoromethylsulfonyl)imide  $((\text{CH}_3)_3\text{N}^+(\text{C}_3\text{H}_7)\text{N}^-(\text{SO}_2\text{CF}_3)_2)$  alone as an electrolyte, as shown in Inventive Example 1.

[0107]

20           (Inventive Example 10)

In Inventive Example 10, the same non-aqueous electrolyte as that in the above-mentioned Inventive Example 9 was used. Otherwise, the test cell in Inventive Example 10 was prepared as in the case of the test cell of the  
25 above-mentioned Inventive Example 2.

[0108]

(Evaluation 10)

The test cell of Inventive Example 10 was charged to a charge cutoff potential of 0.0 V (vs. Li/Li<sup>+</sup>) at a charge  
5 current of 0.05 mA/cm<sup>2</sup>, and then discharged to a discharge cutoff potential of 2.0 V (vs. Li/Li<sup>+</sup>) at a discharge current of 0.05 mA/cm<sup>2</sup>, to examine the initial charge-discharge characteristics. The results are given in Fig. 21. Note that the solid line represents a discharge curve showing the  
10 relationship between the potential and the capacity per 1 g of active material during charging, and the broken line represents a charge curve showing the relationship between the potential and the capacity per 1 g of active material during discharging.

15 [0109]

As a result, in the test cell of Inventive Example 10, the initial specific charge and discharge capacities per 1 g of active material were approximately 3417 mAh/g and 2989 mAh/g, respectively. The specific charge/discharge capacity  
20 was markedly increased, compared with that of a carbon material used in a general positive electrode. The reversible reaction of the silicon thin film was also proved.

[0110]

Further, with this test cell of Inventive Example 10,  
25 the operation of charging the cell to a charge cutoff

potential of 0.0 V (vs. Li/Li<sup>+</sup>) at a charge current of 0.05 mA/cm<sup>2</sup>, and then discharging the cell to a discharge cutoff potential of 2.0 V (vs. Li/Li<sup>+</sup>) at a discharge current of 0.05 mA/cm<sup>2</sup> was repeated, to measure the charge capacity Q<sub>a</sub> (mAh/g) and discharge capacity Q<sub>b</sub> (mAh/g) in each cycle, and also find out the charge-discharge efficiency (%) in each cycle in accordance with the above-mentioned equation. In Fig. 22, the white circle and solid line represent the discharge capacity (mAh/g) in each cycle, and the triangle and broken line represent the charge-discharge efficiency (%) in each cycle.

[0111]

As a result, in the test cell in Inventive Example 10, the specific discharge capacities in the third cycle and thereafter were kept constant at approximately 3243 mAh/g, and the charge/discharge efficiencies were also kept constant at approximately 94%.

[0112]

(Inventive Example 11)

In Inventive Example 11, a non-aqueous electrolyte including a lithium salt, LiN(CF<sub>3</sub>SO<sub>2</sub>)<sub>2</sub> dissolved at a concentration of 0.5 mol/l in a mixture of 25% by volume of 1,3-dioxolane and 75% by volume of trimethylpropylammonium bis(trifluoromethylsulfonyl)imide ((CH<sub>3</sub>)<sub>3</sub>N<sup>+</sup>(C<sub>3</sub>H<sub>7</sub>)N<sup>-</sup>(SO<sub>2</sub>CF<sub>3</sub>)<sub>2</sub>) was used. Otherwise, the test cell

of Inventive Example 11 was prepared as in the case of the above-mentioned Inventive Example 1.

[0113]

(Evaluation 11)

5        Using the test cell of Inventive Example 11 thus prepared, the potential of the active electrode 11 relative to the reference electrode 13 was scanned starting at an initial potential of 2.4 V (vs.  $\text{Li/Li}^+$ ) in a reduction direction, and then in an oxidation direction for three  
10 cycles, at a scan rate of 1.0 mV/s in a scan range of 1.0 to 3.3 V (vs.  $\text{Li/Li}^+$ ), to measure the cyclic voltammetry in each cycle. The results are given in Fig. 23.

[0114]

As a result, in the case of the test cell of Inventive  
15 Example 11, a reduction peak appeared at around 1.9 V (vs.  $\text{Li/Li}^+$ ) during scanning in the reduction direction, and so it is presumed that the elemental sulfur was reduced. In addition, an oxidation peak appeared around 2.4 V (vs.  $\text{Li/Li}^+$ ) during scanning in the oxidation direction, and so it is  
20 presumed that the above-mentioned reduced elemental sulfur was oxidized at around this potential. Also in the second cycle and thereafter, there were reduction peaks at around 1.5 V (vs.  $\text{Li/Li}^+$ ) during scanning in the reduction direction, and oxidation peaks at around 2.4 V (vs.  $\text{Li/Li}^+$ ) during  
25 scanning in the oxidation direction. It is therefore presumed

that the reversible reaction of elemental sulfur was carried out.

[0115]

Further, the test cell of Inventive Example 11 was  
5 discharged to a discharge cutoff potential of 1.0 V (vs. Li/Li<sup>+</sup>) at a discharge current of 0.13 mA/cm<sup>2</sup>, and then charged to a charge cutoff potential of 3.0 V (vs. Li/Li<sup>+</sup>) at a charge current of 0.13 mA/cm<sup>2</sup>, to examine the initial charge-discharge characteristics. The results are given in  
10 Fig.24. Note that the solid line represents a discharge curve showing the relationship between the potential and the capacity per 1 g of elemental sulfur during discharging, and the broken line represents a charge curve showing the relationship between the potential and the capacity per 1 g  
15 of elemental sulfur during charging.

[0116]

As a result, in the test cell of Inventive Example 11, the initial specific discharge capacity per 1 g of elemental sulfur was 2291 mAh/g, and the specific discharge capacity  
20 was markedly increased, compared with that of LiCoO<sub>2</sub> used in a general positive electrode. Further, the mixture of 1,3-dioxolane and trimethylpropylammonium bis(trifluoromethylsulfonyl)imide  
((CH<sub>3</sub>)<sub>3</sub>N<sup>+</sup>(C<sub>3</sub>H<sub>7</sub>)N<sup>-</sup>(SO<sub>2</sub>CF<sub>3</sub>)<sub>2</sub>) increased the capacity at around  
25 2.0 V or higher (vs. Li/Li<sup>+</sup>) during discharging, compared with

that obtained using 1,3-dioxolane alone as an electrolyte, as shown in Comparative Example 3 below, and the specific discharge capacity was also greater than that obtained using trimethylpropylammonium bis(trifluoromethylsulfonyl)imide  
5  $((\text{CH}_3)_3\text{N}^+(\text{C}_3\text{H}_7)\text{N}^-(\text{SO}_2\text{CF}_3)_2)$  alone as an electrolyte, as shown in Inventive Example 1.

[0117]

(Inventive Example 12)

In Inventive Example 12, the same non-aqueous  
10 electrolyte as that in the above-mentioned Inventive Example 11 was used. Otherwise, the test cell of Inventive Example 12 was prepared as in the case of the above-mentioned Inventive Example 2.

[0118]

15 (Evaluation 12)

The test cell of Inventive Example 12 was charged to a charge cutoff potential of 0.0 V (vs.  $\text{Li}/\text{Li}^+$ ) at a charge current of  $0.05 \text{ mA}/\text{cm}^2$ , and then discharged to a discharge cutoff potential of 2.0 V (vs.  $\text{Li}/\text{Li}^+$ ) at a discharge current  
20 of  $0.05 \text{ mA}/\text{cm}^2$ , to examine the initial charge-discharge characteristics. The results are given in Fig. 25. Note that the solid line represents a discharge curve showing the relationship between the potential and the capacity per 1 g of active material during charging, and the broken line  
25 represents a charge curve showing the relationship between

the potential and the capacity per 1 g of active material during discharging.

[0119]

As a result, in this test cell of Inventive Example 12,  
5 the initial specific charge and discharge capacities per 1 g of active material were approximately 3417 mAh/g and 2989 mAh/g, respectively. The specific charge/discharge capacity was markedly increased, compared with that of a carbon material used in a general negative electrode. The reversible  
10 reaction of the silicon thin film was also proved.

[0120]

Further, with the test cell of Inventive Example 12, the operation of charging the cell to a charge cutoff potential of 0.0 V (vs. Li/Li<sup>+</sup>) at a charge current of 0.05 mA/cm<sup>2</sup>, and  
15 then discharging the cell to a discharge cutoff potential of 2.0 V (vs. Li/Li<sup>+</sup>) at a discharge current of 0.05 mA/cm<sup>2</sup> was repeated, to measure the charge capacity Q<sub>a</sub> (mAh/g) and discharge capacity Q<sub>b</sub> (mAh/g) in each cycle, and also find out the charge-discharge efficiency (%) in each cycle in  
20 accordance with the above-mentioned equation. In Fig. 26, the solid line and white circle represent the discharge capacity (mAh/g) in each cycle, and the broken line and triangle represent the charge-discharge efficiency (%) in each cycle.

25 [0121]

As a result, in this test cell of Inventive Example 12, the specific discharge capacities in the third cycle and thereafter were kept constant at approximately 3243 mAh/g, and the charge-discharge efficiencies were also kept constant  
5 at approximately 94%.

[0122]

(Comparative Example 3)

In Comparative Example 3, a non-aqueous electrolyte including a lithium salt,  $\text{LiN}(\text{CF}_3\text{SO}_2)_2$  dissolved at a  
10 concentration of 0.5 mol/l in 1,3-dioxolane was used. Otherwise, the test cell of Comparative Example 3 was prepared as in the case of the above-mentioned Inventive Example 1.

[0123]

(Evaluation 13)

15 Using the test cell of Comparative Example 3 thus prepared, the potential of the active electrode 11 relative to the reference electrode 13 was scanned starting at an initial potential of 2.2 V (vs.  $\text{Li}/\text{Li}^+$ ) in a reduction direction, and then in an oxidation direction for three  
20 cycles, at a scan rate of 1.0 mV/s in a scan range of 1.0 to 3.0 V (vs.  $\text{Li}/\text{Li}^+$ ), to measure the cyclic voltammetry in each cycle. The results are given in Fig. 27.

[0124]

As a result, in the case of the test cell of Comparative  
25 Example 3, a reduction peak appeared at around 1.8 V (vs.



Li/Li<sup>+</sup>) during scanning in the reduction direction, and a large reduction current flowed at around 1.2 V or lower (vs. Li/Li<sup>+</sup>). It is thus presumed that the elemental sulfur was reduced. In addition, there was an oxidation peak at around 2.6 V (vs. Li/Li<sup>+</sup>) during scanning in the oxidation direction, and so it is presumed that the above-mentioned reduced elemental sulfur was oxidized at around this potential.

[0125]

The test cell of Comparative Example 3 was discharged to a discharge cutoff potential of 1.0 V (vs. Li/Li<sup>+</sup>) at a discharge current of 0.13 mA/cm<sup>2</sup>, and then charged to a charge cutoff potential of 3.0 V (vs. Li/Li<sup>+</sup>) at a charge current of 0.13 mA/cm<sup>2</sup>, to examine the initial charge-discharge characteristics. The results are given in Fig. 28.

[0126]

Note that the solid line represents a discharge curve showing the relationship between the potential and the capacity per 1 g of elemental sulfur during discharging, and the broken line represents a charge curve showing the relationship between the potential and the capacity per 1 g of elemental sulfur during charging.

[0127]

As a result, in this test cell of Comparative Example 3, the initial specific discharge capacity per 1 g of elemental sulfur was 1677 mAh/g. The specific discharge

capacity was markedly increased, compared with that of  $\text{LiCoO}_2$  used in a general positive electrode, while the discharge potential was as low as approximately 1.2 V (vs.  $\text{Li/Li}^+$ ).

[0128]

5 (Evaluation 14)

The mixture of trimethylpropylammonium bis(trifluoromethylsulfonyl)imide  $((\text{CH}_3)_3\text{N}^+(\text{C}_3\text{H}_7)\text{N}^-(\text{SO}_2\text{CF}_3)_2)$  and 1,3-dioxolane has reduced viscosity in the electrolyte, compared with the electrolyte

10 containing only trimethylpropylammonium

bis(trifluoromethylsulfonyl)imide

$((\text{CH}_3)_3\text{N}^+(\text{C}_3\text{H}_7)\text{N}^-(\text{SO}_2\text{CF}_3)_2)$ . Accordingly, the mixture is preferable for use as an electrolyte.

[0129]

15 (Evaluation 15)

The results of Inventive Examples 1, 9, 11, and Comparative Example 3 show that in the use of a positive electrode including elemental sulfur, it is more preferable to mix trimethylpropylammonium

20 bis(trifluoromethylsulfonyl)imide

$((\text{CH}_3)_3\text{N}^+(\text{C}_3\text{H}_7)\text{N}^-(\text{SO}_2\text{CF}_3)_2)$  with 1,3-dioxolane than to use 1,3-dioxolane or trimethylpropylammonium

bis(trifluoromethylsulfonyl)imide

$((\text{CH}_3)_3\text{N}^+(\text{C}_3\text{H}_7)\text{N}^-(\text{SO}_2\text{CF}_3)_2)$  alone, when comparing the specific  
25 discharge capacities at around 2 V or higher (vs.  $\text{Li/Li}^+$ )

during discharging. The 1,3-dioxolane may be set in the range of 0.1 to 99.9% by volume. Preferably, the ratio of 1,3-dioxolane may be set in the range of 0.1 to 50% by volume, more preferably in the range of 0.1 to 25% by volume.

5 [0130]

(Inventive Example 13)

In Inventive Example 13, a non-aqueous electrolyte including a lithium salt,  $\text{LiN}(\text{CF}_3\text{SO}_2)_2$  dissolved at a concentration of 0.5 mol/l in a mixture of 50% by volume of tetrahydrofuran and 50% by volume of trimethylpropylammonium bis(trifluoromethylsulfonyl)imide  
10  $((\text{CH}_3)_3\text{N}^+(\text{C}_3\text{H}_7)\text{N}^-(\text{SO}_2\text{CF}_3)_2)$  was used. Otherwise, the test cell of Inventive Example 13 was prepared as in the case of the above-mentioned Inventive Example 1.

15 [0131]

(Evaluation 16)

Using the test cell of Inventive Example 13 thus prepared, the potential of the active electrode 11 relative to the reference electrode 13 was scanned starting at an  
20 initial potential of 2.5 V (vs.  $\text{Li}/\text{Li}^+$ ) in a reduction direction, and then in an oxidation direction for three cycles, at a scan rate of 1.0 mV/s in a scan range of 1.0 to 3.0 V (vs.  $\text{Li}/\text{Li}^+$ ), to measure the cyclic voltammetry in each cycle. The results are given in Fig. 29.

25 [0132]

As a result, in the case of the test cell of Inventive Example 13, reduction peaks appeared at around 2.0 V (vs. Li/Li<sup>+</sup>) and 1.5 V (vs. Li/Li<sup>+</sup>) during scanning in the reduction direction, and so it is presumed that the elemental sulfur was reduced. In addition, an oxidation current flowed at around 2.2 V or higher (vs. Li/Li<sup>+</sup>) during scanning in the oxidation direction, and it is presumed that the above-mentioned reduced elemental sulfur was oxidized at this potential range.

10 [0133]

Further, the test cell of Inventive Example 12 was discharged to a discharge cutoff potential of 1.0 V (vs. Li/Li<sup>+</sup>) at a discharge current of 0.13 mA/cm<sup>2</sup>, and then charged to a charge cutoff potential of 3.0 V (vs. Li/Li<sup>+</sup>) at a charge current of 0.13 mA/cm<sup>2</sup>, to examine the initial charge-discharge characteristics. The results are given in Fig. 30. Note that the solid line represents a discharge curve showing the relationship between the potential and the capacity per 1 g of elemental sulfur during discharging, and the broken line represents a charge curve showing the relationship between the potential and the capacity per 1 g of elemental sulfur during charging.

[0134]

As a result, in this test cell of Inventive Example 13, the initial specific discharge capacity per 1 g of elemental

sulfur was 1479 mAh/g. The specific discharge capacity was markedly increased, compared with that of LiCoO<sub>2</sub> used in a general positive electrode. In addition, the mixture of tetrahydrofuran and trimethylpropylammonium

5 bis(trifluoromethylsulfonyl)imide

((CH<sub>3</sub>)<sub>3</sub>N<sup>+</sup>(C<sub>3</sub>H<sub>7</sub>)N<sup>-</sup>(SO<sub>2</sub>CF<sub>3</sub>)<sub>2</sub>) increased the capacity at around 2.0 V or higher (vs. Li/Li<sup>+</sup>) during discharging, compared with that obtained using tetrahydrofuran alone as an electrolyte, as shown in Comparative Example 4 below, and the specific  
10 discharge capacity was also greater than that obtained using trimethylpropylammonium bis(trifluoromethylsulfonyl)imide ((CH<sub>3</sub>)<sub>3</sub>N<sup>+</sup>(C<sub>3</sub>H<sub>7</sub>)N<sup>-</sup>(SO<sub>2</sub>CF<sub>3</sub>)<sub>2</sub>) alone as an electrolyte, as shown in Inventive Example 1.

[0135]

15 (Inventive Example 14)

In Inventive Example 14, the same non-aqueous electrolyte as that in the above-mentioned Inventive Example 13 was used. Otherwise, the test cell of Inventive Example 14 was prepared as in the case of the above-mentioned  
20 Inventive Example 2.

[0136]

(Evaluation 17)

The test cell of Inventive Example 14 was charged to a charge cutoff potential of 0.0 V (vs. Li/Li<sup>+</sup>) at a charge  
25 current of 0.05 mA/cm<sup>2</sup>, and then discharged to a discharge

cutoff potential of 2.0 V (vs. Li/Li<sup>+</sup>) at a discharge current of 0.05 mA/cm<sup>2</sup>, to examine the initial charge-discharge characteristics. The results are given in Fig. 31. Note that the solid line represents a discharge curve showing the relationship between the potential and the capacity per 1 g of active material during charging, and the broken line represents a charge curve showing the relationship between the potential and the capacity per 1 g of active material during discharging.

10 [0137]

As a result, in this test cell of Inventive Example 14, the initial specific charge and discharge capacities per 1 g of active material were 3417 mAh/g and 2989 mAh/g, respectively. The specific charge/discharge capacity was markedly increased, compared with that of a carbon material used in a general negative electrode. The reversible reaction of the silicon thin film was also proved.

[0138]

Further, with the test cell of Inventive Example 14, the operation of charging the cell to a charge cutoff potential of 0.0 V (vs. Li/Li<sup>+</sup>) at a charge current of 0.05 mA/cm<sup>2</sup>, and then discharging the cell to a discharge cutoff potential of 2.0 V (vs. Li/Li<sup>+</sup>) at a discharge current of 0.05 mA/cm<sup>2</sup> was repeated, to measure the charge capacity Q<sub>a</sub> (mAh/g) and discharge capacity Q<sub>b</sub> (mAh/g) in each cycle, and also find

out the charge-discharge efficiency (%) in each cycle in accordance with the above-mentioned equation. In Fig. 32, the white circle and solid line represent the discharge capacity (mAh/g) in each cycle, and the triangle and broken  
5 line represent the charge-discharge efficiency (%) in each cycle.

[0139]

As a result, in this test cell of Inventive Example 14, the specific discharge capacities in the third cycle and  
10 thereafter were kept constant at approximately 3243 mAh/g, and the charge-discharge efficiencies were also kept constant at approximately 94%.

[0140]

(Inventive Example 15)

15 In Inventive Example 15, a non-aqueous electrolyte including a lithium salt,  $\text{LiN}(\text{CF}_3\text{SO}_2)_2$  dissolved at a concentration of 0.5 mol/l in a mixture of 25% by volume of tetrahydrofuran and 75% by volume of trimethylpropylammonium bis(trifluoromethylsulfonyl)imide  
20  $((\text{CH}_3)_3\text{N}^+(\text{C}_3\text{H}_7)\text{N}^-(\text{SO}_2\text{CF}_3)_2)$  was used. Otherwise, the test cell of Inventive Example 15 was prepared as in the case of the above-mentioned Inventive Example 1.

[0141]

(Evaluation 18)

Using the test cell of Inventive Example 15 thus prepared, the potential of the active electrode 11 relative to the reference electrode 13 was scanned starting at an initial potential of 2.6 V (vs.  $\text{Li/Li}^+$ ) in a reduction direction, and then in an oxidation direction for three cycles, at a scan rate of 1.0 mV/s in a scan range of 1.0 to 3.0 V (vs.  $\text{Li/Li}^+$ ), to measure the cyclic voltammetry in each cycle. The results are given in Fig. 33.

[0142]

As a result, in the case of the test cell of Inventive Example 15, a reduction current flowed at around 2.4 V or lower (vs.  $\text{Li/Li}^+$ ) during scanning in the reduction direction, and so it is presumed that elemental sulfur was reduced. In addition, an oxidation peak appeared at around 2.5 V (vs.  $\text{Li/Li}^+$ ) during scanning in the oxidation direction, and so it is presumed that the above-mentioned reduced elemental sulfur was oxidized at around this potential.

[0143]

The test cell of Inventive Example 15 was discharged to a discharge cutoff potential of 1.0 V (vs.  $\text{Li/Li}^+$ ) at a discharge current of 0.13 mA/cm<sup>2</sup>, and then charged to a charge cutoff potential of 3.0 V (vs.  $\text{Li/Li}^+$ ) at a charge current of 0.13 mA/cm<sup>2</sup>, to examine the initial charge-discharge characteristics. The results are given in Fig. 34. Note that the solid line represents a discharge curve showing the



relationship between the potential and the capacity per 1 g of elemental sulfur during discharging, and the broken line represents a charge curve showing the relationship between the potential and the capacity per 1 g of elemental sulfur during charging.

[0144]

As a result, in this test cell of Inventive Example 14, the initial specific discharge capacity per 1 g of elemental sulfur was 1547 mAh/g. The specific discharge capacity was markedly increased, compared with that of LiCoO<sub>2</sub> used in a general positive electrode. Further, the mixture of tetrahydrofuran and trimethylpropylammonium bis(trifluoromethylsulfonyl)imide ((CH<sub>3</sub>)<sub>3</sub>N<sup>+</sup>(C<sub>3</sub>H<sub>7</sub>)N<sup>-</sup>(SO<sub>2</sub>CF<sub>3</sub>)<sub>2</sub>) increased the capacity at around 2.0 V or higher (vs. Li/Li<sup>+</sup>) during discharging, compared with that obtained using tetrahydrofuran alone as an electrolyte, as shown in Comparative Example 4 below, and the specific discharge capacity was also greater than that obtained using trimethylpropylammonium bis(trifluoromethylsulfonyl)imide ((CH<sub>3</sub>)<sub>3</sub>N<sup>+</sup>(C<sub>3</sub>H<sub>7</sub>)N<sup>-</sup>(SO<sub>2</sub>CF<sub>3</sub>)<sub>2</sub>) alone as an electrolyte, as shown in Inventive Example 1.

[0145]

(Inventive Example 16)

In Inventive Example 16, the same non-aqueous electrolyte as that in the above-mentioned Inventive Example

15 was used. Otherwise, the test cell of Inventive Example 16 was prepared as in the case of the above-mentioned Inventive Example 2.

[0146]

5 (Evaluation 19)

The test cell of Inventive Example 16 was charged to a charge cutoff potential of 0.0 V (vs. Li/Li<sup>+</sup>) at a charge current of 0.05 mA/cm<sup>2</sup>, and then discharged to a discharge cutoff potential of 2.0 V (vs. Li/Li<sup>+</sup>) at a discharge current of 0.05 mA/cm<sup>2</sup>, to examine the initial charge-discharge characteristics. The results are given in Fig. 35. Note that the solid line represents a discharge curve showing the relationship between the potential and the capacity per 1 g of active material during charging, and the broken line represents a charge curve showing the relationship between the potential and the capacity per 1 g of active material during discharging.

[0147]

As a result, in this test cell of Inventive Example 16, the initial specific charge and discharge capacities per 1 g of active material were approximately 3417 mAh/g and 2989 mAh/g, respectively. The specific charge/discharge capacity was markedly increased, compared with that of a carbon material used in a general negative electrode. The reversible reaction of the silicon thin film was also proved.

[0148]

Further, with the test cell of Inventive Example 16, the operation of charging the cell to a charge cutoff potential of 0.0 V (vs. Li/Li<sup>+</sup>) at a charge current of 0.05 mA/cm<sup>2</sup>, and then discharging the cell to a discharge cutoff potential of 2.0 V (vs. Li/Li<sup>+</sup>) at a discharge current of 0.05 mA/cm<sup>2</sup> was repeated, to measure the charge capacity Q<sub>a</sub> (mAh/g) and discharge capacity Q<sub>b</sub> (mAh/g) in each cycle, and also find out the charge-discharge efficiency (%) in each cycle in accordance with the above-mentioned equation. In Fig. 36, the white circle and solid line represent the discharge capacity (mAh/g) in each cycle, and the triangle and broken line represent the charge-discharge efficiency (%) in each cycle.

15 [0149]

As a result, in this test cell of Inventive Example 16, the specific discharge capacities in the third cycle and thereafter were kept constant at approximately 3243 mAh/g, and the charge-discharge efficiencies were also kept constant at approximately 94%.

[0150]

(Comparative Example 4)

In Comparative Example 4, a non-aqueous electrolyte including a lithium salt, LiN(CF<sub>3</sub>SO<sub>2</sub>)<sub>2</sub> dissolved at a concentration of 0.5 mol/l in tetrahydrofuran was used.

Otherwise, the test cell of Comparative Example 4 was prepared as in the case of the above-mentioned Inventive Example 1.

[0151]

(Evaluation 20)

5        Using the test cell of Comparative Example 4 thus prepared, the potential of the active electrode 11 relative to the reference electrode 13 was scanned starting at an initial potential of 2.3 V (vs.  $\text{Li/Li}^+$ ) in a reduction direction, and then in an oxidation direction for three  
10 cycles, at a scan rate of 1.0 mV/s in a scan range of 1.0 to 3.0 V (vs.  $\text{Li/Li}^+$ ), to measure the cyclic voltammetry in each cycle. The results are given in Fig. 37.

[0152]

As a result, in the case of the test cell of Comparative  
15 Example 4, a reduction peak appeared at around 1.6 V (vs.  $\text{Li/Li}^+$ ), and a large reduction current flowed at around 1.2 V or lower (vs.  $\text{Li/Li}^+$ ) during scanning in the reduction direction, and so it is presumed that elemental sulfur was reduced. In addition, there was an oxidation peak at around  
20 2.5 V (vs.  $\text{Li/Li}^+$ ) during scanning in the oxidation direction, and it is presumed that the above-mentioned reduced elemental sulfur was oxidized at around this potential.

[0153]

Further, the test cell of Comparative Example 4 was  
25 discharged to a discharge cutoff potential of 1.0 V (vs.

Li/Li<sup>+</sup>) at a discharge current of 0.13 mA/cm<sup>2</sup>, and then charged to a charge cutoff potential of 3.3 V (vs. Li/Li<sup>+</sup>) at a charge current of 0.13 mA/cm<sup>2</sup>, to examine the initial charge-discharge characteristics. The results are given in Fig. 38. Note that the solid line represents a discharge curve showing the relationship between the potential and the capacity per 1 g of elemental sulfur during discharging, and the broken line represents a charge curve showing the relationship between the potential and the capacity per 1 g of elemental sulfur during charging.

[0154]

As a result, in this test cell of Comparative Example 4, the initial specific discharge capacity per 1 g of elemental sulfur was 1065 mAh/g. The specific discharge capacity was markedly increased, compared with that of LiCoO<sub>2</sub> used in a general positive electrode, while the discharge potential was as low as approximately 1.2 V (vs. Li/Li<sup>+</sup>).

[0155]

(Evaluation 21)

The mixture of trimethylpropylammonium bis(trifluoromethylsulfonyl)imide ((CH<sub>3</sub>)<sub>3</sub>N<sup>+</sup>(C<sub>3</sub>H<sub>7</sub>)N<sup>-</sup>(SO<sub>2</sub>CF<sub>3</sub>)<sub>2</sub>) and tetrahydrofuran has reduced viscosity in the electrolyte, compared with the electrolyte containing only trimethylpropylammonium bis(trifluoromethylsulfonyl)imide

$((\text{CH}_3)_3\text{N}^+(\text{C}_3\text{H}_7)\text{N}^-(\text{SO}_2\text{CF}_3)_2)$ . Accordingly, the mixture is preferable for use as an electrolyte.

[0156]

(Evaluation 22)

5 Further, the results of Inventive Examples 1, 13, 17, and Comparative Example 4 show that in the use of a positive electrode including elemental sulfur, it is preferable to mix trimethylpropylammonium bis(trifluoromethylsulfonyl)imide  $((\text{CH}_3)_3\text{N}^+(\text{C}_3\text{H}_7)\text{N}^-(\text{SO}_2\text{CF}_3)_2)$  with tetrahydrofuran than to use  
10 trimethylpropylammonium bis(trifluoromethylsulfonyl)imide  $((\text{CH}_3)_3\text{N}^+(\text{C}_3\text{H}_7)\text{N}^-(\text{SO}_2\text{CF}_3)_2)$  or tetrahydrofuran alone, when comparing the specific discharge capacities in plateaus at around 2.0 V or higher (vs.  $\text{Li}/\text{Li}^+$ ) in the discharge characteristics. The tetrahydrofuran may be set in the range  
15 of 0.1 to 99.9% by volume. Preferably, the ratio of tetrahydrofuran may be set in the range of 0.1 to 50% by volume, more preferably, in the range of 0.1 to 25% by volume.  
[0157]

(Inventive Example 17)

20 In Inventive Example 17, a non-aqueous electrolyte including a lithium salt,  $\text{LiN}(\text{CF}_3\text{SO}_2)_2$  dissolved at a concentration of 0.5 mol/l in a mixture of 50% by volume of 1,2-dimethoxyethane and 50% by volume of trimethylpropylammonium bis(trifluoromethylsulfonyl)imide  
25  $((\text{CH}_3)_3\text{N}^+(\text{C}_3\text{H}_7)\text{N}^-(\text{SO}_2\text{CF}_3)_2)$  was used. Otherwise, the test cell

of Inventive Example 17 was prepared as in the case of the above-mentioned Inventive Example 1.

[0158]

(Evaluation 23)

5        Using the test cell of Inventive Example 17 thus prepared, the potential of the active electrode 11 relative to the reference electrode 13 was scanned starting at an initial potential of 2.8 V (vs.  $\text{Li/Li}^+$ ) in a reduction direction, and then in an oxidation direction for three  
10 cycles, at a scan rate of 1.0 mV/s in a scan range of 1.0 to 3.0 V (vs.  $\text{Li/Li}^+$ ), to measure the cyclic voltammetry in each cycle. The results are given in Fig. 39.

[0159]

As a result, in the case of the test cell of Inventive  
15 Example 17, a reduction peak appeared at around 2.0 V (vs.  $\text{Li/Li}^+$ ) during scanning in the reduction direction, and so it is presumed that the elemental sulfur was reduced. In addition, an oxidation current flowed at around 2.2 V or higher (vs.  $\text{Li/Li}^+$ ) during scanning in the oxidation  
20 direction, and so it is presumed that the above-mentioned reduced elemental sulfur was oxidized at this potential range.

[0160]

Further, the test cell of Inventive Example 17 was  
25 discharged to a discharge cutoff potential of 1.0 V (vs.

Li/Li<sup>+</sup>) at a discharge current of 0.13 mA/cm<sup>2</sup>, and then charged to a charge cutoff potential of 3.0 V (vs. Li/Li<sup>+</sup>) at a charge current of 0.13 mA/cm<sup>2</sup>, to examine the initial charge-discharge characteristics. The results are given in Fig. 40. Note that the solid line represents a discharge curve showing the relationship between the potential and the capacity per 1 g of elemental sulfur during discharging, and the broken line represents a charge curve showing the relationship between the potential and the capacity per 1 g of elemental sulfur during charging.

[0161]

As a result, in this test cell of Inventive Example 17, the initial specific discharge capacity per 1 g of elemental sulfur was 1919 mAh/g. The specific discharge capacity was markedly increased, compared with that of LiCoO<sub>2</sub> used in a general positive electrode. Further, the mixture of tetrahydrofuran and trimethylpropylammonium bis(trifluoromethylsulfonyl)imide ((CH<sub>3</sub>)<sub>3</sub>N<sup>+</sup>(C<sub>3</sub>H<sub>7</sub>)N<sup>-</sup>(SO<sub>2</sub>CF<sub>3</sub>)<sub>2</sub>) increased the specific capacity at around 1.5 V or higher (vs. Li/Li<sup>+</sup>) during discharging, compared with that obtained using tetrahydrofuran alone as an electrolyte, as shown in Comparative Example 5, and the specific discharge capacity was also greater than that obtained using trimethylpropylammonium bis(trifluoromethylsulfonyl)imide



$((\text{CH}_3)_3\text{N}^+(\text{C}_3\text{H}_7)\text{N}^-(\text{SO}_2\text{CF}_3)_2)$  alone as an electrolyte, as shown in Inventive Example 1.

[0162]

(Inventive Example 18)

5 In Inventive Example 18, the same non-aqueous electrolyte as that in the above-mentioned Inventive Example 17 was used. Otherwise, the test cell of Inventive Example 18 was prepared as in the case of the above-mentioned Inventive Example 2.

10 [0163]

(Evaluation 24)

The test cell of Inventive Example 18 was charged to a charge cutoff potential of 0.0 V (vs.  $\text{Li}/\text{Li}^+$ ) at a charge current of  $0.05 \text{ mA}/\text{cm}^2$ , and then discharged to a discharge cutoff potential of 2.0 V (vs.  $\text{Li}/\text{Li}^+$ ) at a discharge current of  $0.05 \text{ mA}/\text{cm}^2$ , to examine the initial charge-discharge characteristics. The results are given in Fig. 41. Note that the solid line represents a discharge curve showing the relationship between the potential and the capacity per 1 g of active material during charging, and the broken line represents a charge curve showing the relationship between the potential and the capacity per 1 g of active material during discharging.

[0164]

As a result, in this test cell of Inventive Example 18, the initial specific charge and discharge capacities per 1 g of active material were approximately 3417 mAh/g and 2989 mAh/g, respectively. The specific charge/discharge capacity was markedly increased, compared with that of a carbon material used in a negative electrode. The reversible reaction of the silicon thin film was also proved.

[0165]

Further, with the test cell of Inventive Example 18, the operation of charging the cell to a charge cutoff potential of 0.0 V (vs. Li/Li<sup>+</sup>) at a charge current of 0.05 mA/cm<sup>2</sup>, and then discharging the cell to a discharge cutoff potential of 2.0 V (vs. Li/Li<sup>+</sup>) at a discharge current of 0.05 mA/cm<sup>2</sup> was repeated, to measure the charge capacity Q<sub>a</sub> (mAh/g) and discharge capacity Q<sub>b</sub> (mAh/g) in each cycle, and also find out the charge-discharge efficiency (%) in each cycle in accordance with the above-mentioned equation. In Fig. 42, the white circle and solid line represent the discharge capacity (mAh/g) in each cycle, and the triangle and broken line represent the charge-discharge efficiency (%) in each cycle.

[0166]

As a result, in this test cell of Inventive Example 18, the specific discharge capacities in the third cycle and thereafter were kept constant at approximately 3243 mAh/g,

and the charge-discharge efficiencies were also kept constant at approximately 94%.

[0167]

(Inventive Example 19)

5 In Inventive Example 19, a non-aqueous electrolyte including a lithium salt,  $\text{LiN}(\text{CF}_3\text{SO}_2)_2$  dissolved at a concentration of 0.5 mol/l in a mixture of 25% by volume of 1,2-dimethoxyethane and 75% by volume of trimethylpropylammonium bis(trifluoromethylsulfonyl)imide  
10  $((\text{CH}_3)_3\text{N}^+(\text{C}_3\text{H}_7)\text{N}^-(\text{SO}_2\text{CF}_3)_2)$  was used. Otherwise, the test cell of Inventive Example 19 was prepared as in the case of the above-mentioned Inventive Example 1.

[0168]

(Evaluation 25)

15 Using the test cell of Inventive Example 19 thus prepared, the potential of the active electrode 11 relative to the reference electrode 13 was scanned starting at an initial potential of 2.4 V (vs.  $\text{Li}/\text{Li}^+$ ) in a reduction direction, and then in an oxidation direction for three  
20 cycles, at a scan rate of 1.0 mV/s in a scan range of 1.0 to 3.3 V (vs.  $\text{Li}/\text{Li}^+$ ), to measure the cyclic voltammetry in each cycle. The results are given in Fig. 43.

[0169]

As a result, in the case of the test cell of Inventive  
25 Example 19, a reduction current flowed at around 2.4 V or lower

(vs.  $\text{Li/Li}^+$ ) during scanning in the reduction direction, and so it is presumed that elemental sulfur was reduced. In addition, an oxidation peak appeared at around 2.5 V (vs.  $\text{Li/Li}^+$ ) during scanning in the oxidation direction, and so it is presumed that the above-mentioned reduced elemental sulfur was oxidized at this potential range.

[0170]

Further, the test cell of Inventive Example 19 was discharged to a discharge cutoff potential of 1.0 V (vs.  $\text{Li/Li}^+$ ) at a discharge current of  $0.13 \text{ mA/cm}^2$ , and then charged to a charge cutoff potential of 3.0 V (vs.  $\text{Li/Li}^+$ ) at a charge current of  $0.13 \text{ mA/cm}^2$ , to examine the initial charge-discharge characteristics. The results are given in Fig. 44. Note that the solid line represents a discharge curve showing the relationship between the potential and the capacity per 1 g of elemental sulfur during discharging, and the broken line represents a charge curve showing the relationship between the potential and the capacity per 1 g of elemental sulfur during charging.

[0171]

As a result, in this test cell of Inventive Example 19, the initial specific discharge capacity per 1 g of elemental sulfur was 1636 mAh/g. The specific discharge capacity was markedly increased, compared with that of  $\text{LiCoO}_2$  used in a general positive electrode. Further, the mixture of

tetrahydrofuran and trimethylpropylammonium

bis(trifluoromethylsulfonyl)imide

$((\text{CH}_3)_3\text{N}^+(\text{C}_3\text{H}_7)\text{N}^-(\text{SO}_2\text{CF}_3)_2)$  increased the specific capacity at around 1.5 V or higher (vs.  $\text{Li}/\text{Li}^+$ ) during discharging,

5 compared with that obtained using 1,2-dimethoxyethane alone as an electrolyte, as shown in Comparative Example 5 below, and the specific discharge capacity was also greater than that obtained using trimethylpropylammonium

bis(trifluoromethylsulfonyl)imide

10  $((\text{CH}_3)_3\text{N}^+(\text{C}_3\text{H}_7)\text{N}^-(\text{SO}_2\text{CF}_3)_2)$  alone as an electrolyte, as shown in Inventive Example 1.

[0172]

(Inventive Example 20)

In Inventive Example 20, the same non-aqueous  
15 electrolyte as that in the above-mentioned Inventive Example 19 was used. Otherwise, the test cell of Inventive Example 20 was prepared as in the case of the above-mentioned Inventive Example 2.

[0173]

20 (Evaluation 26)

The test cell of Inventive Example 20 was charged to a charge cutoff potential of 0.0 V (vs.  $\text{Li}/\text{Li}^+$ ) at a charge current of 0.05  $\text{mA}/\text{cm}^2$ , and then discharged to a discharge cutoff potential of 2.0 V (vs.  $\text{Li}/\text{Li}^+$ ) at a discharge current  
25 of 0.05  $\text{mA}/\text{cm}^2$ , to examine the initial charge-discharge

characteristics. The results are given in Fig. 45. Note that the solid line represents a discharge curve showing the relationship between the potential and the capacity per 1 g of active material during charging, and the broken line represents a charge curve showing the relationship between the potential and the capacity per 1 g of active material during discharging.

[0174]

As a result, in this test cell of Inventive Example 20, the initial specific charge and discharge capacities per 1 g of active material were approximately 3417 mAh/g and 2989 mAh/g, respectively. The specific charge/discharge capacity was markedly increased, compared with that of a carbon material used in a general negative electrode. The reversible reaction of the silicon thin film was also proved.

[0175]

Further, with the test cell of Inventive Example 20, the operation of charging the cell to a charge cutoff potential of 0.0 V (vs. Li/Li<sup>+</sup>) at a charge current of 0.05 mA/cm<sup>2</sup>, and then discharging the cell to a discharge cutoff potential of 2.0 V (vs. Li/Li<sup>+</sup>) at a discharge current of 0.05 mA/cm<sup>2</sup> was repeated, to measure the charge capacity  $Q_a$  (mAh/g) and discharge capacity  $Q_b$  (mAh/g) in each cycle, and also find out the charge-discharge efficiency (%) in each cycle in accordance with the above-mentioned equation. In Fig. 46,

the white circle and solid line represent the discharge capacity (mAh/g) in each cycle, and the triangle and broken line represent the charge-discharge efficiency (%) in each cycle.

5 [0176]

As a result, in this test cell of Inventive Example 20, the specific discharge capacities in the third cycle and thereafter were kept constant at approximately 3243 mAh/g, and the charge-discharge efficiencies were also kept constant  
10 at approximately 94%.

[0177]

(Comparative Example 5)

In Comparative Example 5, a non-aqueous electrolyte including a lithium salt,  $\text{LiN}(\text{CF}_3\text{SO}_2)_2$  dissolved at a  
15 concentration of 0.5 mol/l in 1,2-dimethoxyethane was used. Otherwise, the test cell of Comparative Example 5 was prepared as in the case of the above-mentioned Inventive Example 1.

[0178]

(Evaluation 27)

20 Using the test cell of Comparative Example 5 thus prepared, the potential of the active electrode 11 relative to the reference electrode 13 was scanned starting at an initial potential of 2.4 V (vs.  $\text{Li}/\text{Li}^+$ ) in a reduction direction, and then in an oxidation direction for three  
25 cycles, at a scan rate of 1.0 mV/s in a scan range of 1.0 to

3.0 V (vs.  $\text{Li/Li}^+$ ), to measure the cyclic voltammetry in each cycle. The results are given in Fig. 47.

[0179]

As a result, in the case of the test cell of Comparative Example 5, a reduction peak appeared at around 1.8 V (vs.  $\text{Li/Li}^+$ ) and a large reduction current flowed at around 1.2 V or lower (vs.  $\text{Li/Li}^+$ ) during scanning in the reduction direction, and so it is presumed that elemental sulfur was reduced. In addition, there was an oxidation peak at around 2.5 V (vs.  $\text{Li/Li}^+$ ) during scanning in the oxidation direction, and so it is presumed that the above-mentioned reduced elemental sulfur was oxidized at around this potential.

[0180]

Further, the test cell of Comparative Example 5 was discharged to a discharge cutoff potential of 1.0 V (vs.  $\text{Li/Li}^+$ ) at a discharge current of  $0.13 \text{ mA/cm}^2$ , and then charged to a charge cutoff potential of 3.0 V (vs.  $\text{Li/Li}^+$ ) at a charge current of  $0.13 \text{ mA/cm}^2$ , to examine the initial charge-discharge characteristics. The results are given in Fig. 48. Note that the solid line represents a discharge curve showing the relationship between the potential and the capacity per 1 g of elemental sulfur during discharging, and the broken line represents a charge curve showing the relationship between the potential and the capacity per 1 g of elemental sulfur during charging.



[0181]

As a result, in this test cell of Comparative Example 5, the initial specific discharge capacity per 1 g of elemental sulfur was 1921 mAh/g. The specific discharge capacity was markedly increased, compared with that of  $\text{LiCoO}_2$  used in a general positive electrode. However, the capacity at around 2 V or higher (vs.  $\text{Li/Li}^+$ ) was small in the discharge characteristics, and most of the discharge potentials were as low as approximately 1.2 V (vs.  $\text{Li/Li}^+$ ).

10 [0182]

(Evaluation 28)

The mixture of trimethylpropylammonium bis(trifluoromethylsulfonyl)imide

$((\text{CH}_3)_3\text{N}^+(\text{C}_3\text{H}_7)\text{N}^-(\text{SO}_2\text{CF}_3)_2)$  and 1,2-dimethoxyethane has reduced viscosity in the electrolyte, compared with the electrolyte containing only trimethylpropylammonium bis(trifluoromethylsulfonyl)imide  $((\text{CH}_3)_3\text{N}^+(\text{C}_3\text{H}_7)\text{N}^-(\text{SO}_2\text{CF}_3)_2)$ . Accordingly, the mixture is preferable for use as an electrolyte.

20 [0183]

(Evaluation 29)

Moreover, the results of Inventive Examples 1, 17, 19, and Comparative Example 5 show that in the use of a positive electrode including elemental sulfur, it is more preferable to mix trimethylpropylammonium

bis(trifluoromethylsulfonyl)imide

$((\text{CH}_3)_3\text{N}^+(\text{C}_3\text{H}_7)\text{N}^-(\text{SO}_2\text{CF}_3)_2)$  with 1,2-dimethoxyethane than to use trimethylpropylammonium

bis(trifluoromethylsulfonyl)imide

- 5  $((\text{CH}_3)_3\text{N}^+(\text{C}_3\text{H}_7)\text{N}^-(\text{SO}_2\text{CF}_3)_2)$  or 1,2-dimethoxyethane alone, when comparing the specific discharge capacities at around 1.5 V or higher (vs.  $\text{Li}/\text{Li}^+$ ) in the discharge characteristics. The 1,2-dimethoxyethane may be set in the range of 0.1 to 99.9% by volume. Preferably, the ratio of 1,2-dimethoxyethane may  
10 be set in the range of 0.1 to 50% by volume, more preferably, in the range of 0.1 to 25% by volume.

[0184]

- The results above show that increased specific discharge capacity can be obtained by mixing a quaternary  
15 ammonium salt, such as trimethylpropylammonium bis(trifluoromethylsulfonyl)imide  $((\text{CH}_3)_3\text{N}^+(\text{C}_3\text{H}_7)\text{N}^-(\text{SO}_2\text{CF}_3)_2)$ , trimethyloctylammonium bis(trifluoromethylsulfonyl)imide  
 $((\text{CH}_3)_3\text{N}^+(\text{C}_8\text{H}_{17})\text{N}^-(\text{SO}_2\text{CF}_3)_2)$ , trimethylallylammonium  
20 bis(trifluoromethylsulfonyl)imide  $((\text{CH}_3)_3\text{N}^+(\text{Allyl})\text{N}^-(\text{SO}_2\text{CF}_3)_2)$ , trimethylhexylammonium bis(trifluoromethylsulfonyl)imide  
 $((\text{CH}_3)_3\text{N}^+(\text{C}_6\text{H}_{13})\text{N}^-(\text{SO}_2\text{CF}_3)_2)$ , trimethylethylammonium  
2,2,2-trifluoro-N-(trifluoromethylsulfonyl)acetamide

$((\text{CH}_3)_3\text{N}^+(\text{C}_2\text{H}_5)(\text{CF}_3\text{CO})\text{N}^-(\text{SO}_2\text{CF}_3))$ , trimethylallylammonium  
 2,2,2-trifluoro-N-(trifluoromethylsulfonyl)acetamide  
 $((\text{CH}_3)_3\text{N}^+(\text{Allyl})(\text{CF}_3\text{CO})\text{N}^-(\text{SO}_2\text{CF}_3))$ , trimethylpropylammonium  
 2,2,2-trifluoro-N-(trifluoromethylsulfonyl)acetamide  
 5  $((\text{CH}_3)_3\text{N}^+(\text{C}_3\text{H}_7)(\text{CF}_3\text{CO})\text{N}^-(\text{SO}_2\text{CF}_3))$ , tetraethylammonium  
 2,2,2-trifluoro-N-(trifluoromethylsulfonyl)acetamide  
 $((\text{C}_2\text{H}_5)_4\text{N}^+(\text{CF}_3\text{CO})\text{N}^-(\text{SO}_2\text{CF}_3))$ , or triethylmethylanmonium  
 2,2,2-trifluoro-N-(trifluoromethylsulfonyl)acetamide  
 $((\text{C}_2\text{H}_5)_3\text{N}^+(\text{CH}_3)(\text{CF}_3\text{CO})\text{N}^-(\text{SO}_2\text{CF}_3))$ ; or a room temperature  
 10 molten salt having a melting point of not higher than 60°C,  
 such as an imidazolium salt illustrated by  
 1-ethyl-3-methylimidazolium  
 bis(pentafluoroethylsulfonyl)imide  
 $((\text{C}_2\text{H}_5)(\text{C}_3\text{H}_3\text{N}_2)^+(\text{CH}_3)\text{N}^-(\text{SO}_2\text{C}_2\text{F}_5)_2)$ ,  
 15 1-ethyl-3-methylimidazolium  
 bis(trifluoromethylsulfonyl)imide  
 $((\text{C}_2\text{H}_5)(\text{C}_3\text{H}_3\text{N}_2)^+(\text{CH}_3)\text{N}^-(\text{SO}_2\text{CF}_3)_2)$ ,  
 1-ethyl-3-methylimidazolium tetrafluoroborate  
 $((\text{C}_2\text{H}_5)(\text{C}_3\text{H}_3\text{N}_2)^+(\text{CH}_3)\text{BF}_4^-)$ , 1-ethyl-3-methylimidazolium  
 20 pentafluoroborate  $((\text{C}_2\text{H}_5)(\text{C}_3\text{H}_3\text{N}_2)^+(\text{CH}_3)\text{PF}_6^-)$  with at least one  
 type of an organic solvent selected from fluorinated cyclic  
 carbonates, such as trifluoropropylene carbonate and  
 fluoroethyl carbonate; cyclic ethers, such as 1,3-dioxolane,  
 4-methyl-1,3-dioxolane, tetrahydrofuran, 2-methyl  
 25 tetrahydrofuran, propylene oxide, 1,2-butylene oxide,

1,4-dioxane, 1,3,5-trioxane, furan, 2-methylfuran,  
1,8-cineole, and crown ether; or chain ethers, such as  
1,2-dimethoxyethane, diethyl ether, dipropyl ether,  
diisopropyl ether, dibutyl ether, dihexyl ether, ethyl vinyl  
5 ether, butyl vinyl ether, methyl phenyl ether, ethyl phenyl  
ether, butyl phenyl ether, pentyl phenyl ether,  
methoxytoluene, benzyl ethyl ether, diphenyl ether, dibenzyl  
ether, o-dimethoxybenzene, 1,2-diethoxyethane,  
1,2-dibutoxyethane, diethylene glycol dimethyl ether,  
10 diethylene glycol diethyl ether, diethylene glycol dibutyl  
ether, 1,1-dimethoxymethane, 1,1-diethoxyethane,  
triethylene glycol dimethyl ether, and tetraethylene glycol  
dimethyl ether. Needless to say, a mixture of at least two  
types of room temperature molten salts having a melting point  
15 of not higher than 60°C may also be used.

[Brief Description of the Drawings]

[FIG. 1]

A schematic diagram for use in explaining a test cell  
prepared in each of Inventive Examples 1 to 20 and Comparative  
20 Examples 1 to 5 of this invention

[FIG. 2]

A diagram showing the cyclic voltammetry of a working  
electrode measured by scanning the potential of the working  
electrode in the test cell of Inventive Example 1

25 [FIG. 3]

A diagram showing the cyclic voltammetry of a working electrode measured by scanning the potential of the working electrode in the test cell of Comparative Example 1

[FIG. 4]

5 A diagram showing initial charge-discharge characteristics of the test cell of Inventive Example 1

[FIG. 5]

A diagram showing the discharge capacity and charge-discharge efficiency in each cycle obtained when the  
10 test cell of Inventive Example 1 was repeatedly charged/discharged

[FIG. 6]

A diagram showing initial charge-discharge characteristics of the test cell of Inventive Example 2

15 [FIG. 7]

A diagram showing the discharge capacity and charge-discharge efficiency in each cycle obtained when the test cell of Inventive Example 2 was repeatedly charged/discharged

20 [FIG. 8]

A diagram showing the cyclic voltammetry of a working electrode measured by scanning the potential of the working electrode in the test cell of Inventive Example 3

[FIG. 9]

A diagram showing the cyclic voltammetry of a working electrode measured by scanning the potential of the working electrode in the test cell of Comparative Example 2

[FIG. 10]

5 A diagram showing initial charge/discharge characteristics of the test cell of Inventive Example 4

[FIG. 11]

A diagram showing the discharge capacity and charge-discharge efficiency in each cycle obtained when the  
10 test cell of Inventive Example 5 was repeatedly charged/discharged

[FIG. 12]

A diagram showing the cyclic voltammetry of a working electrode measured by scanning the working electrode in the  
15 test cell of Inventive Example 5

[FIG. 13]

A diagram showing initial charge/discharge characteristics of the test cell of Inventive Example 5

[FIG. 14]

20 A diagram showing the cyclic voltammetry of a working electrode measured by scanning the working electrode in the test cell of Inventive Example 6

[FIG. 15]

A diagram showing the cyclic voltammetry of a working electrode measured by scanning the working electrode in the test cell of Inventive Example 7

[FIG. 16]

5 A diagram showing initial charge/discharge characteristics of the test cell of Inventive Example 7

[FIG. 17]

A diagram showing initial charge/discharge characteristics of the test cell of Inventive Example 8

10 [FIG. 18]

A diagram showing the discharge capacity and charge-discharge efficiency in each cycle obtained when the test cell of Inventive Example 8 was repeatedly charged/discharged

15 [FIG. 19]

A diagram showing the cyclic voltammetry of a working electrode measured by scanning the working electrode in the test cell of Inventive Example 9

[FIG. 20]

20 A diagram showing initial charge/discharge characteristics of the test cell of Inventive Example 9

[FIG. 21]

A diagram showing initial charge/discharge characteristics of the test cell of Inventive Example 10

25 [FIG. 22]

A diagram showing the discharge capacity and charge-discharge efficiency in each cycle obtained when the test cell of Inventive Example 10 was repeatedly charged/discharged

5 [FIG. 23]

A diagram showing the cyclic voltammetry of a working electrode measured by scanning the working electrode in the test cell of Inventive Example 11

[FIG. 24]

10 A diagram showing initial charge/discharge characteristics of the test cell of Inventive Example 11

[FIG. 25]

A diagram showing initial charge/discharge characteristics of the test cell of Inventive Example 12

15 [FIG. 26]

A diagram showing the discharge capacity and charge-discharge efficiency in each cycle obtained when the test cell of Inventive Example 12 was repeatedly charged/discharged

20 [FIG. 27]

A diagram showing the cyclic voltammetry of a working electrode measured by scanning the working electrode in the test cell of Comparative Example 3

[FIG. 28]



A diagram showing initial charge/discharge characteristics of the test cell of Comparative Example 3  
[FIG. 29]

A diagram showing the cyclic voltammetry of a working  
5 electrode measured by scanning the working electrode in the test cell of Inventive Example 13  
[FIG. 30]

A diagram showing initial charge/discharge characteristics of the test cell of Inventive Example 13  
10 [FIG. 31]

A diagram showing initial charge/discharge characteristics of the test cell of Inventive Example 14  
[FIG. 32]

A diagram showing the discharge capacity and  
15 charge-discharge efficiency in each cycle obtained when the test cell of Inventive Example 14 was repeatedly charged/discharged  
[FIG. 33]

A diagram showing the cyclic voltammetry of a working  
20 electrode measured by scanning the working electrode in the test cell of Inventive Example 15  
[FIG. 34]

A diagram showing initial charge/discharge characteristics of the test cell of Inventive Example 15  
25 [FIG. 35]

A diagram showing initial charge/discharge characteristics of the test cell of Inventive Example 16

[FIG. 36]

A diagram showing the discharge capacity and  
5 charge-discharge efficiency in each cycle obtained when the test cell of Inventive Example 16 was repeatedly charged/discharged

[FIG. 37]

A diagram showing the cyclic voltammetry of a working  
10 electrode measured by scanning the working electrode in the test cell of Comparative Example 4

[FIG. 38]

A diagram showing initial charge/discharge characteristics of the test cell of Comparative Example 4

15 [FIG. 39]

A diagram showing the cyclic voltammetry of a working electrode measured by scanning the working electrode in the test cell of Inventive Example 17

[FIG. 40]

20 A diagram showing initial charge/discharge characteristics of the test cell of Inventive Example 17

[FIG. 41]

A diagram showing initial charge/discharge characteristics of the test cell of Inventive Example 18

25 [FIG. 42]

Fig 42 is a diagram showing the discharge capacity and charge-discharge efficiency in each cycle obtained when the test cell of Inventive Example 18 was repeatedly charged/discharged

5 [FIG. 43]

A diagram showing the cyclic voltammetry of a working electrode measured by scanning the working electrode in the test cell of Inventive Example 19

[FIG. 44]

10 A diagram showing initial charge/discharge characteristics of the test cell of Inventive Example 19

[FIG. 45]

A diagram showing initial charge/discharge characteristics of the test cell of Inventive Example 20

15 [FIG. 46]

A diagram showing the discharge capacity and charge-discharge efficiency in each cycle obtained when the test cell of Inventive Example 20 was repeatedly charged/discharged

20 [FIG. 47]

A diagram showing the cyclic voltammetry of a working electrode measured by scanning the working electrode in the test cell of Comparative Example 5

[FIG. 48]

A diagram showing initial charge/discharge characteristics of the test cell of Comparative Example 5

[Description of Reference Numerals]

- 10 Test cell vessel
- 5 11 Working electrode
- 12 Counter electrode
- 13 Reference electrode
- 14 Non-aqueous electrolyte

10

Fig. 1

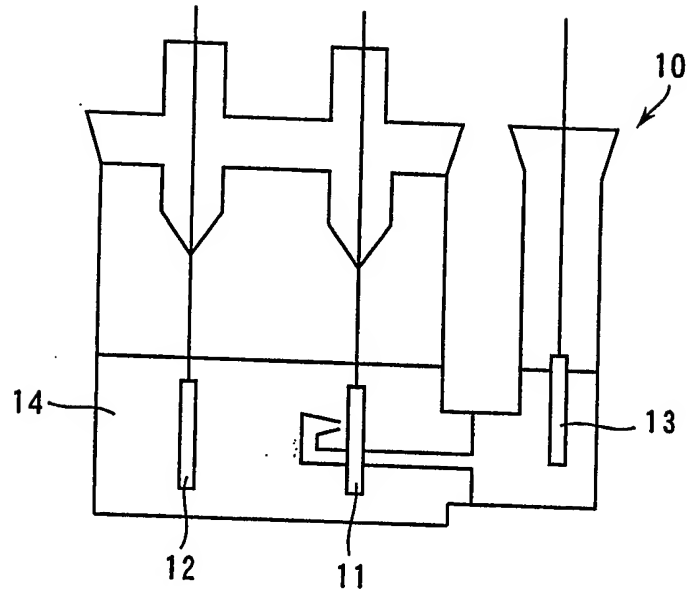


Fig.2

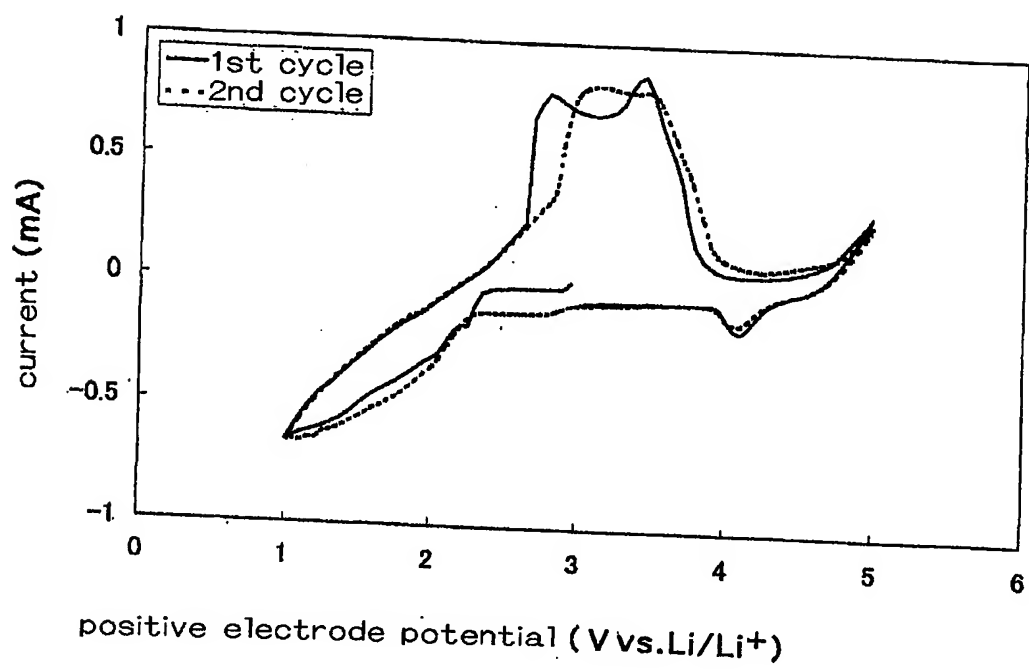


Fig. 3

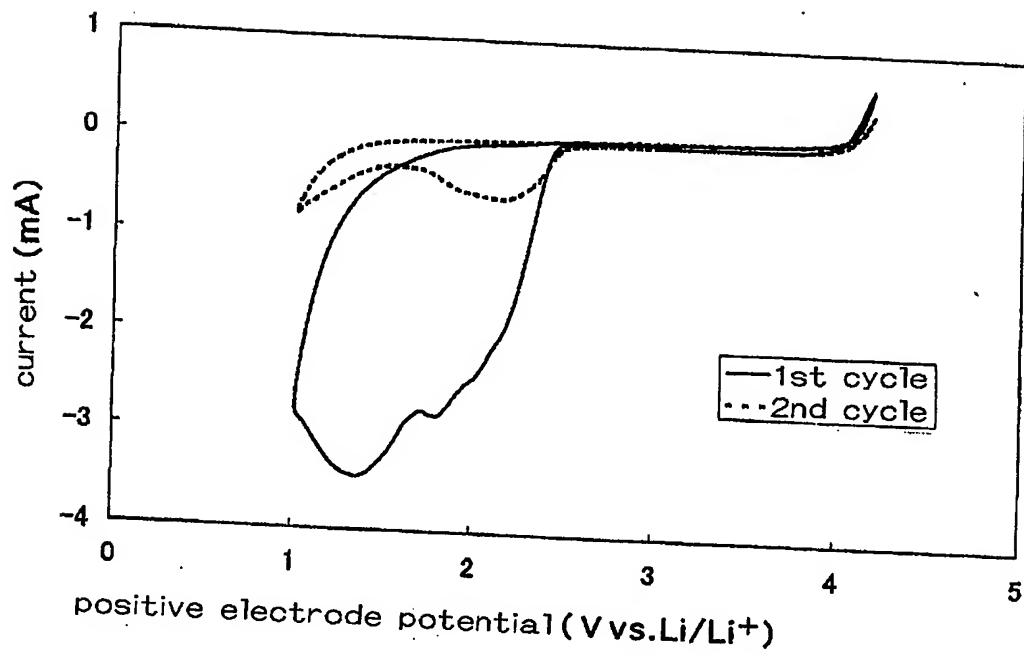


Fig. 4

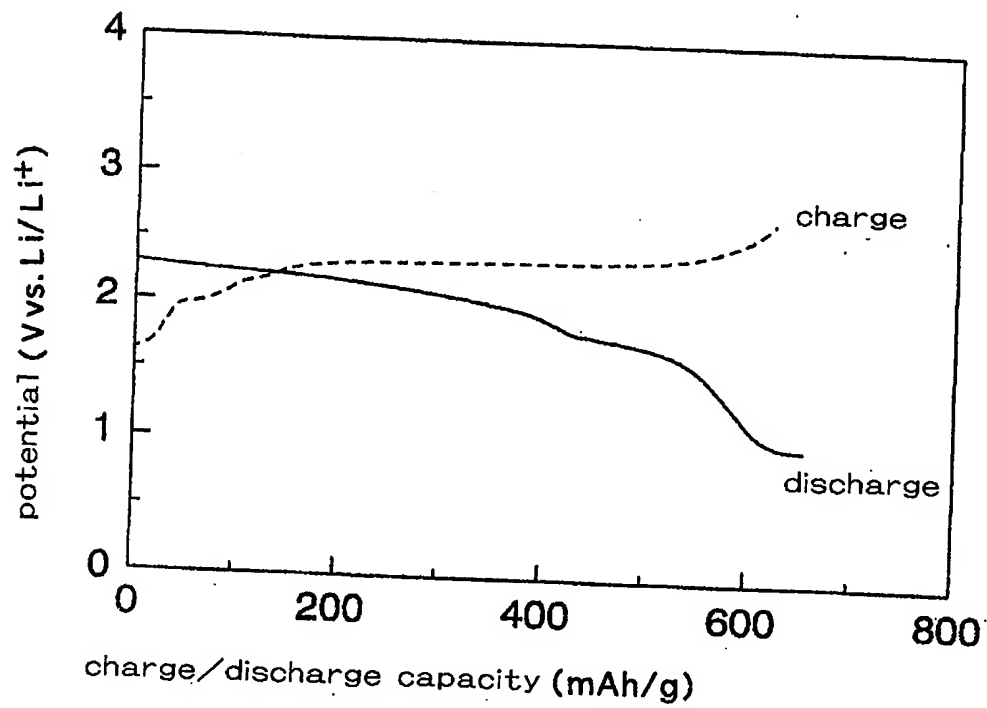


Fig.5

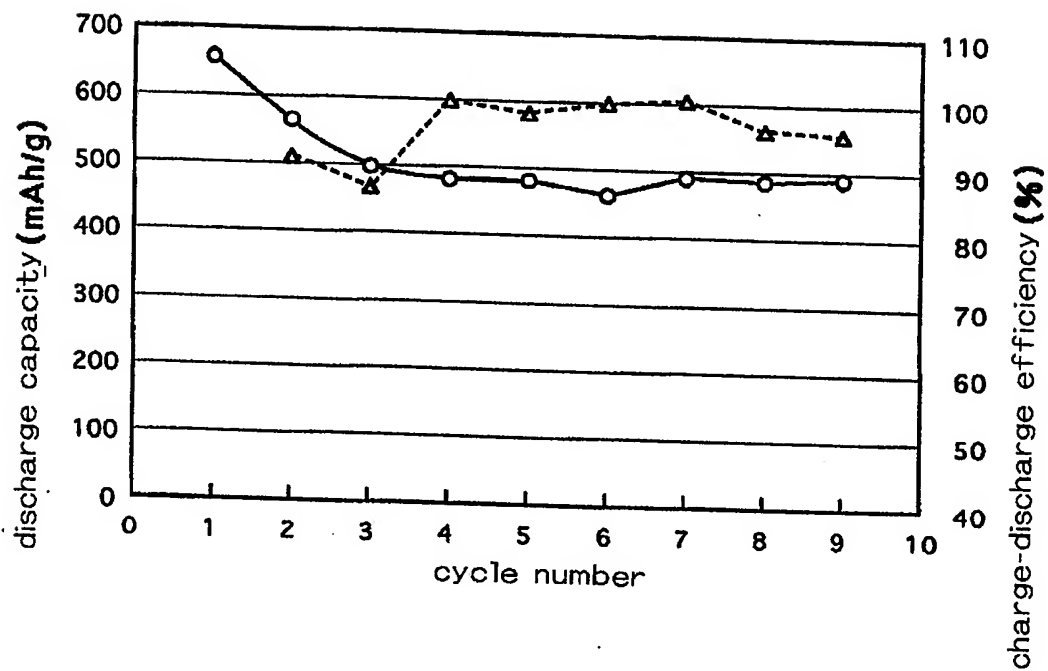


Fig.6

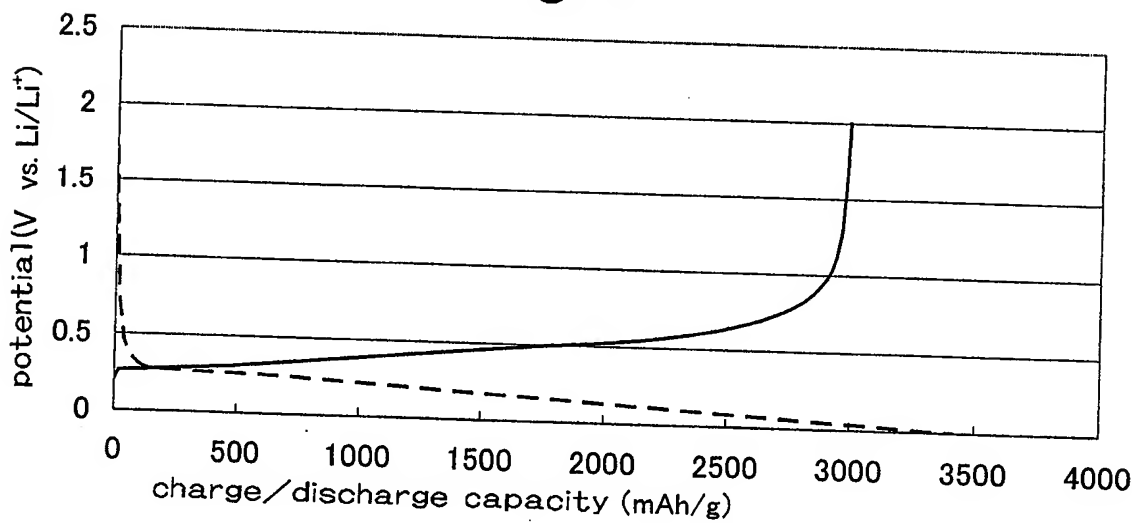




Fig. 7

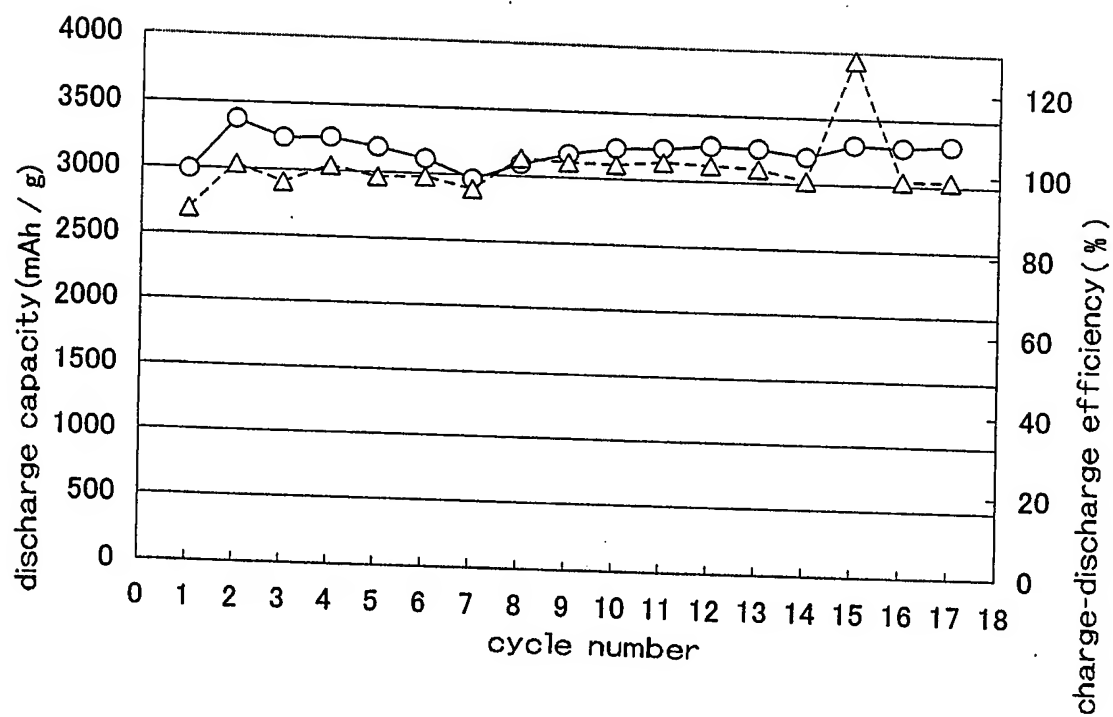


Fig. 8

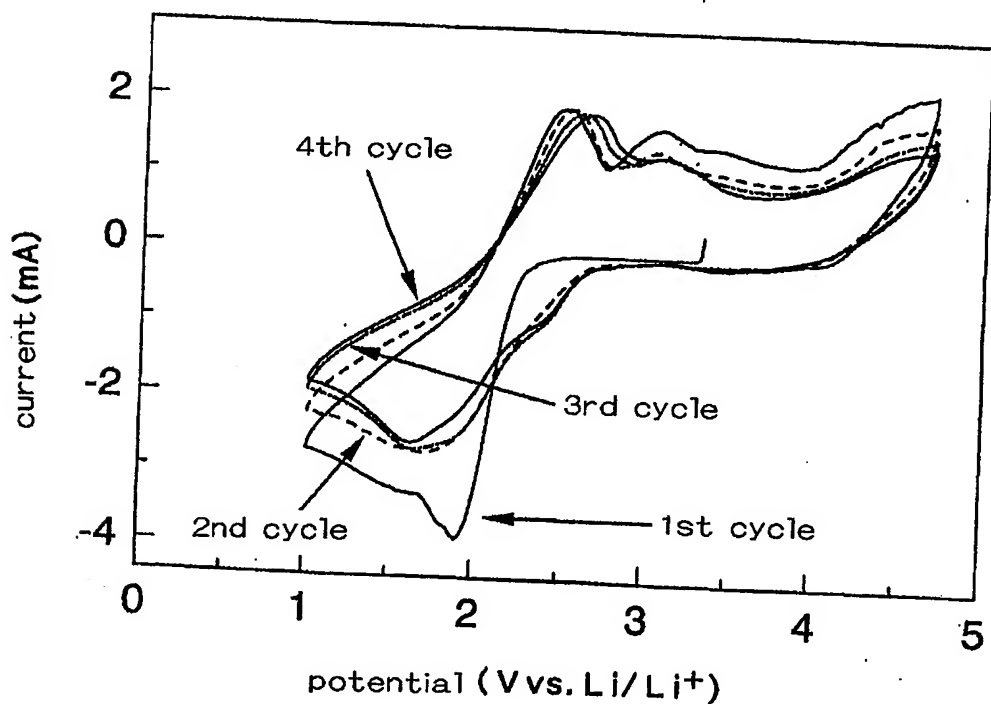


Fig. 9

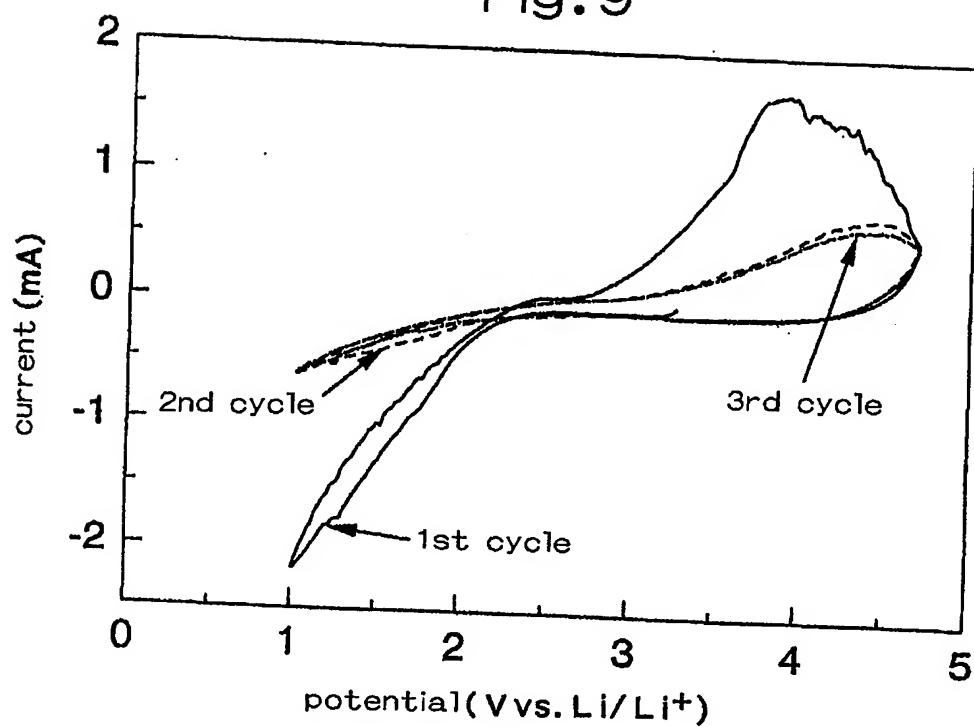


Fig. 10

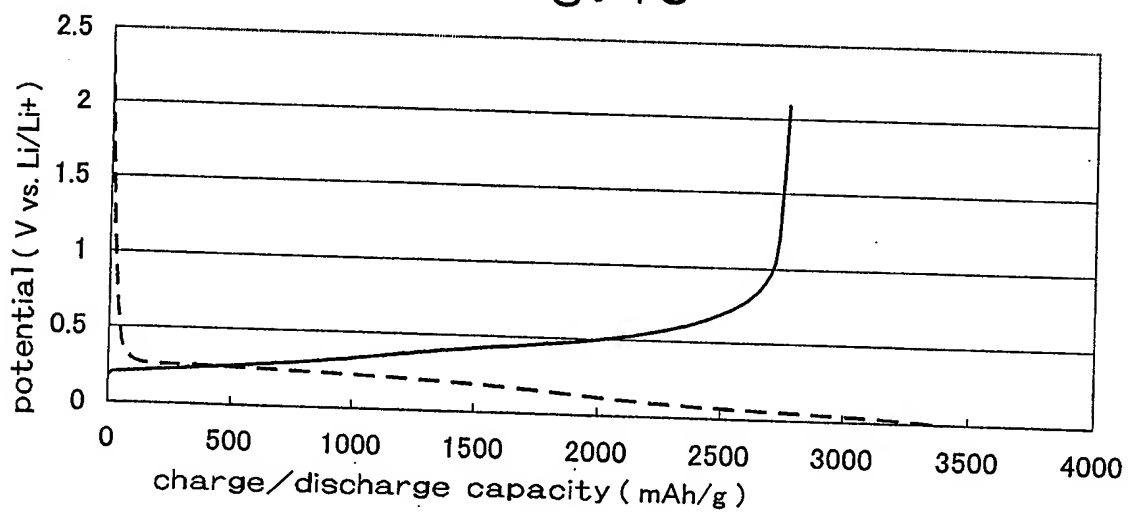


Fig. 11

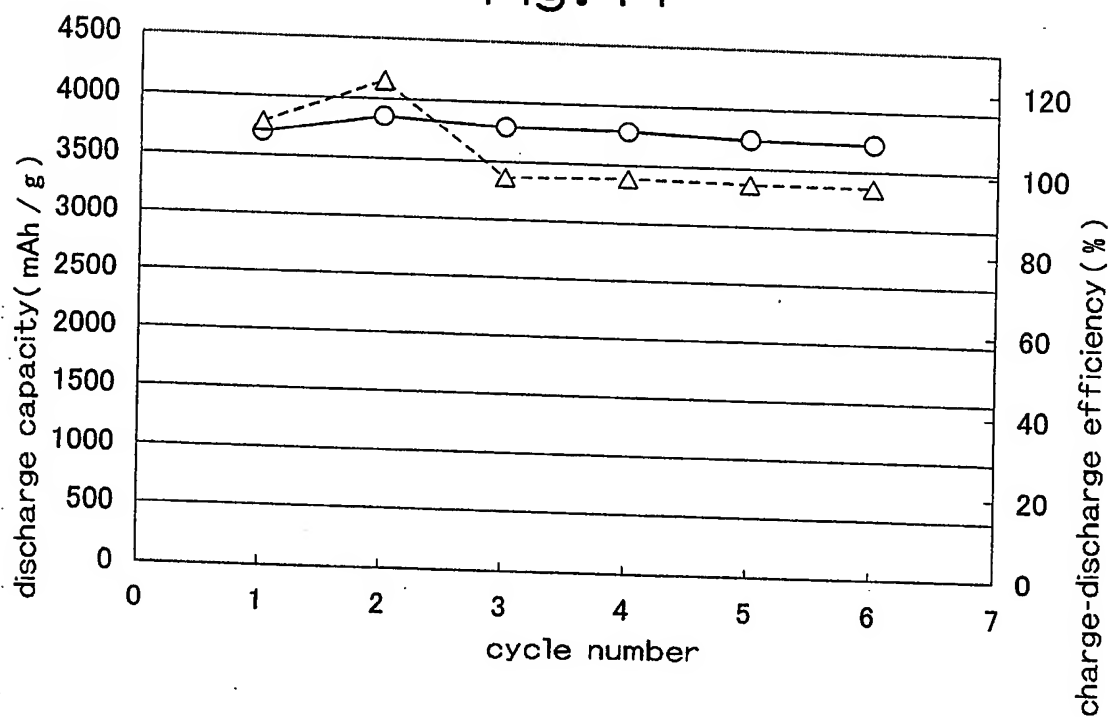


Fig. 12

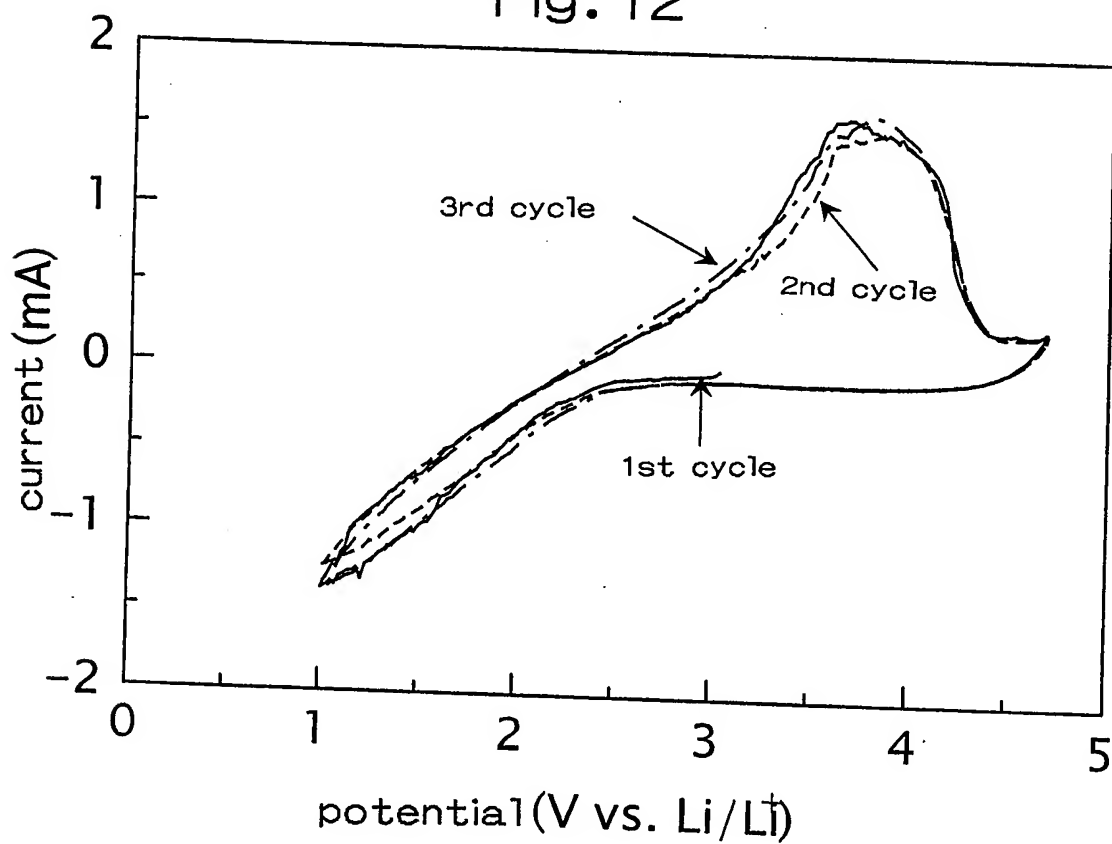


Fig. 13

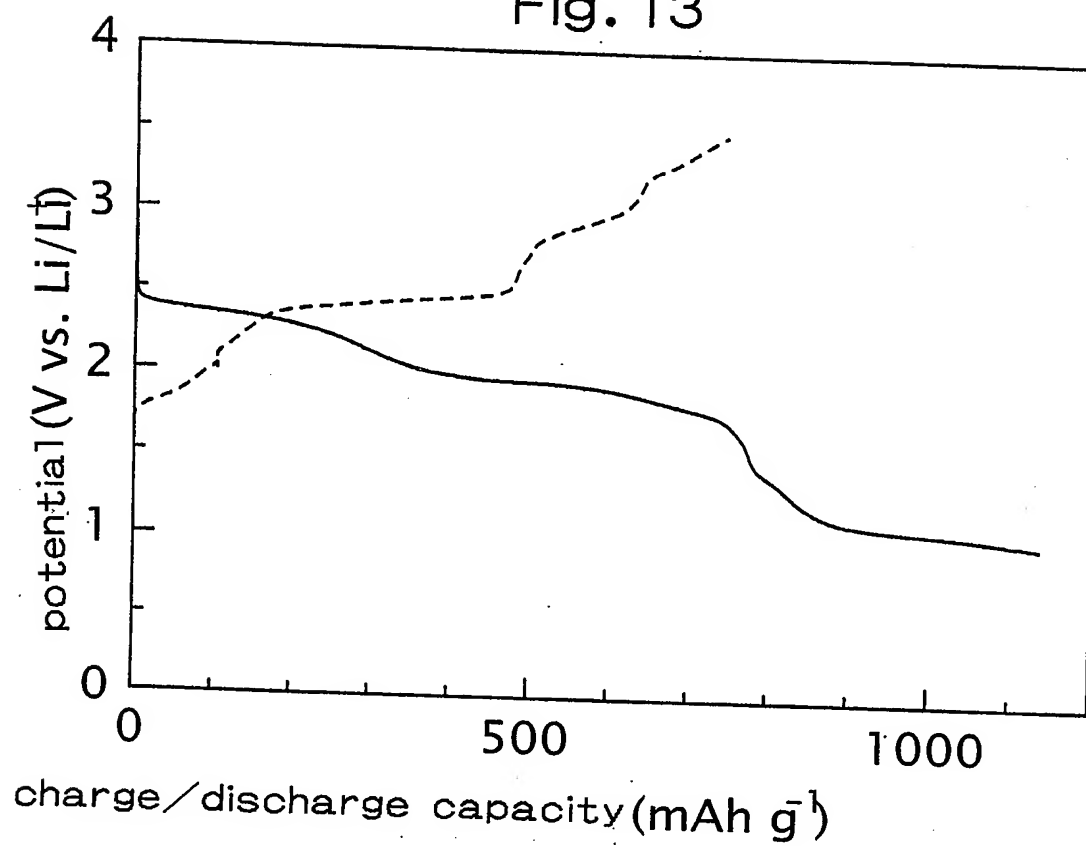


Fig. 14

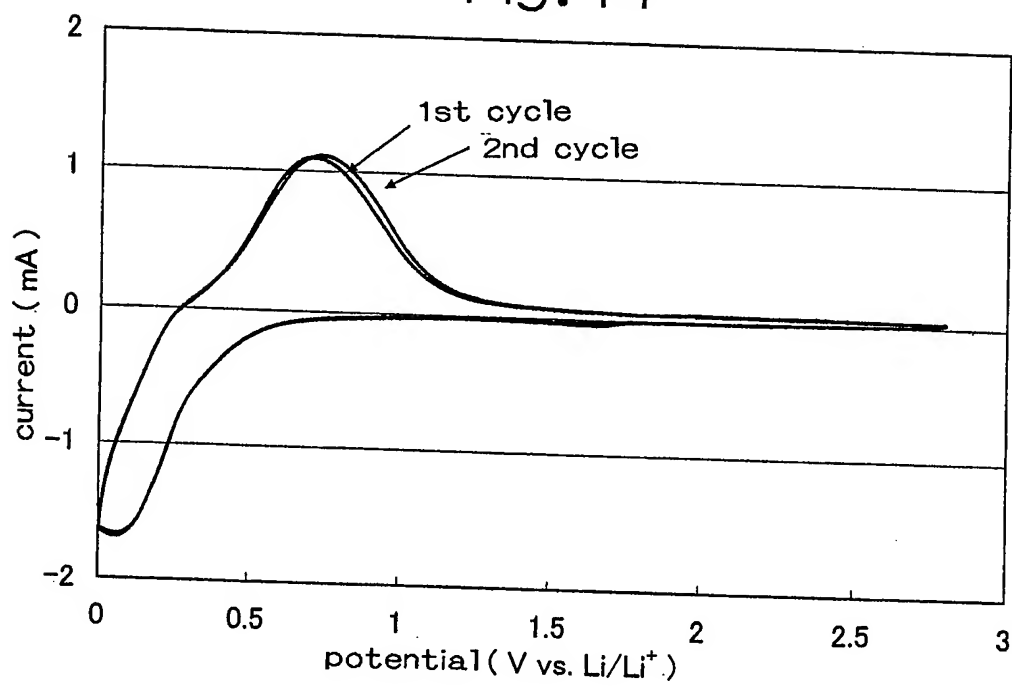


Fig. 15

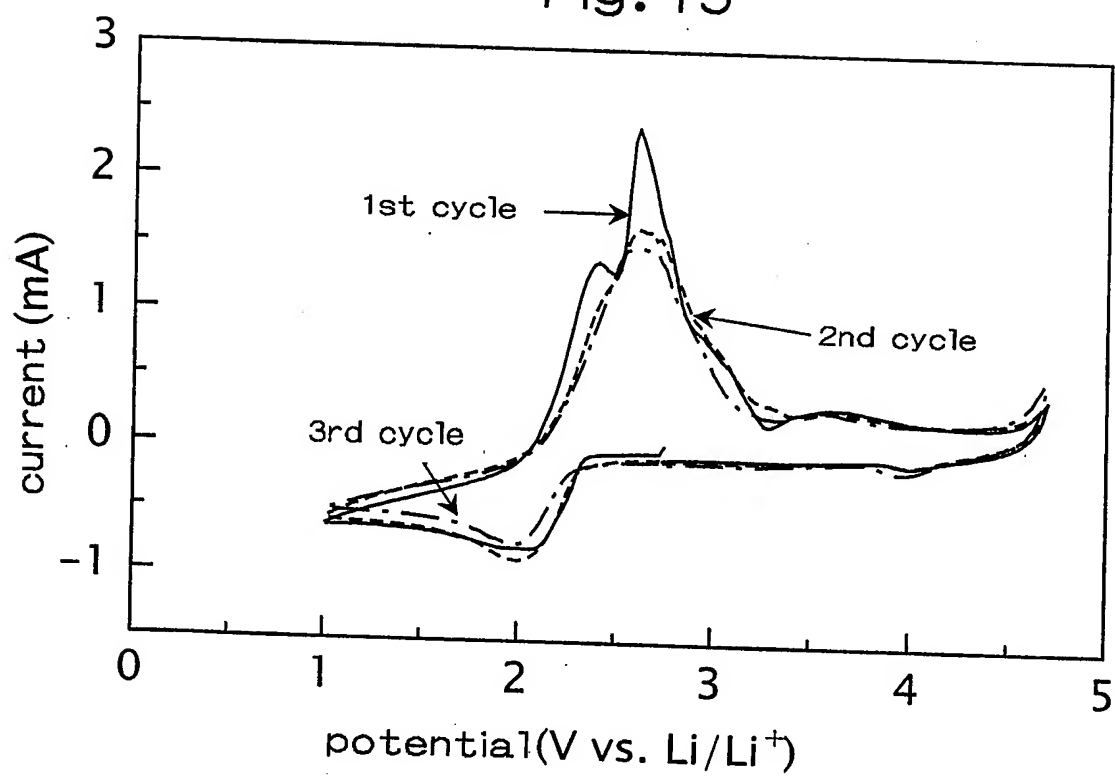


Fig. 16

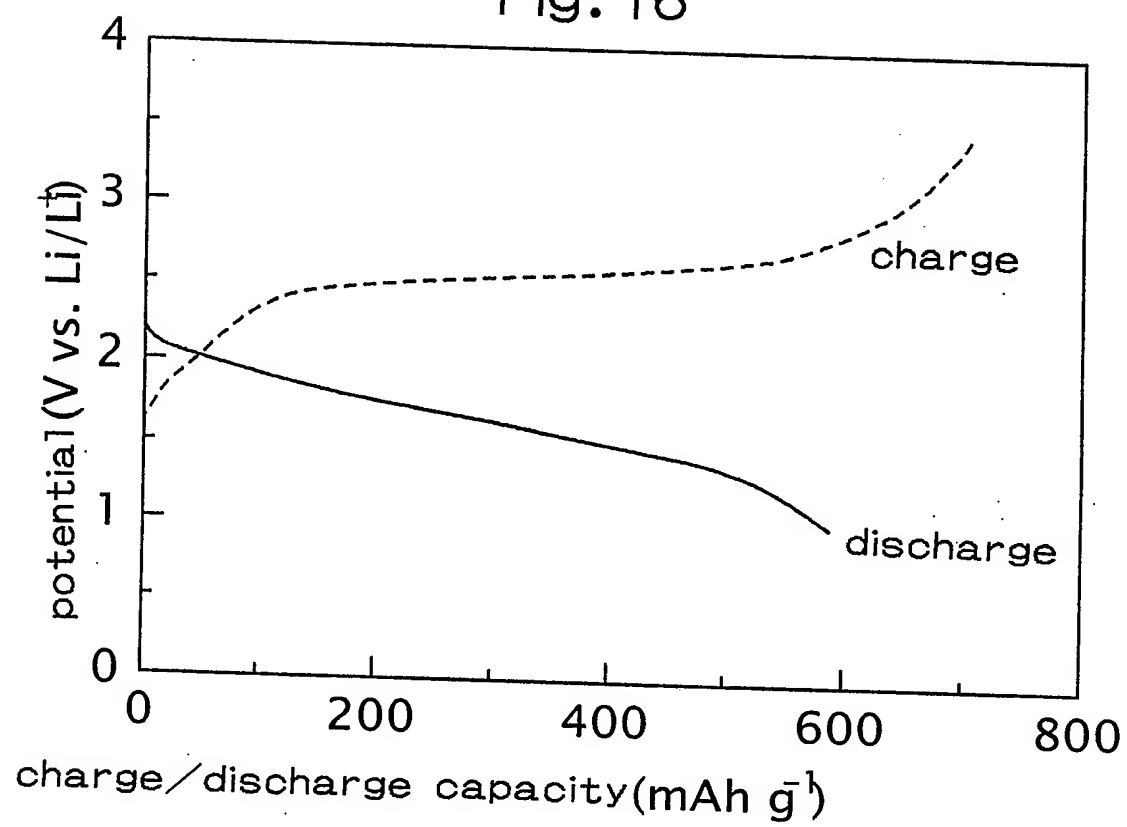


Fig. 17

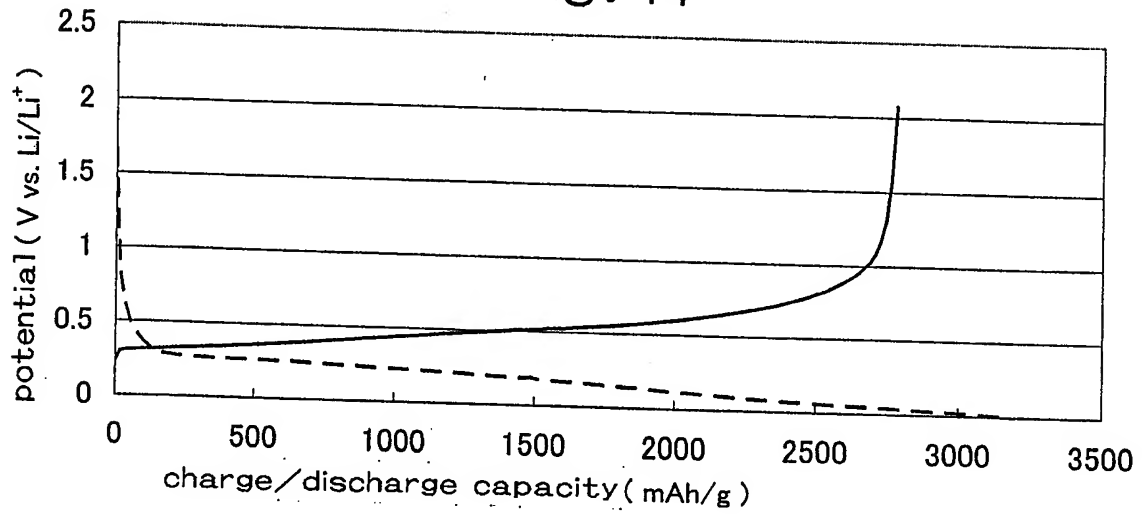


Fig. 18

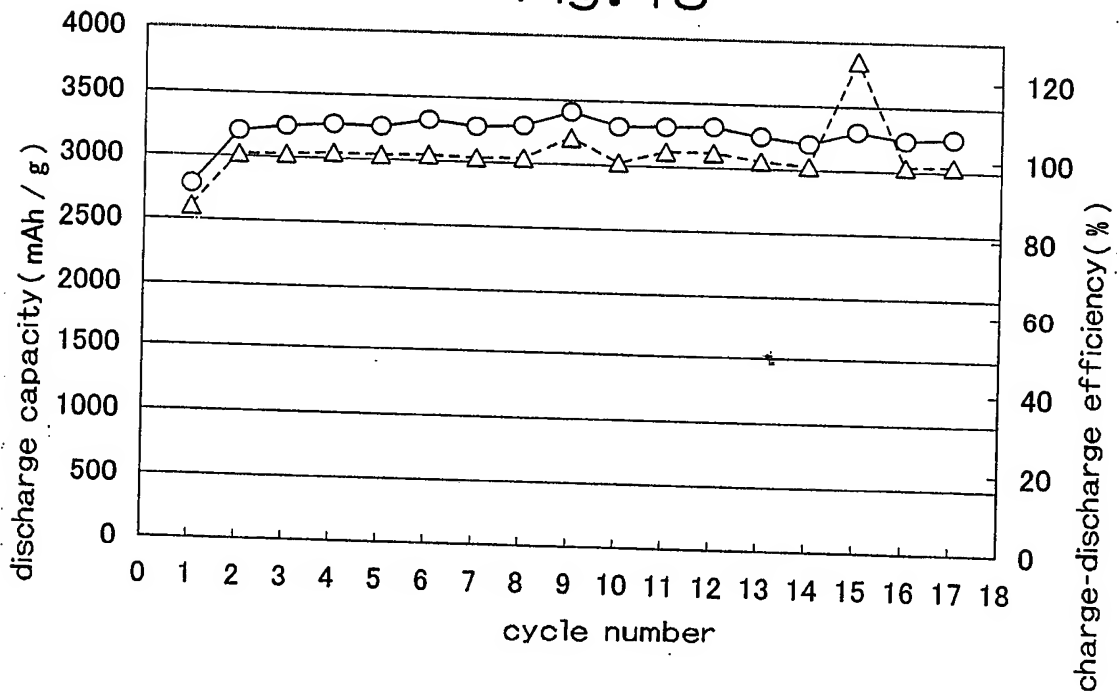




Fig. 19

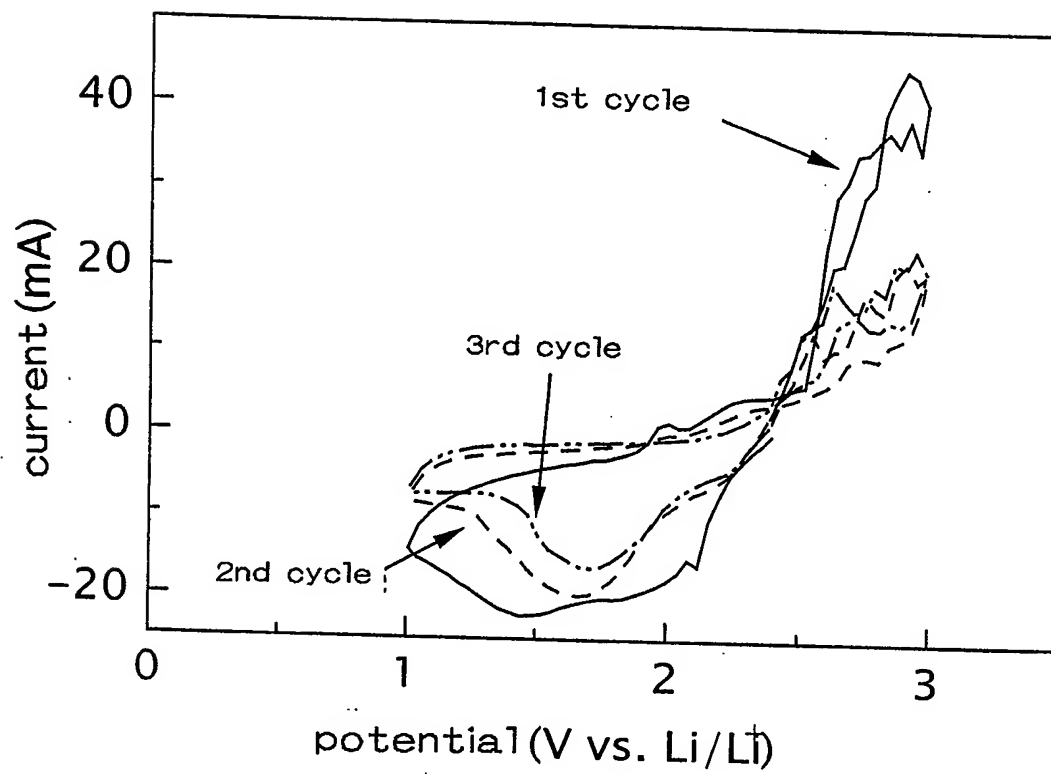


Fig. 20

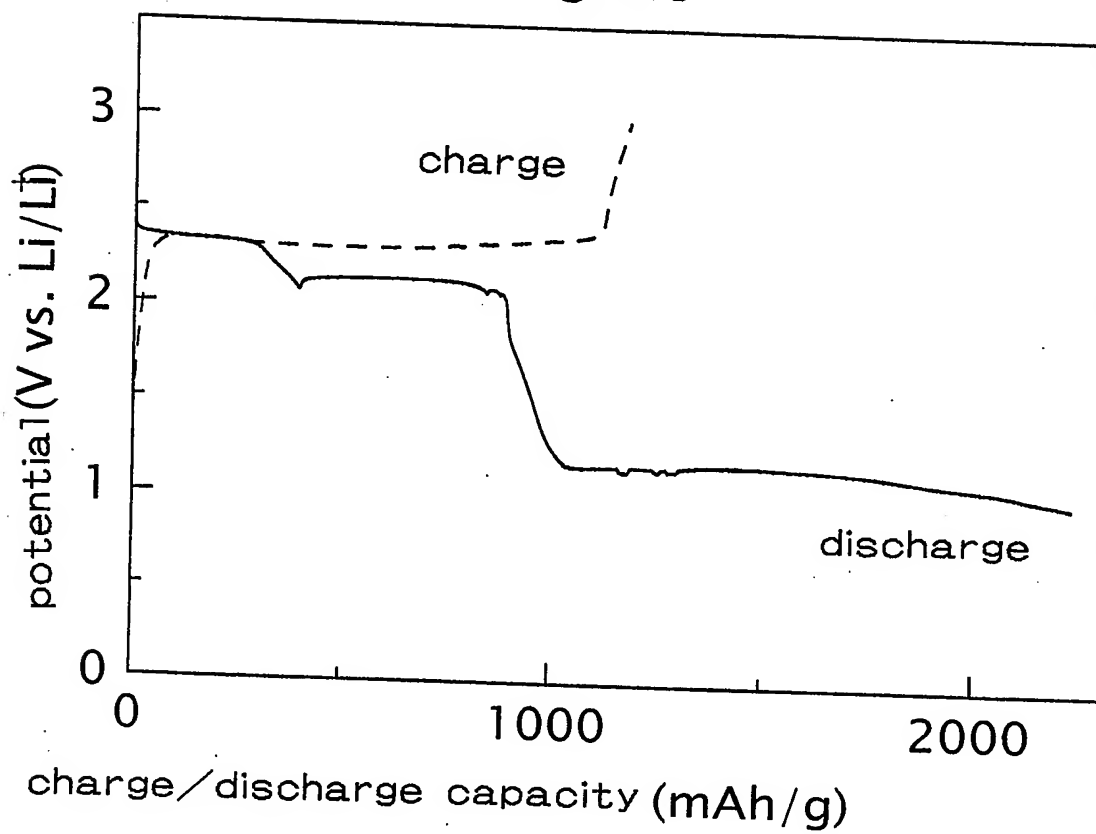


Fig.21

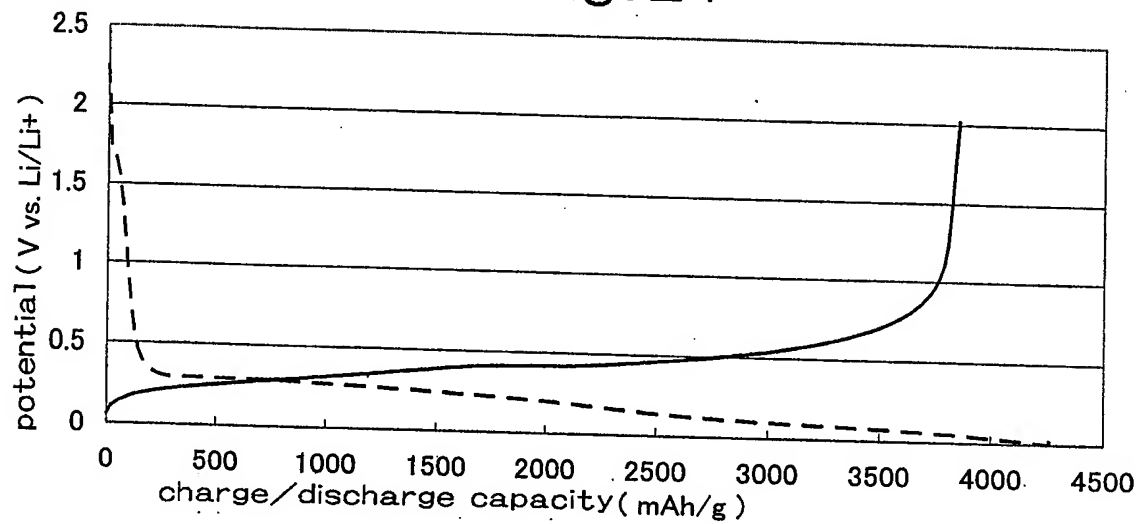


Fig.22

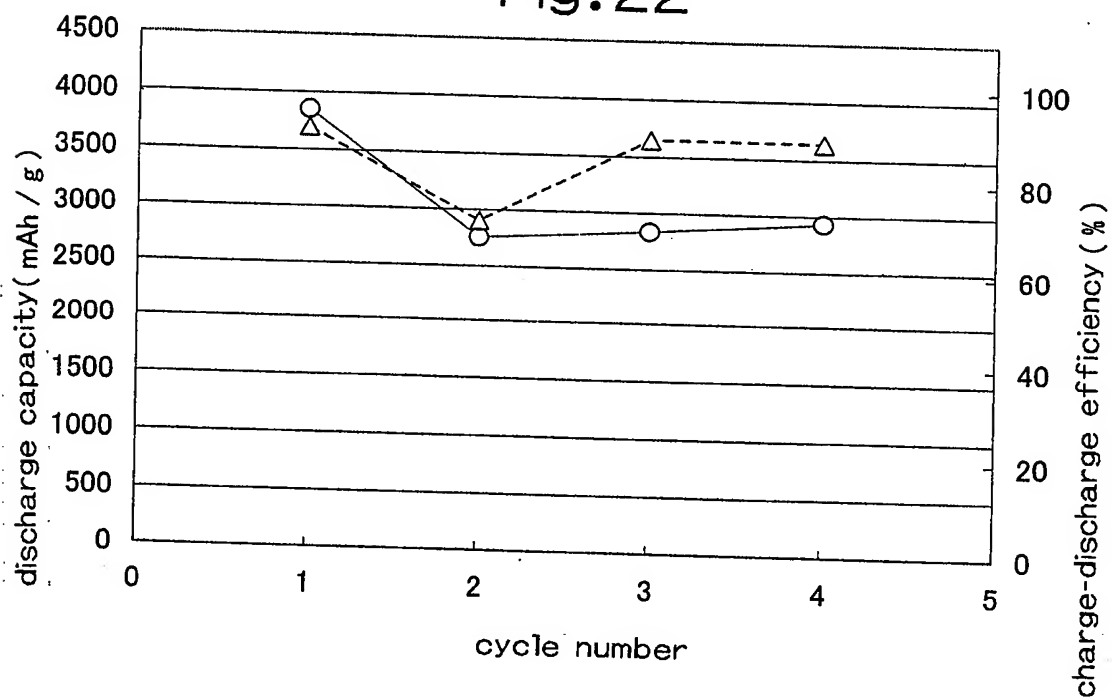


Fig.23

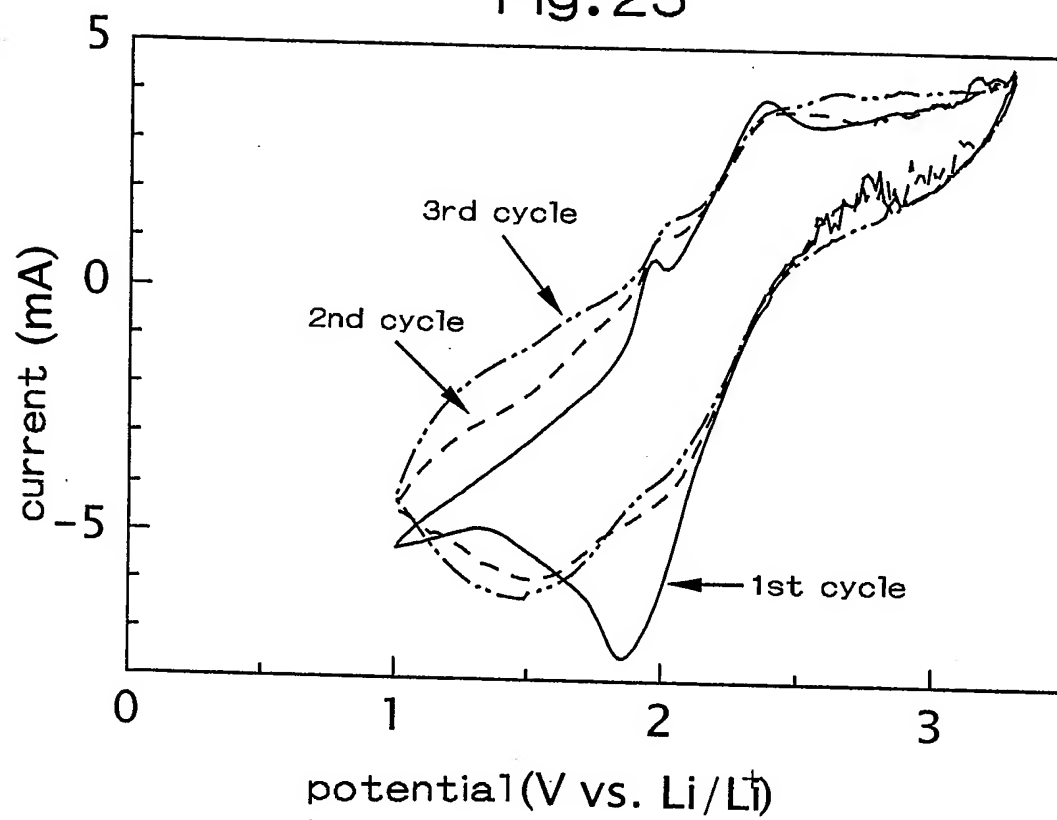


Fig. 24

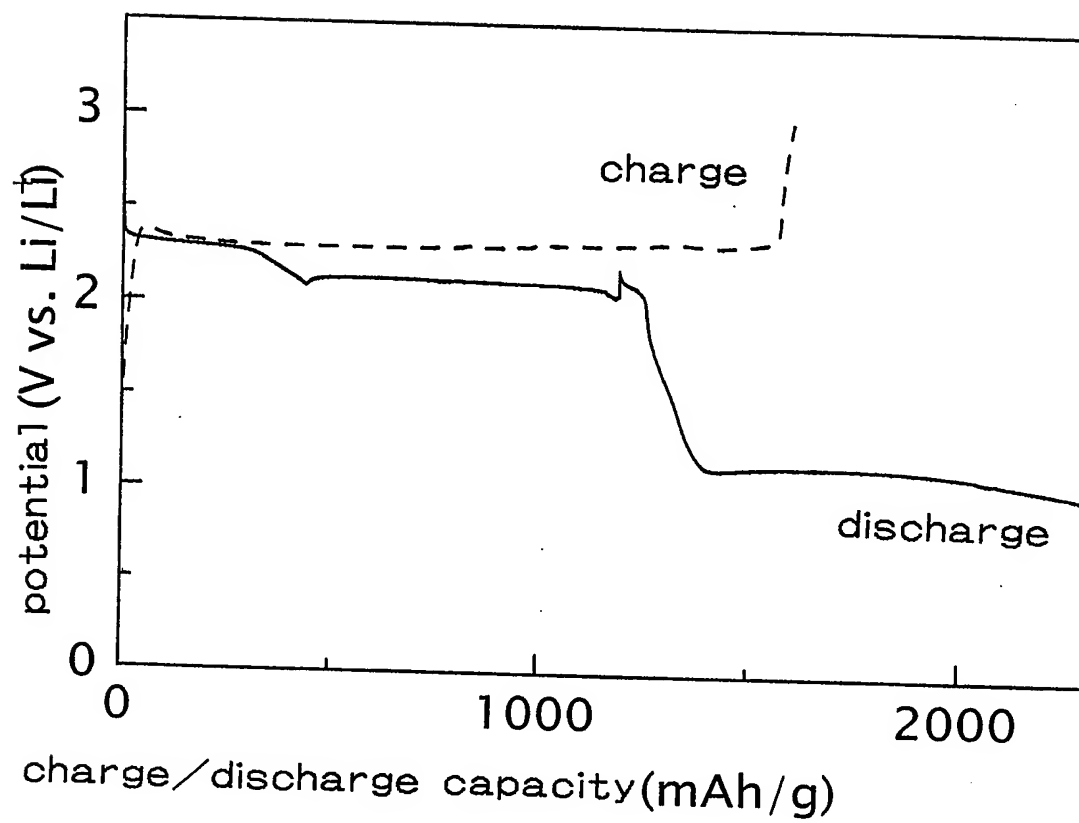


Fig. 25

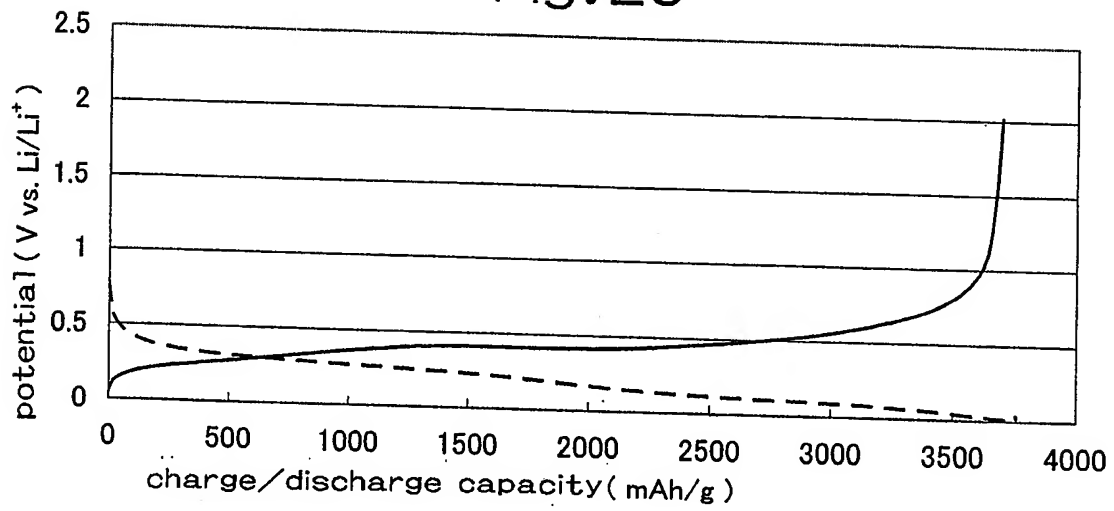


Fig. 26

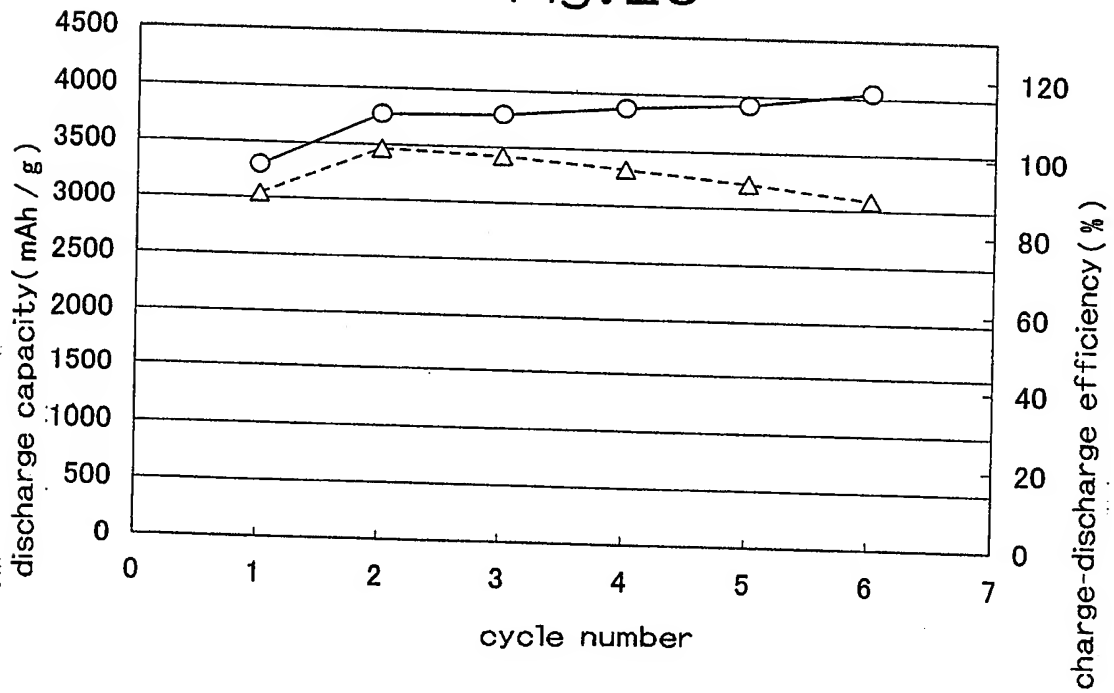


Fig. 27

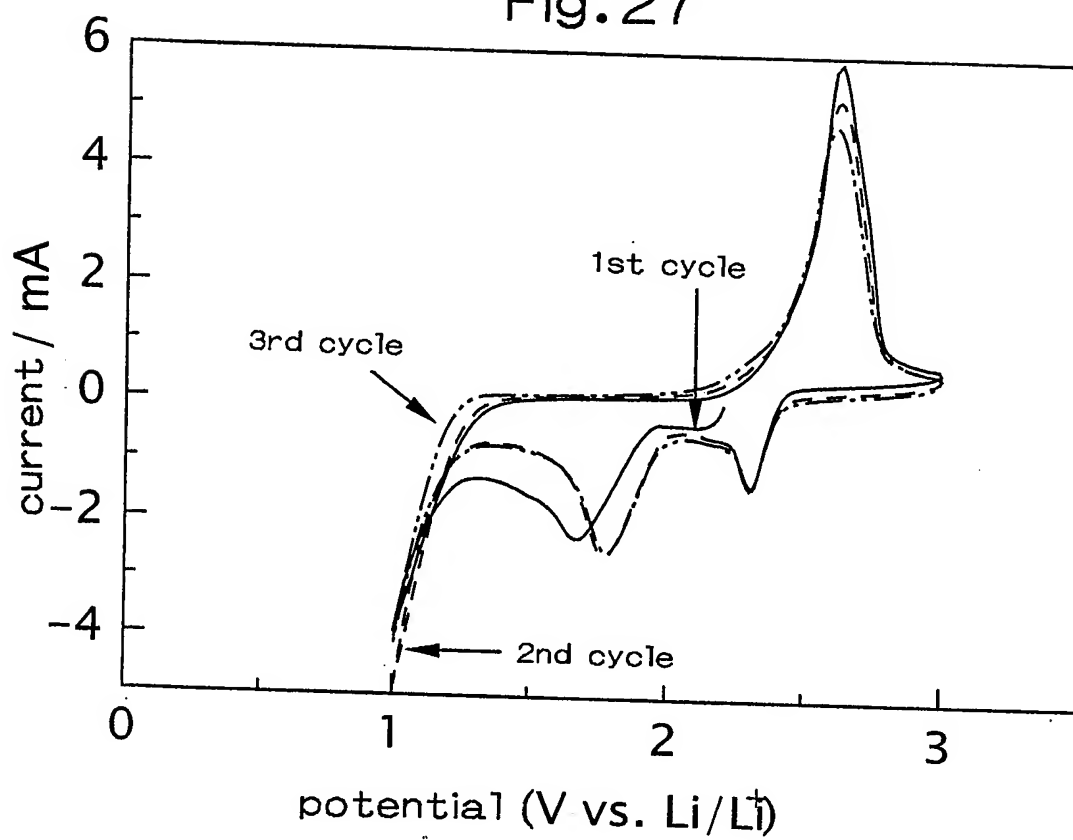


Fig. 28

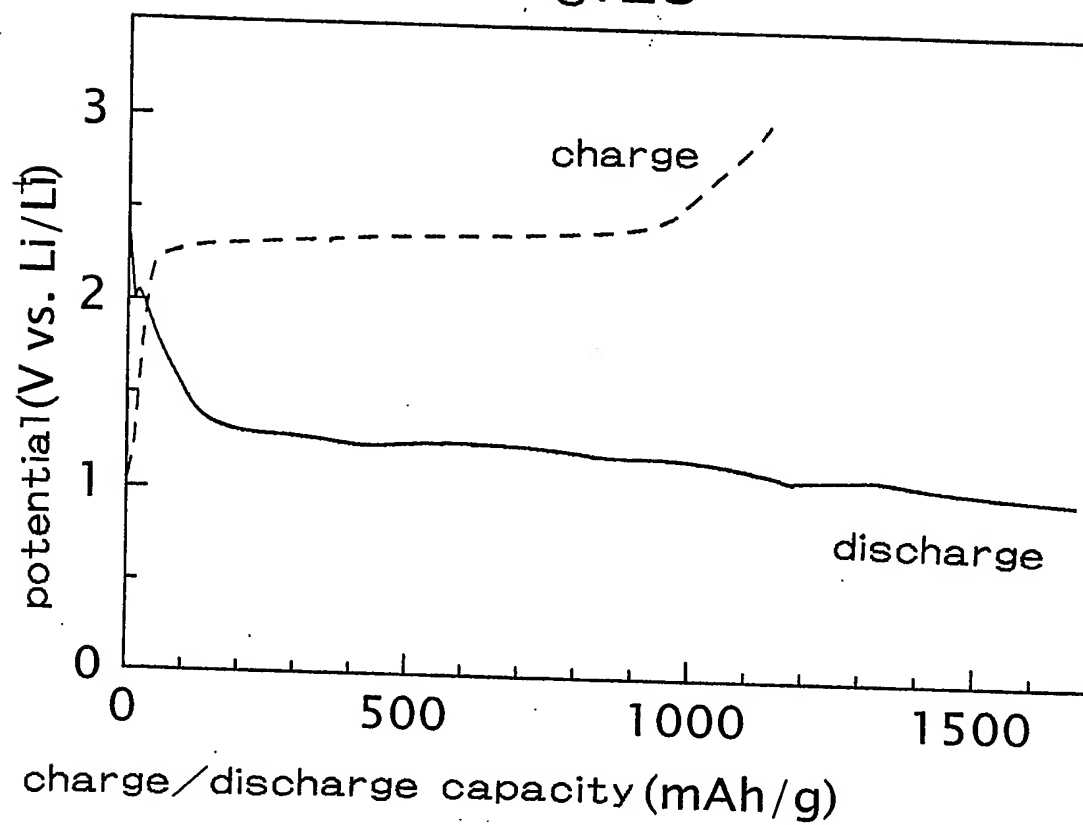




Fig.29

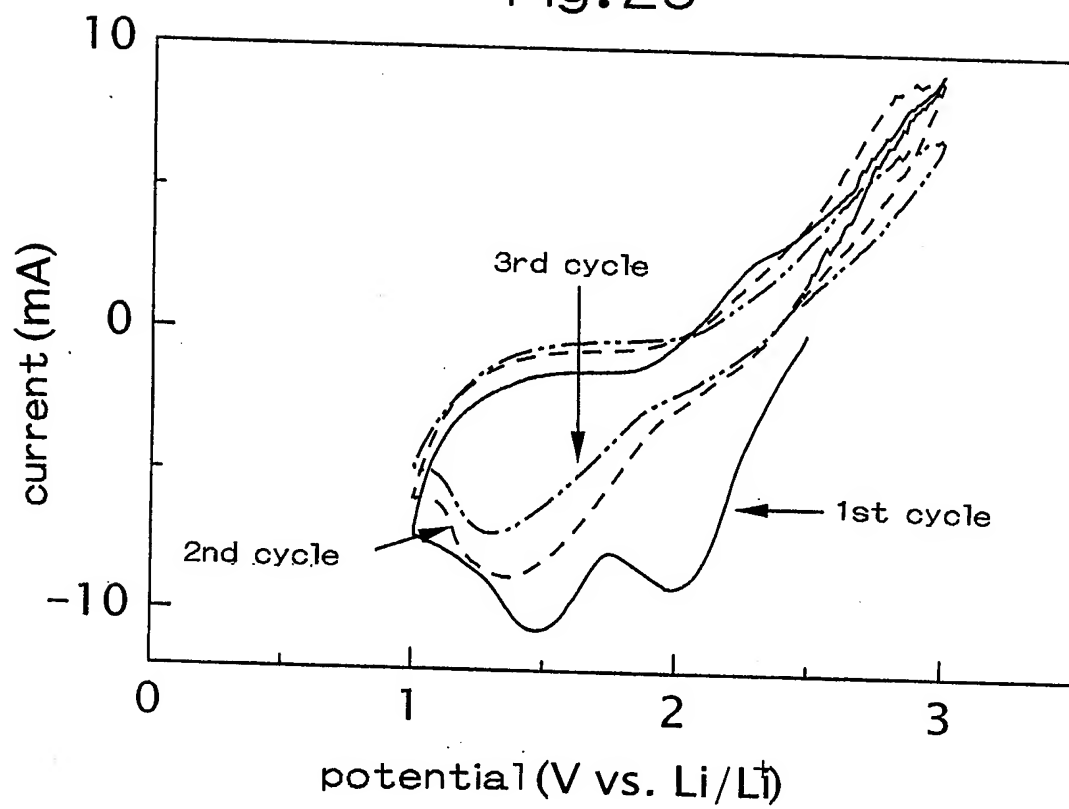


Fig. 30

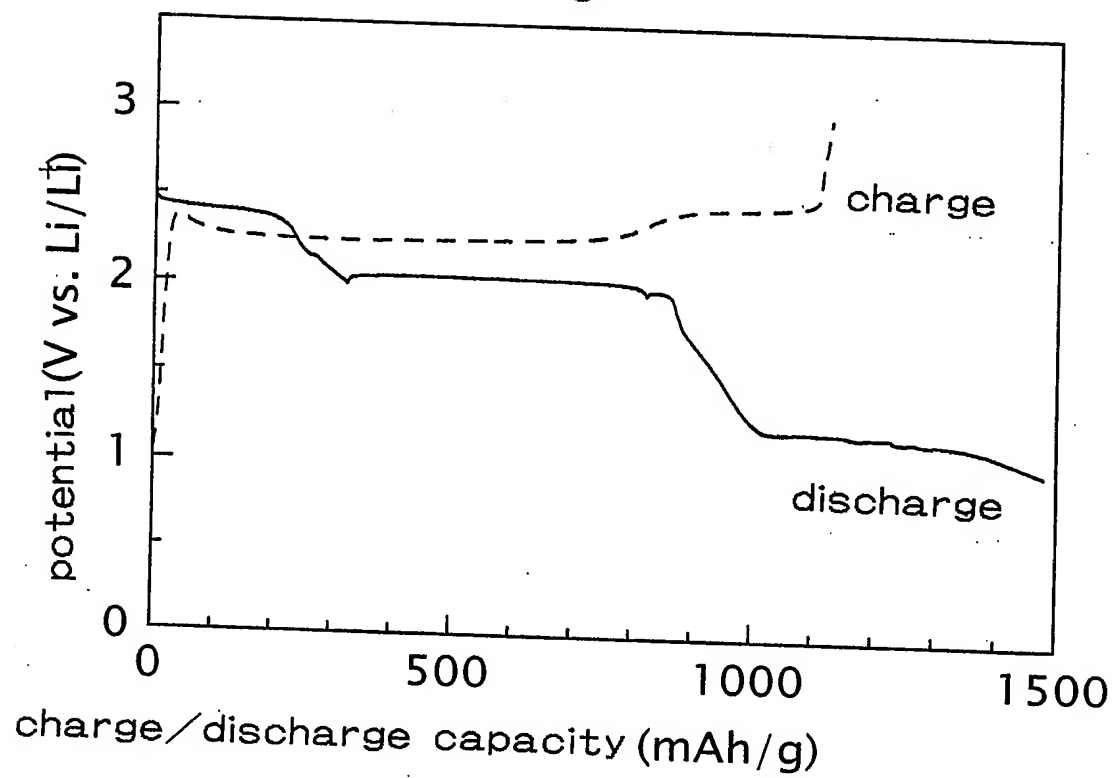


Fig. 31

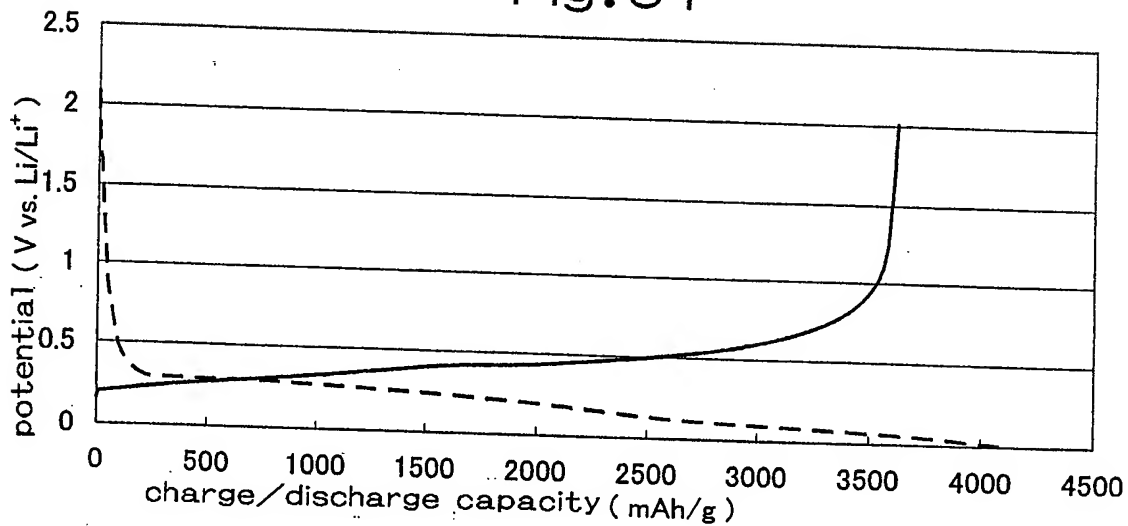


Fig. 32

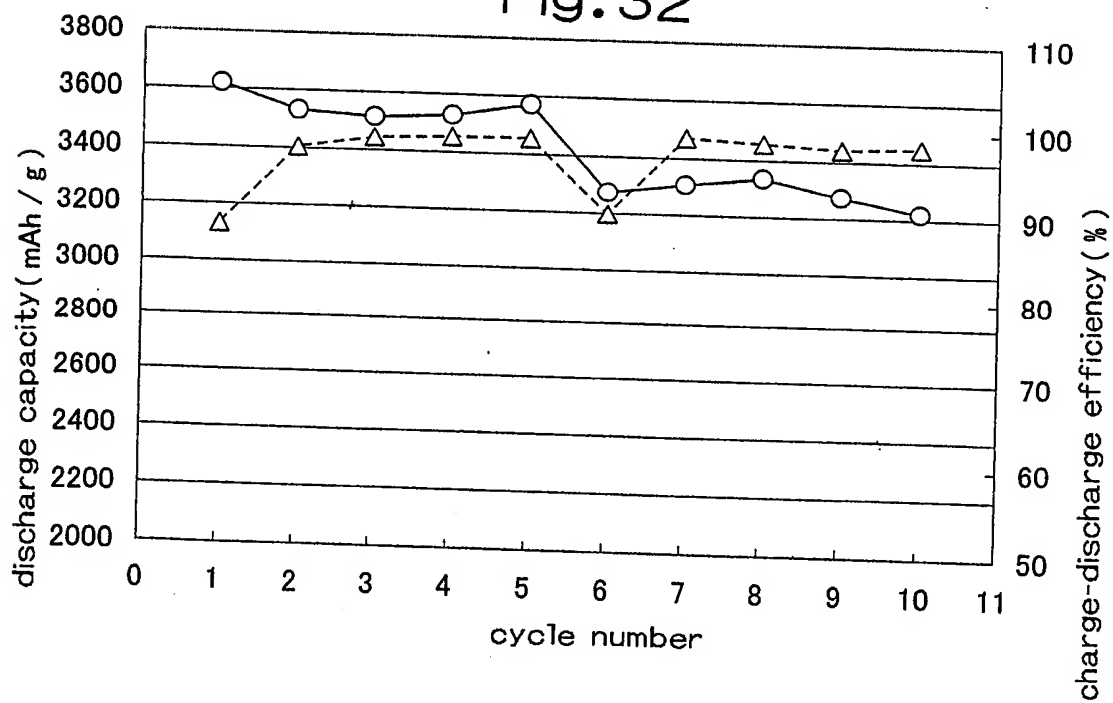


Fig.33

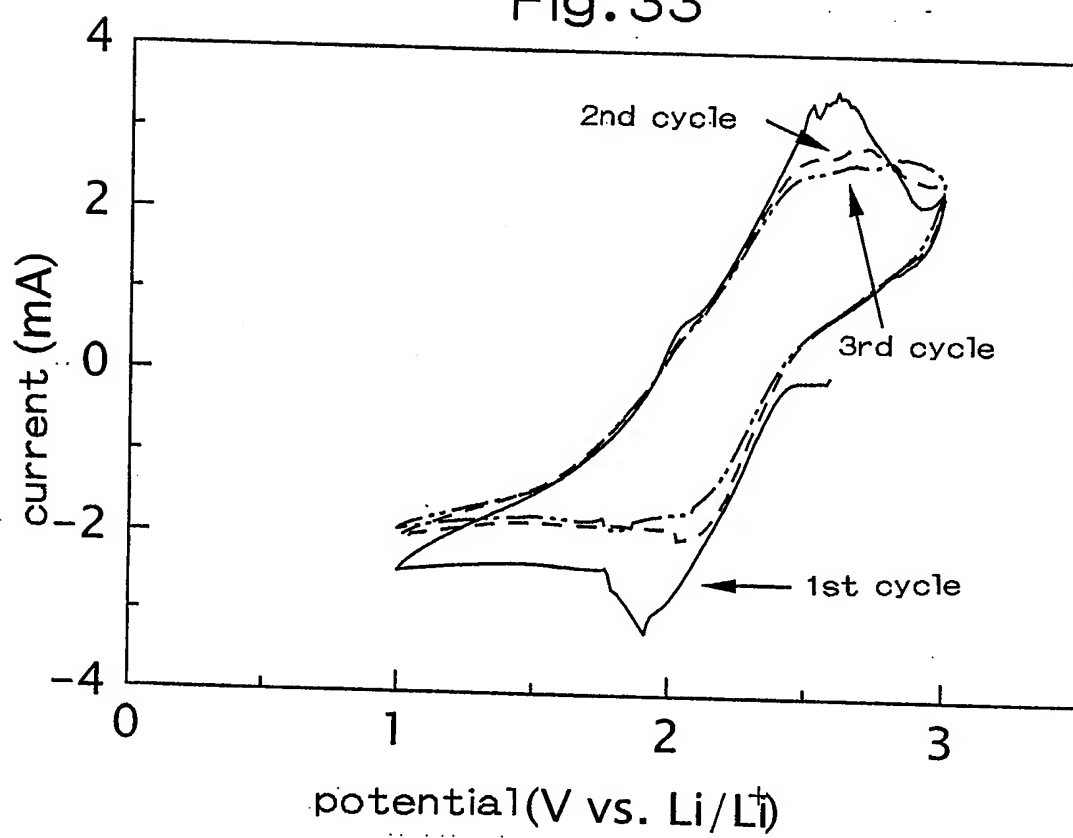


Fig.34

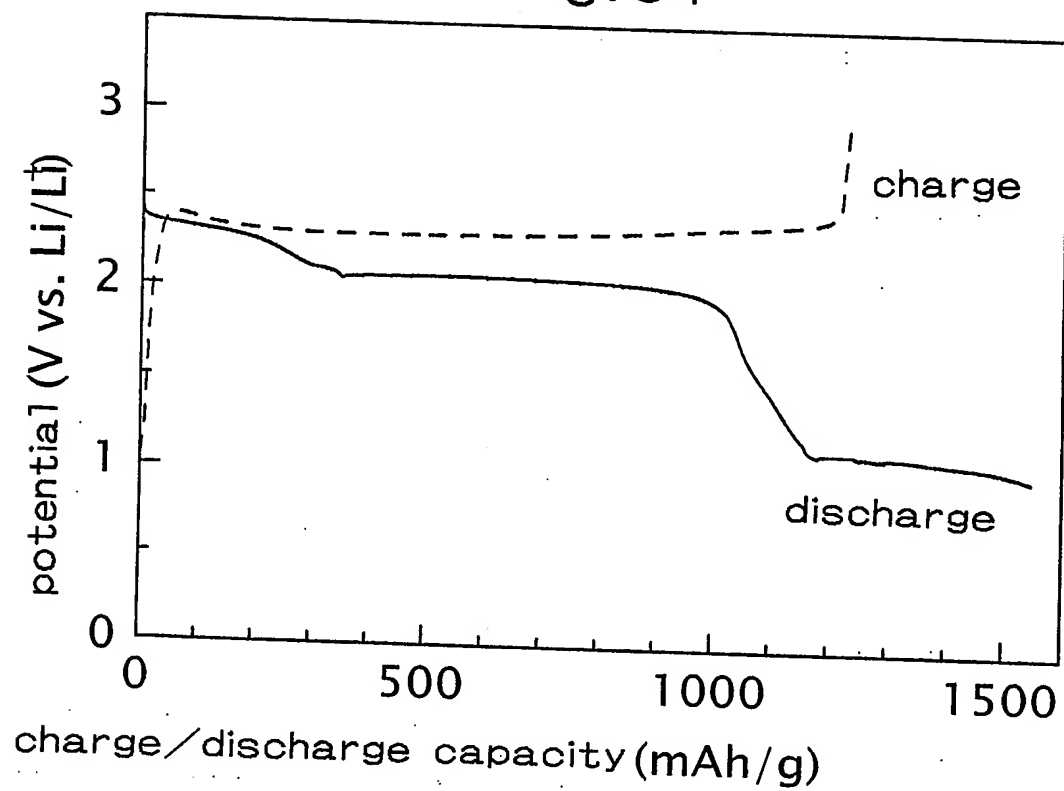


Fig. 35

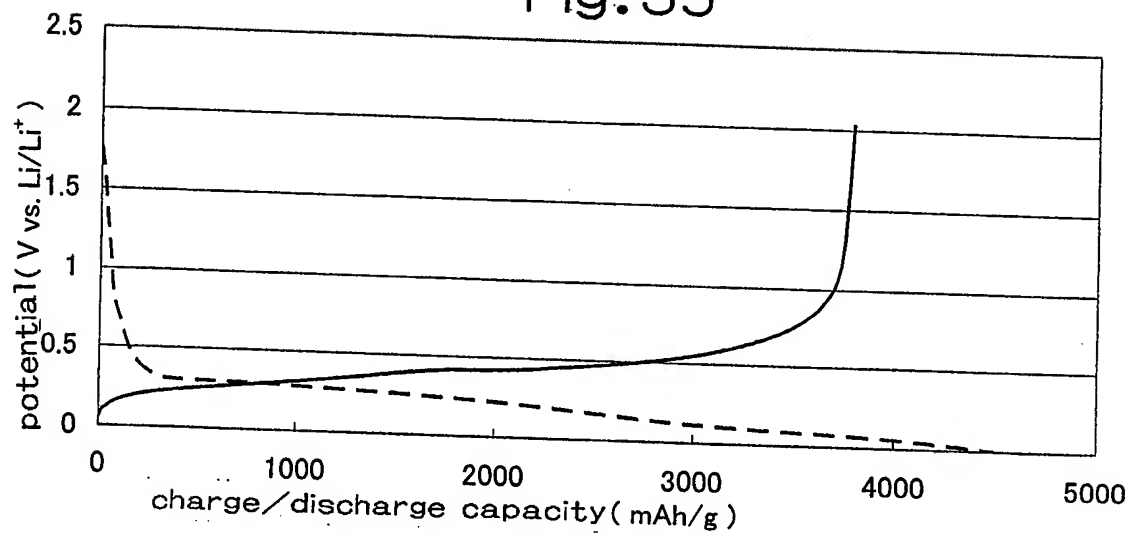


Fig. 36

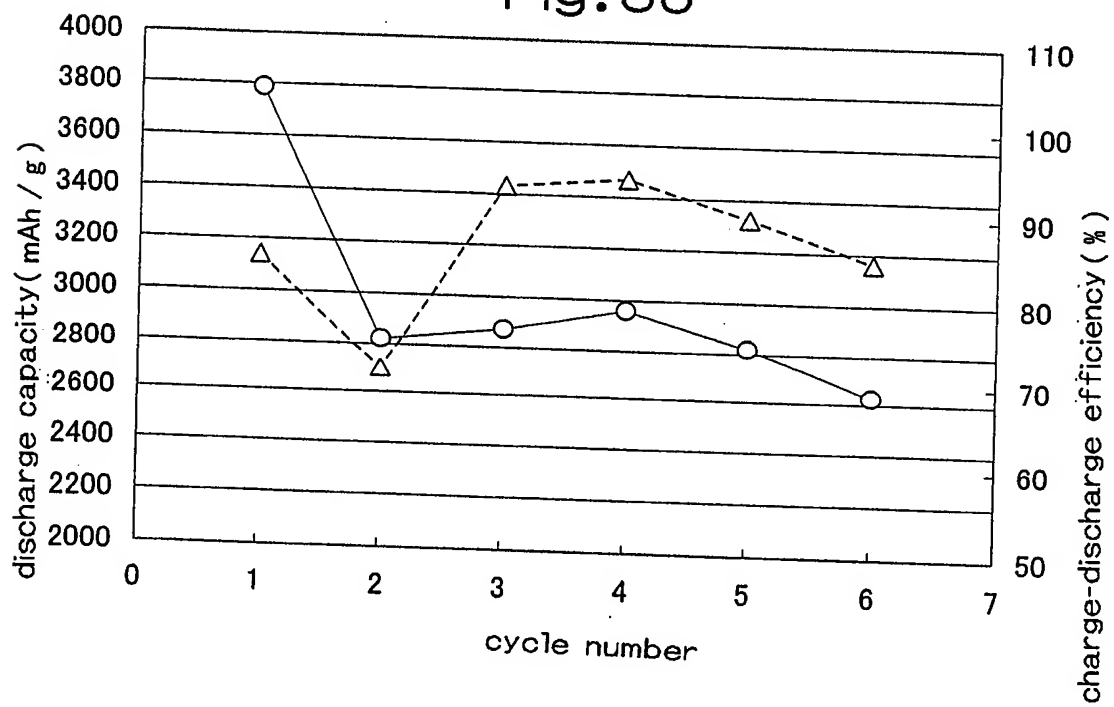


Fig.37

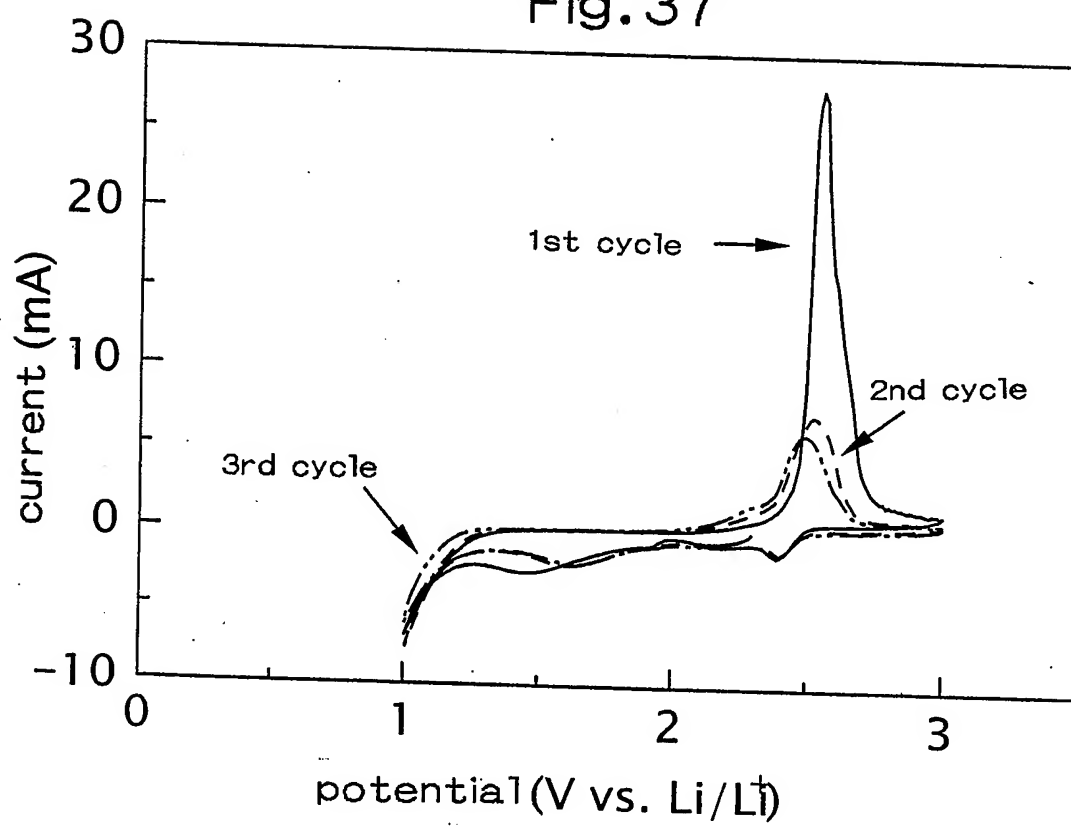


Fig.38

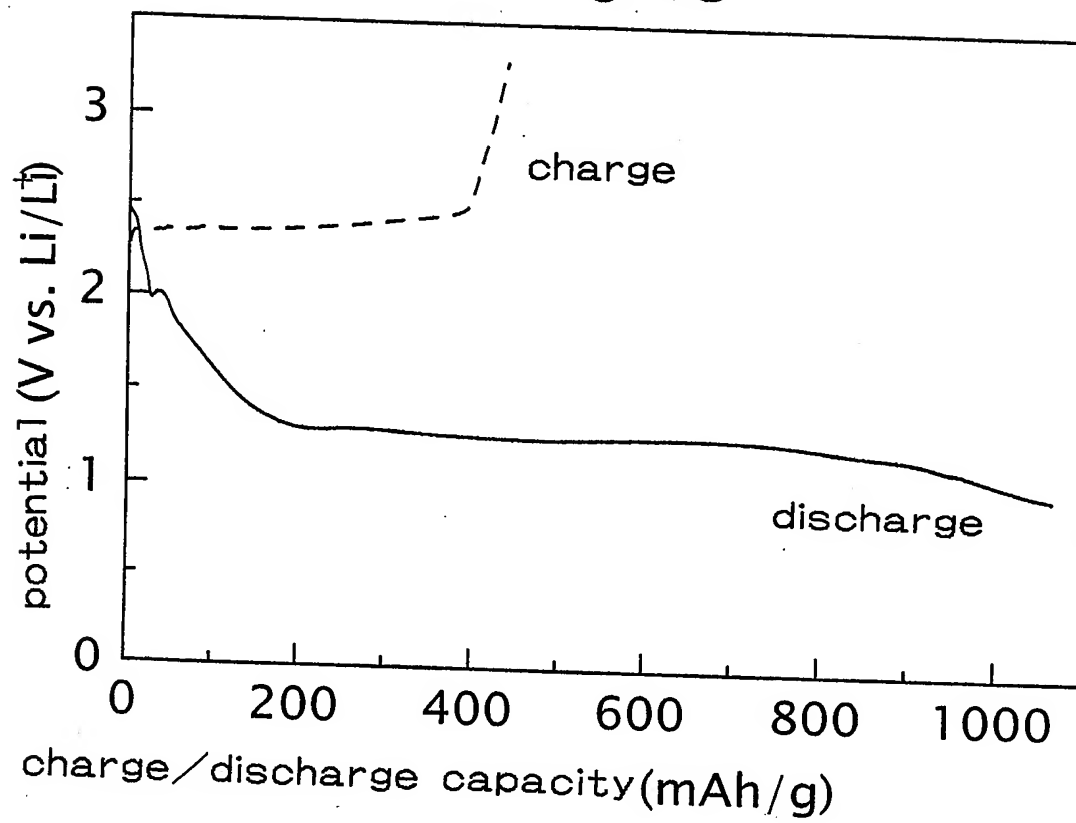




Fig. 39

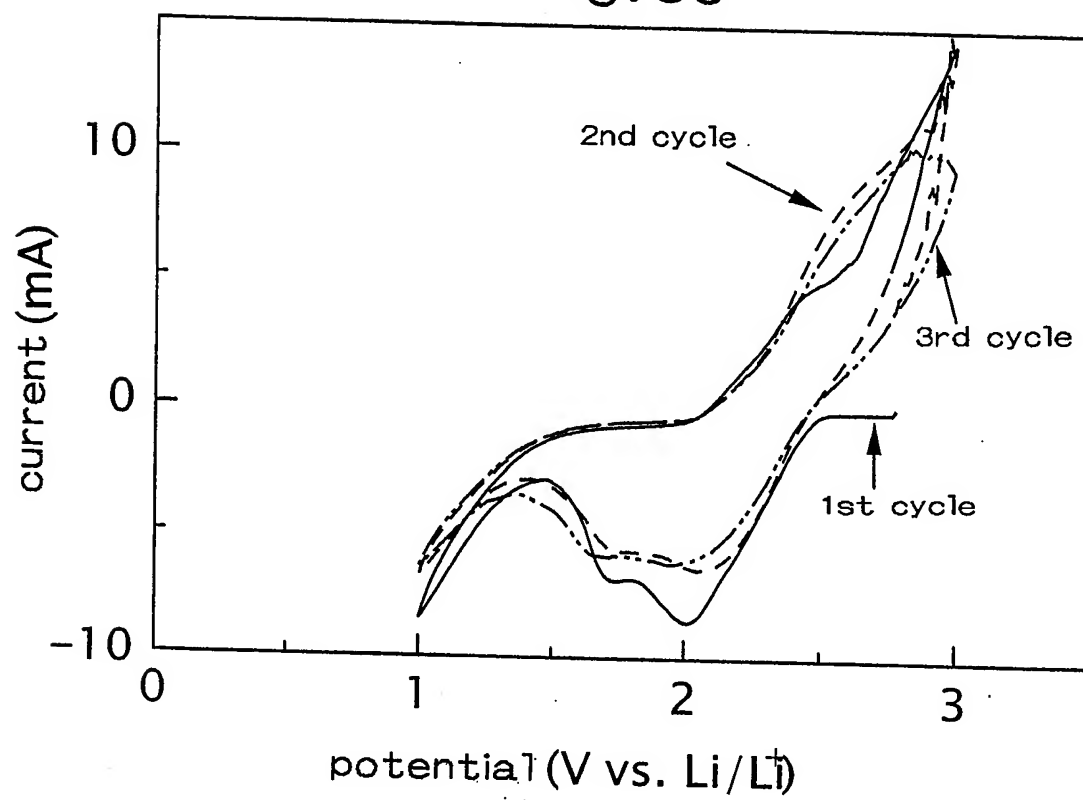


Fig. 40

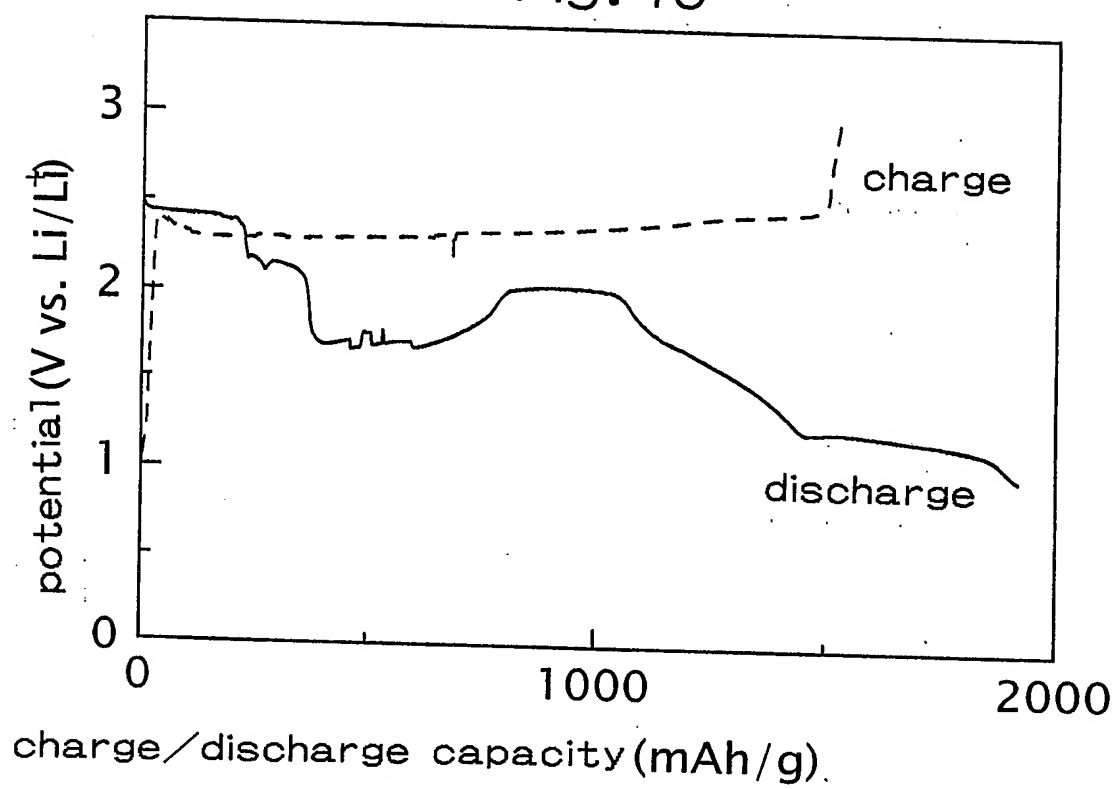


Fig.41

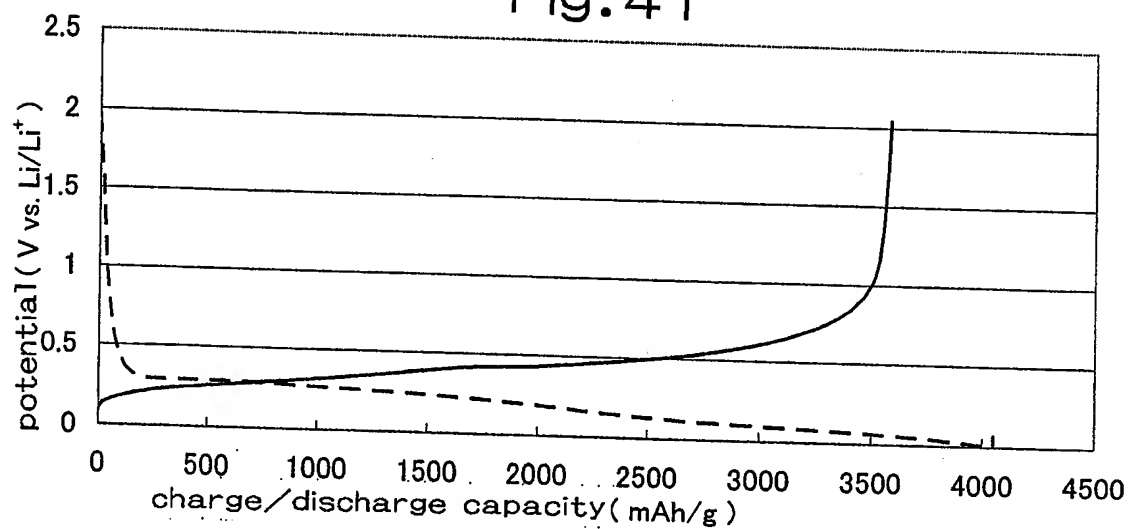


Fig.42

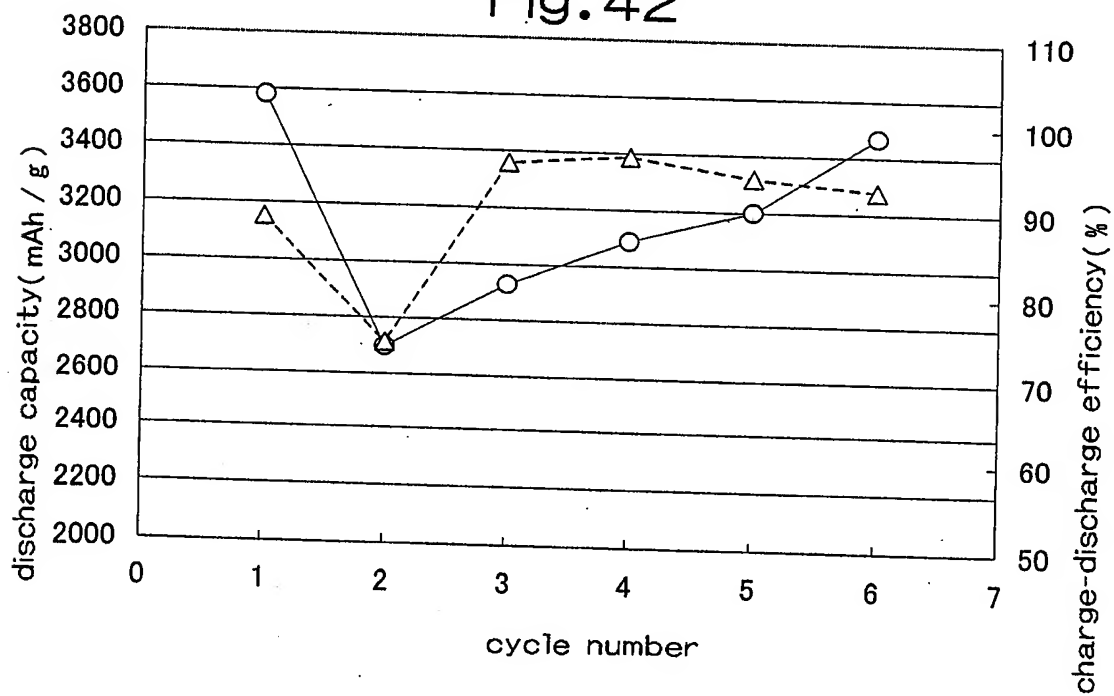


Fig.43

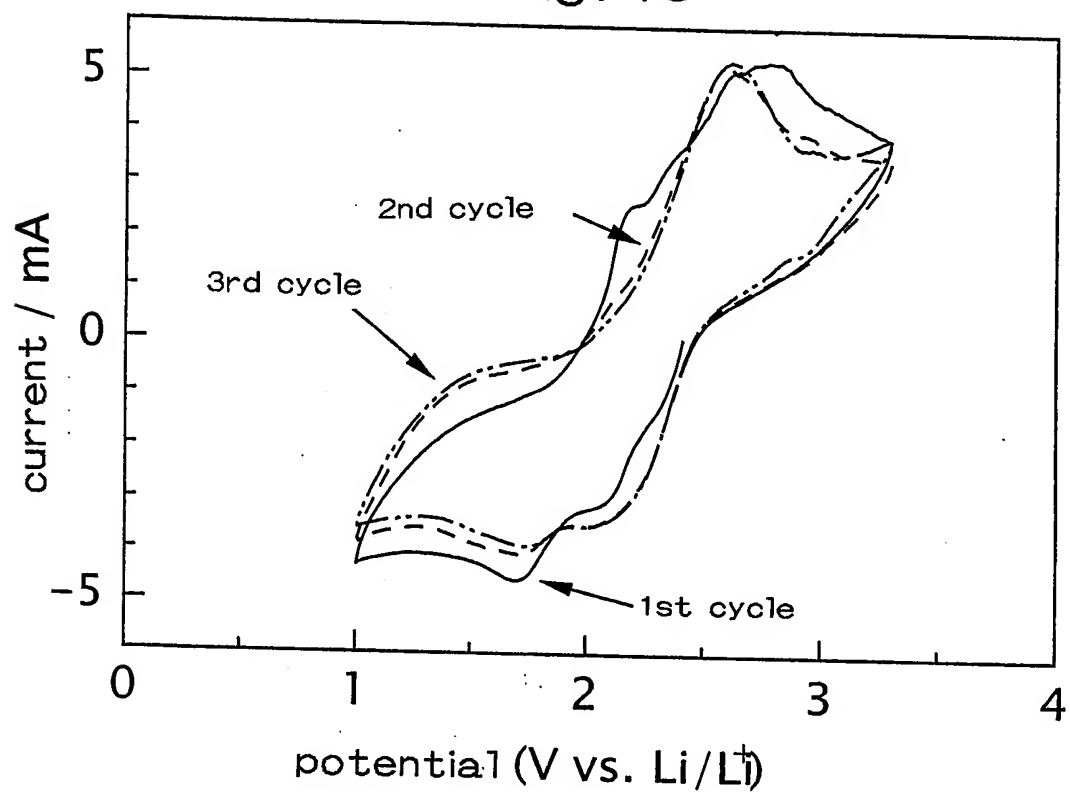


Fig. 44

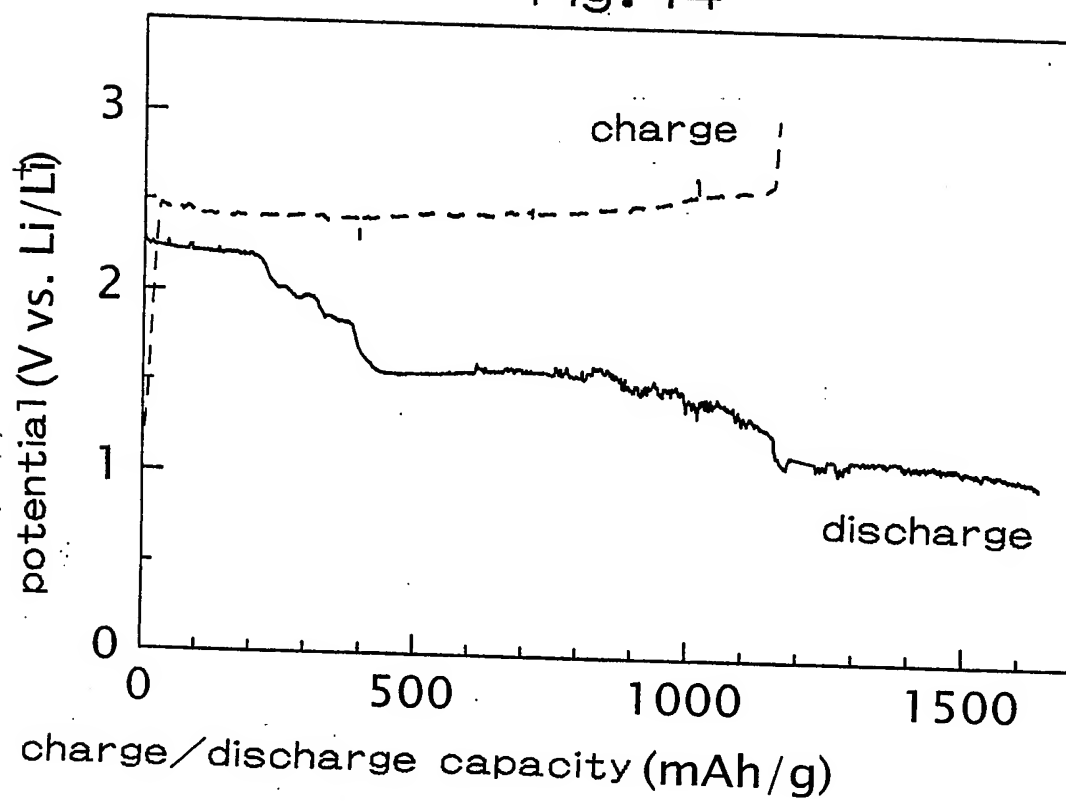


Fig.45

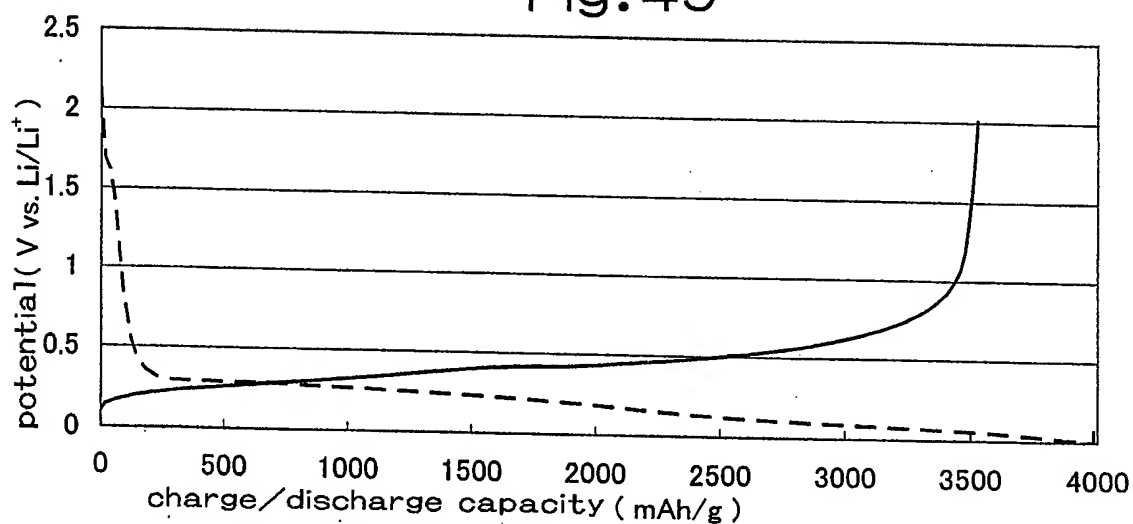


Fig.46

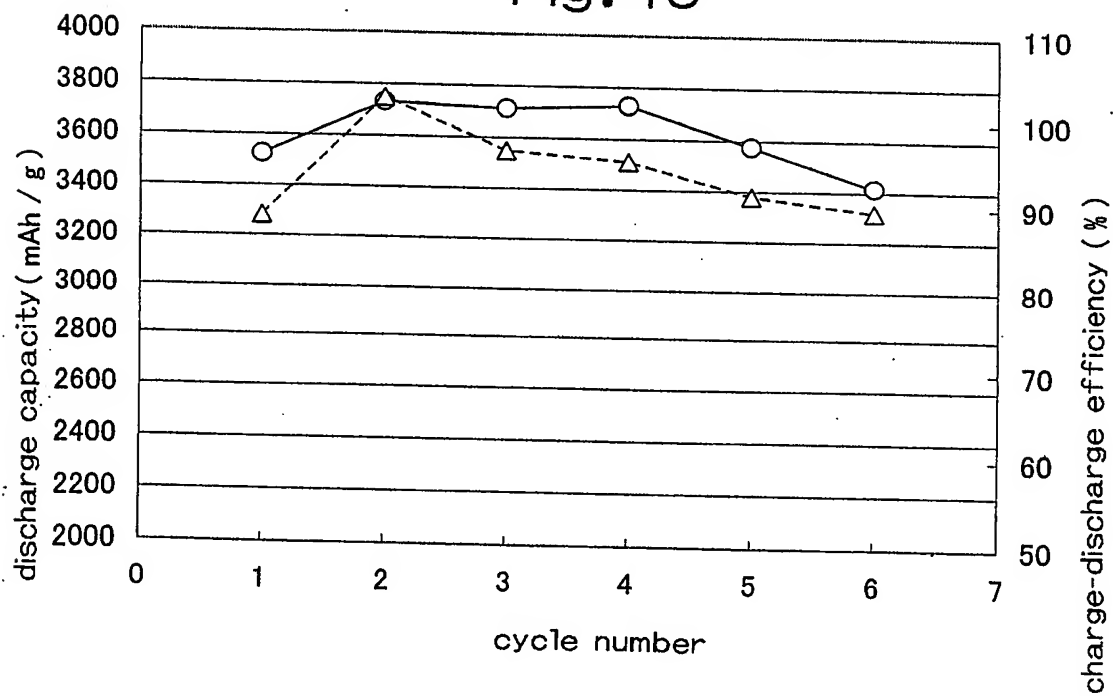


Fig.47

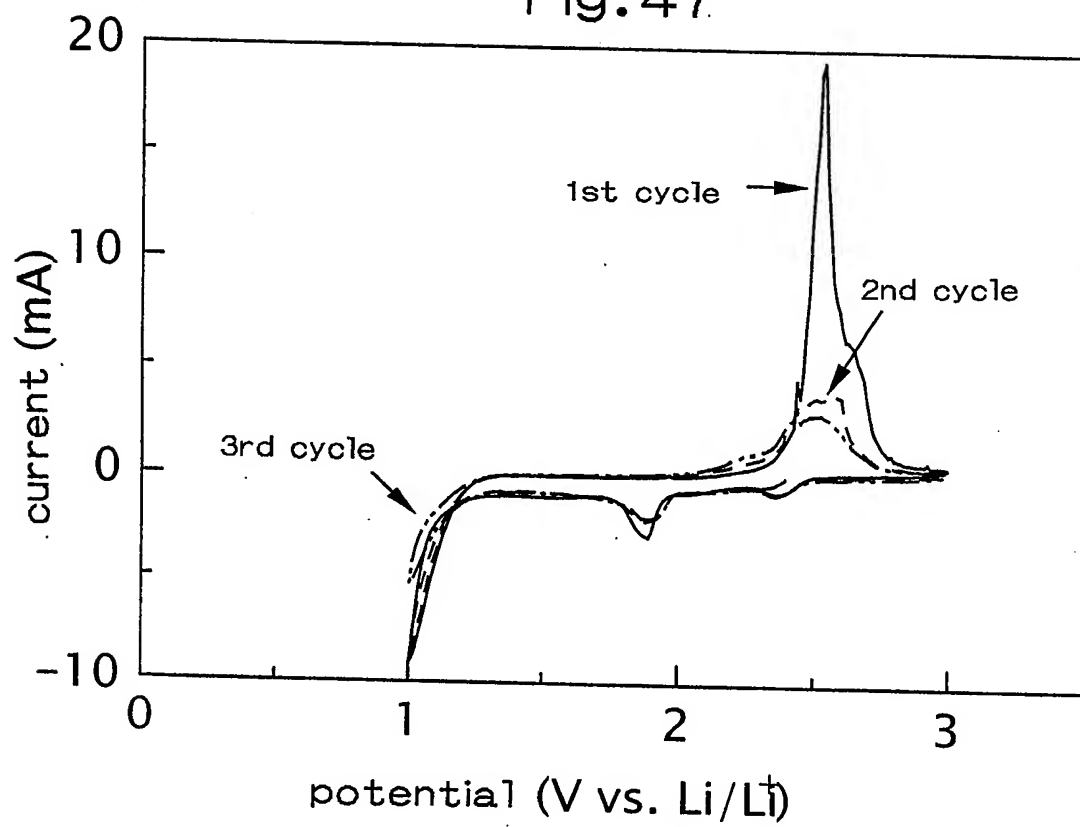
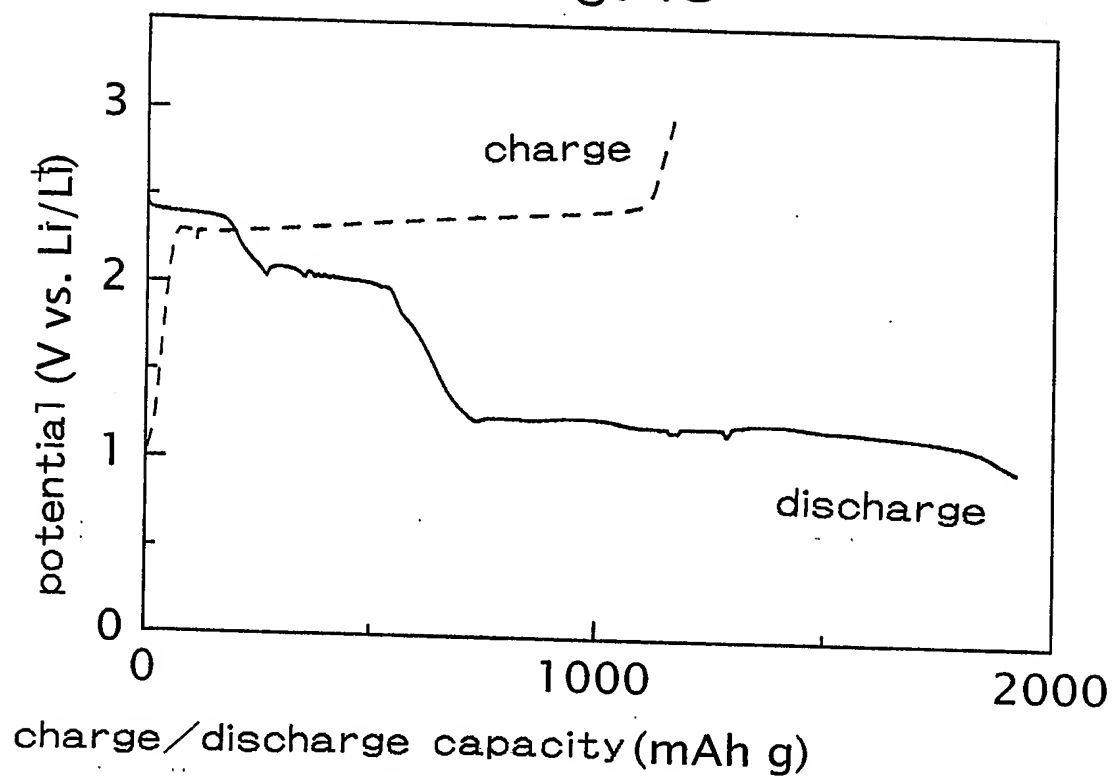


Fig. 48





[Document Name] Abstract

[Abstract]

[Subject] A non-aqueous electrolyte secondary battery having increased capacity and energy density is provided.

5 [Solving Means] A non-aqueous electrolyte secondary battery comprises a positive electrode including elemental sulfur, a negative electrode including silicon that stores lithium, and a non-aqueous electrolyte including a room temperature molten salt having a melting point of not higher than 60°C.

10 The non-aqueous electrolyte may further include at least one type of solvent selected from cyclic ether, chain ether, and fluorinated carbonate. The non-aqueous electrolyte may include a room temperature molten salt having a melting point of not higher than 60°C and a reduction product of elemental

15 sulfur.

[Selected Drawing] Fig. 1